UNIVERSITAT POLITÈCNICA DE CATALUNYA
BARCELONATECH
Escola d'Enginyeria de Barcelona Est

Politecnico di Bari

TREBALL FI DE GRAU

Grau en Enginyeria Electrònica Industrial i Automàtica

STUDY AND DESIGN OF A BALANCE POSTURAL CONTROL SYSTEM

Memòria i Annexos

Autor: Andrea Fonseca Benítez
Director: Prof. Ing. Biagio Turchiano
Co-Director: Prof. Ing. Paolo Lino

Convocatòria: Juny 2017

Resum

L'habilitat de mantenir una postura correcta s'està convertint en un important tema d'estudi ja que és necessari comprendre el comportament del cos humà per tal d'aplicar aquests coneixements en altres camps com la robòtica o la mecànica

Al llarg d'aquest projecte s'ha realitzat el disseny i estudi d'un sistema de control per l'equilibri de la postura tot seguint un enfocament frontal. Per tal de trobar paràmetres antropomètrics realistes ha estat necessari realitzar una àmplia recerca sobre els diversos paràmetres biomecànics. En quant al model, per tal de centrar l'atenció en les bases del moviment, s'ha escollit un model simplificat basat en el doble pèndul. Pel que reguarda el sistema de control, s'han utilitzat dos mètodes diferents; d'una banda el mètode LQR (per les seves sigles en anglès, "*Linear Quadratic Regulator*") ja que deixa al dissenyador la capacitat de triar quant pes es vol donar a l'efecte del controlador, i per l'altra banda un controlador no linear. A més a més, s'ha dissenyat un segon model que inclou un element elàstic com a aproximació del comportament del maluc. És per això que s'ha realitzat una exhaustiva recerca sobre les diverses aproximacions en el disseny de les articulacions. Finalment, la simulació dels diferents models i els diversos escenaris considerats ha permès la comparació de tots ells, arribant a proporcionar quins paràmetres poden ser negligits i quins tenen una gran influència en els resultats.

Resumen

La capacidad de mantener una postura correcta se está convirtiendo en un importante tema de estudio ya que es necesario entender el comportamiento del cuerpo humano para poder aplicar esos conocimientos a campos como la robótica y la mecánica.

En este proyecto se ha realizado el diseño y estudio de un sistema de control de balance postural siguiendo un enfoque frontal. Con tal de encontrar parámetros antropométricos realistas ha sido necesario realizar una exhausta investigación sobre parámetros biomecánicos. En cuanto al modelo, con la finalidad de centrar la atención en las bases del movimiento, se ha elegido un modelo simplificado basado en un doble péndulo. Por lo que reguarda el sistema de control, se han usado dos métodos; por un lado, el método LQR (por sus siglas en inglés, "*Linear quadratic regulator"*) ya que deja al diseñador la capacidad de elegir cuanto peso se quiere dar al efecto del control, mientras por el otro un controlador no linear. Se ha diseñado también un segundo modelo que incluye un elemento elástico como aproximación del comportamiento de la cadera. Con tal fin, se ha tenido que realizar una amplia investigación sobre las distintas aproximaciones en la modelación de las articulaciones. Finalmente, la simulación de los distintos modelos y los diversos escenarios considerados ha permitido la comparación de todos ellos, llegando a proporcional qué parámetros pueden ser descuidados y cuales tienen un gran peso en los resultados.

Abstract

The ability to maintain a proper posture is becoming a more interesting topic as it is necessary to understand the behavior of the human body to be able to apply this knowledge to robotics and mechanics.

In this project the design and study of a balance postural control system has been developed, by following a frontal modeling approach. An extensive research on biomechanical parameters has been necessary to find realistic anthropometric values to be implemented. A simplified model, based on the double pendulum, has been chosen because it allowed focusing on the basis of the balance movement. Regarding the control system, two different methods have been used. On the one hand, the Linear-quadratic regulator (LQR) has been used as it allowed to decide how much weight the controller could have, while on the other hand, a non linear controller has been studied. Moreover, a second model that included an elastic element to simulate the hip joint has been designed;to do so, a wide research on different approximations of the human body's joints has been performed. Finally, the simulation of the different models and the numerous scenarios considered has allowed an extensive comparison determining which parameters could be neglected and which ones havea strong influence on the system dynamics.

Acknowledgments

I would first like to thank my thesis supervisors, Prof. Ing. Biagio Turchianoand Prof. Ing. Paolo Lino, at Politecnico di Bari. The door to Prof. Ing. Lino office was always open whenever I ran into a trouble spot or had a question on how to approach my research. He consistently allowed this thesis to be my own work, but steered me in the right direction whenever he thought I needed it.

Besides my supervisors, I would also like to express my gratitude to my coordinator Prof. Ing. TizianoPoliti for guiding me through the bureaucracy of writing a thesis in a foreign country and for his help when choosing my thesis supervisors.

Finally, my sincere thanks also goes to my friend Juan Hurtado that helped me with his physiotherapy knowledge when I was surrounded by anthropometric parameters and, of course, with his unconditional support.

Index

1. Preamble

1.1. Background of the project

Posture is a key element of the daily life. There are significant number of studies that show the relationship between keeping a proper posture and numerous health benefits. On the one hand, from a psychological perspective, it is well known how the posture can influence a person's mood, the way to face the day and even how other people perceive them and treat them accordingly. On the other hand, from a medical perception, maintaining a good posture is the easiest way to prevent present and future injuries and deformations. The ability of maintaining a posture is due to a huge number of muscular contractions and efforts. It's a continuous process, in which the body regulates every single part of its components to face the effects of gravity and punctual external disturbances.

Biomechanics has a strong relationship with physiology and anatomy. The tension that acts at the tendons is controlled by the patterns generated by the release of metabolic energy by the neuromuscular system. That tension waveform depends on physiological characteristics of the body like the muscles and if they are rested or fatigued. With the reduction of the mortality rate and the constant increase of the lifespan, the degenerative illnesses are becoming more and more important. However, this is not the main source of the increasing rate of physical postural injuries. Due to the lifestyle adopted by the majority of the occidental society, a lot of injuries occur. This lifestyle is characterized by a constant bad posture in desk related jobs or the constant use of Smartphones that lead to an unhealthy position of the neck.

Setting aside the biomedical background, the modeling of the body is a different problem to tackle. There are different models depending on the precision needed and the case of study. In this project, a frontal standing modeling approach is used. As the main objective is to study the basics of the stabilization movement, a simple model is suitable to analyze the system dynamics. More specifically, the so called Pendubot is considered as a reference.

The Pendubot [8] is a two link robot with an actuator at one of the ends of the open chain. Different versions with the actuation in between the links have been also designed and studied, such as the Acrobot from the University of Illinois. However, the analysis of Pendubot kinematics and dynamics is more useful for this project (Fig. 1.1.).

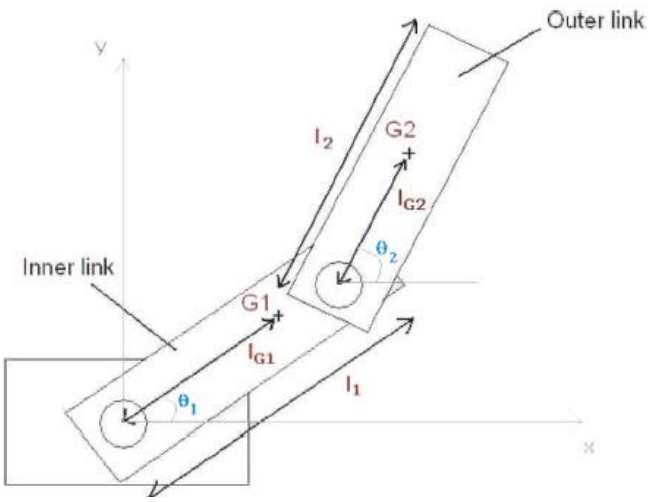

Fig. 1.1. *Pendubot diagram [7].*

As it can be seen in Fig. 1.1, the actuator acts directly the inner link, while the movement of the outer link is due to the transmitted torque through the inner link, and therefore cannot be controlled directly. The mechanical equations that describe the Pendubot can be easily obtained either with a Newton-Euler strategy or using Lagrange's equation. In literature, a common approach to control the system is based on LQR or pole placement methods. To this aim, it is necessary to linearize the Pendubot dynamical equations (e.g. by means of the Taylor series).

The Pendubot design itself allows a 360º motion, and therefore, depending on the application, the control system (Fig. 1.2) needs to include angle restrictions.

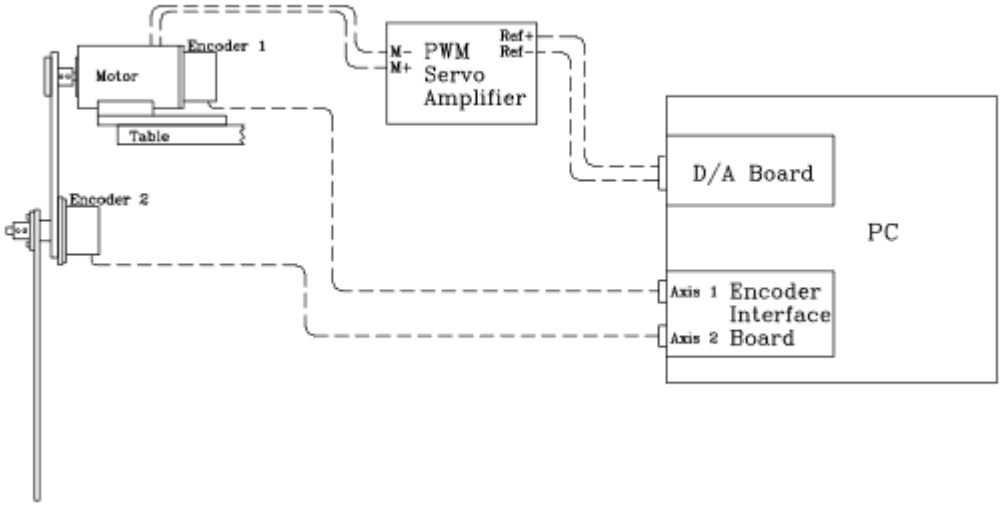

Fig. 1.2. *Scheme of the Pendubot's interface with its controller. [8]*

Following a similar approach, A.Tenerelli developed a model based on a frontal approach, thus obtaining a system of dynamical equations similar to those representing a double pendulum dynamics. As it can be seen in Fig. 1.3, an additional body corresponding to the arms was added to the system model.

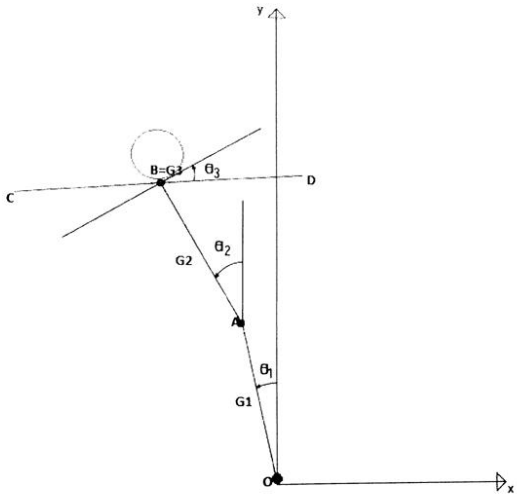

Fig. 1.3. *Schematics of the model used by A.Tenerelli [22].*

The original model in Tenerelli's thesis was affected by errors on parameters and compensation momentums in joints, and on simulation models implemented in Matlab/Simulink environment. Finally, the original work did not consider reliable biomechanical parameters within the model.

However, it represented a suitable starting point to develop different modeling and control strategies, and implementation approaches.

1.2. Motivation

Decrypting the mechanisms of the human body has always been an intriguing topic in various disciplines. Such a natural mechanism like the posture balance takes hundreds of considerations and regulating actions performed unconsciously every second of a person's life. However, it is not only interesting to analyze it from a physical and medical point of view, but also to try to replicate it through the knowledge provided by different engineering fields. Moreover, the proper understanding of such mechanisms and its replication is the first milestone for biomechanical and automation studies aiming at developing support posture devices. Maintaining an upright position is a natural human struggle in certain circumstances, for example among the elder population or in some medical health conditions like sclerosis. The increase of the life expectancy of the population has motivated a large number of studies among the medical field, as it has opened a completely new

window of circumstances unreachable a few years ago. Both the medical and military research on exoskeletons has increased in the past 50 years, requiring a better understanding of the human body and regulating mechanisms. Therefore, this is an extremely interesting topic as it allows the communion of fields such as biomechanics and control and regulation of systems.

1.3. Previous requirements

For the proper development and understanding of this project the knowledge on different fields of engineering is required. As stated before, this project has been inspired by the thesis work of A.Tenerelli [22]. Derivation of the system equations requires the knowledge of systems dynamics, to adopt either the Newton-Euler approach or the Lagrange approach. Moreover, notions in biomechanics will be needed to properly define the model parameters. Among other engineering fields, control systems knowledge is needed to design the stabilizing controller. In this work, Maple16 and Matlab software environments have been used, the former to linearize the system and the latter as a simulation tool. Matlab/Simulink environment allowed to directly compute the solution of model differential equations for each simulation time instant.

2. Introduction

2.1. Objectives of the project

This project objective is to obtain a better understanding of the dynamics of the balance system of the human body, by improving the work of A.Tenerelli [22] who derived a simplified model of the system. More in details, the objective is to go further and obtain a non-linear system equivalent to the frontal approach of the human body, which is able, even in presence of external disturbances, to stabilize the unstable vertical position.

To this aim, different milestones have been set. First, the proper definition of model parameters and equations. Then, the design of the controller for a linear version of the system. After the basic study is achieved, the next milestone is to control a non-linear system. Finally, the last step is to design a non-linear controller.

To follow through each step and achieving the different objectives, two software environments are used. More specifically, Maple16 is used as a symbolic math tool, to perform some of the mathematical computations. Matlab/Simulink environments are used to develop the simulation model and to integrate the dynamical system differential equations.

2.2. Scope of the project

The development of this project required a background in different engineering fields.

First of all, in the biomechanics field a state of the art research is performed to find the most accurate parameters as possible including fraction lengths and masses of each body component. In addition to the anatomic parameters, a range of options are considered for the moment of inertia. Each body is approximated by different geometrical shapes to reach a wider knowledge in the influence of these values in the stabilization.

In the mathematical approach, different options are considered evaluating the advantages and disadvantages of a Newton-Euler approach versus a Lagrange's approach to obtain the non-linear model. The advantages of using different mathematical tools are discussed.

When considering the different control techniques, the linearization of the non-linear system is required by the LQR control. The different parameters of this control are explained and reviewed in order to choose the most appropriate ones. The necessity to linearize the system leads to a research

among the different mathematical techniques and the use of software such as Maple16 to perform the most complicated operations avoiding unnecessary mistakes and allowing a faster result and modification when implementing different models. Later on, a non-linear control law is developed to substitute the LQR method.

Finally, different simulations are performed in order to compare the results for each possibility. The knowledge in Matlab/ Simulink allows determining the importance of each parameter and the range in which the stabilization is possible.

3. Biomechanical data

3.1. Background

Biomechanics has been a widely studied subject in the last years, usually with medical applications such as the design of prosthesis or external skeletons. To do so, there have been different methods developed to determine the human body segment parameters. Some authors like W. Braune and O. Fisher, and later W.T. Dempster, studied cadavers to determine coefficients that allowed estimating the segment mass, center of mass and moment of inertia [13]. The formers have been widely used while the latter raised some doubts because of the use of a small and segmented range of data. R. Contini also used cadavers, but in this case a different strategy was followed [13]. In order to determine the parameters of the lower limbs, a whole body density of each sample was determined mathematically by using an accurate weight and an estimation of the volume. However, the range of cases in which the final coefficients could be used was rather small as it depended on a short range of height and weight. A third method was developed by E.P. Hanavan [13]. In this case, the limbs of the body were modeled as geometric solids determining easily then the center of mass and moments of inertia.

In 1985 S.H. Koozekanani and J. Duerk compared the accuracy of Dempster, Contini and Hanavan methods in the article "*Determination of Body Segment Parameters and Their Effect in The Calculations of the Position of Center of Pressure During Postural Sway"* [13]. To do so, the center of pressure in the horizontal direction of a lateral approach was computed using dynamic model with the data provided by the three different models. To compare the accuracy, the experimental values were obtained using a Kistler model 9216 for plate. According to the results, even though the chosen subject did not belong to the range of age taken into account by Dempster (Fig. *3.1*), the results followed the same tendency, even if they were far from being accurate. In the case of Contini, the calculated results differed widely from the measured ones (Fig. *3.2*). Finally, Hanavan model, using general geometric solids, was the most accurate one (Fig. 3.3).

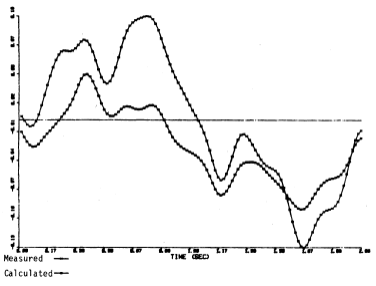

Fig. 3.1. Dempster method (starting below) compared to experimental method (starting above) [13].

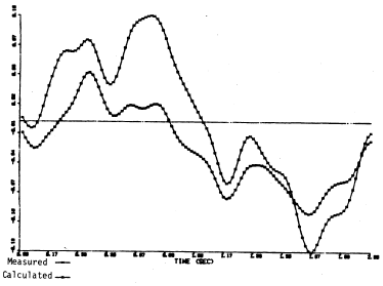

Fig. 3.2. *Contini method (starting below) compared to experimental method (starting above) [13].*

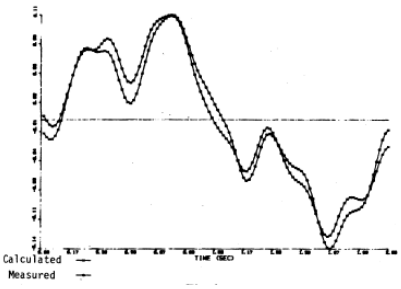

Fig. 3.3.*Hanavan method (starting below) compared to experimental method (starging above) [13].*

A different side of the body modeling issue is the control system. In 1998 P.Gorce and F. El Hafi studied the decision mechanism of humans while stepping over an object. Even though a better understanding of the control scheme is not the scope of this project, for the simulation a model had to be implemented, so biomechanical parameters had to be used. However the parameters where not explained in the paper, so its relevance lies in a future project but not in a biomechanical focused one.

In the article "*Beyond Parameter Estimation: Extending Biomechanical Modeling by the Explicit Exploration of Model Topology" from 2007* [2] the use of topology techniques to study and simulate complex tendon networks is developed. Even though this article is too much detailed for the simplified model studied in this project, it is important to understand also how the studies of biomechanical modeling have evolved.

The authors used an approach based on the explicit distinction between topology and parameter values. Thus, the topology refers to the structure of a model, defined by the organization of the elementary building blocks such as tendons, muscles, ligaments. While the parameter values are associated to the specifications of each building block like shape, size, material properties, etc. [2]. In order to test the methodology, the modeling of hand tendons was considered. The authors' simulation system (Fig. 3.4) differentiated topology and parameter values in two blocks. So when discrepancies were found in the results, they could be corrected modifying one of the two blocks.

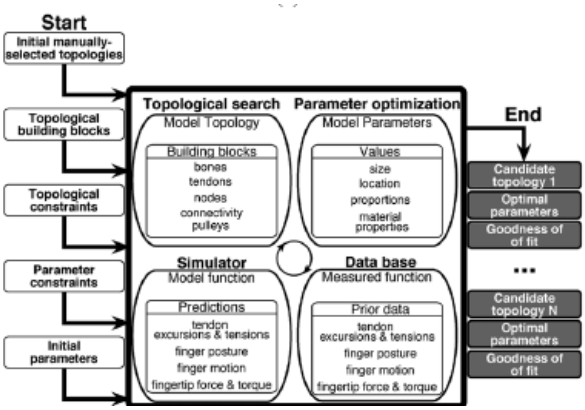

Fig. 3.4. *Bloc diagram of the model where both topology and paramters can be adjusted to fit the data [2].*

To model the structures, the research team developed a biomechanical model simulator, where they defined each building block by proper parameters, and then described them by a strain-stress bond.

It is also interesting to pay attention to the article *"Identification of isolated biomechanical parameters with a wireless body sensor network"* [19]. Even though it is focused on the knee joint and therefore too specific for the purpose of this project, it points out useful information. The main goal of the article is to develop a body sensor able to measure surface electromyogram and 9-degrees of freedom inertial/magnetic data at high sample rates [19], in order to minimize the instrumentation effort done by the subject nowadays. This article points out that typically in biomechanics the behavior of a joint is described as a mechanical impedance, so time-varying and non-linear and also a function of frequency. Taking all into account a dynamic system model of the test bench and the human knee has been developed (Fig. 3.5).

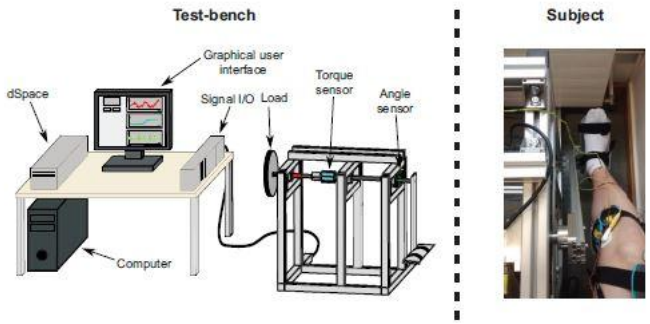

Fig. 3.5. *Test-bench design (left) for a knee model validation with subject (right) [19].*

The test-bench model is represented by a simplified mechanical model taking into account the following elements: two fixed moments of inertia J_1 and J_2 and two non linear viscous damping terms; D_1 and D_2. Being D_1 and D_2 a function of the time derivative of the rotation angle, ($d\varphi/dt = \omega$). Moreover, the sensor torque is given by the spring constant that denotes the stiffness and the relative angle. Therefore the obtained system is the following (Fig. 3.6):

$$\begin{aligned}
\dot{\varphi}_1 &= \omega_1 \\
\dot{\omega}_1 &= \frac{1}{J_1}\left(k_{sens}(\varphi_2 - \varphi_1) - D_1(\omega_1)\right) \\
\dot{\varphi}_2 &= \omega_2 \\
\dot{\omega}_2 &= \frac{1}{J_2}\left(-k_{sens}(\varphi_2 - \varphi_1) - D_2(\omega_2) + G_{mp}(\varphi_{mp})\right),
\end{aligned} \tag{3.1.}$$

Fig. 3.6. *Mechanical equivalent diagram of the test-bench [19].*

Regarding the human knee kinematics model, the authors have based it on the dynamic model by Riener and Fuhr [19]. All detailed information can be found in the paper [19]. But even though the precision of it, it is interesting to analyze the followed approach, especially when trying to add some elastic component to the hip joint in the projects model.

After analyzing the different studies made in the last years, a more basic literature is needed. In the book "*Biomechanics and Motor Control of Human Movement*" by David A. Winter a wide variety of information is found. The most interesting chapter for this project is the anthropometry one. It is exclusively dedicated to the studies of physical measurements of the human body. And though historically the purpose of the field had been evolutionary and historical, nowadays it has become really important for human body modeling.

Regarding segment dimensions, both Dempster and Contini's teams collected estimated data. However it was Drillis and Cotini [23] to express them as a fraction of body height (Fig. 3.7).

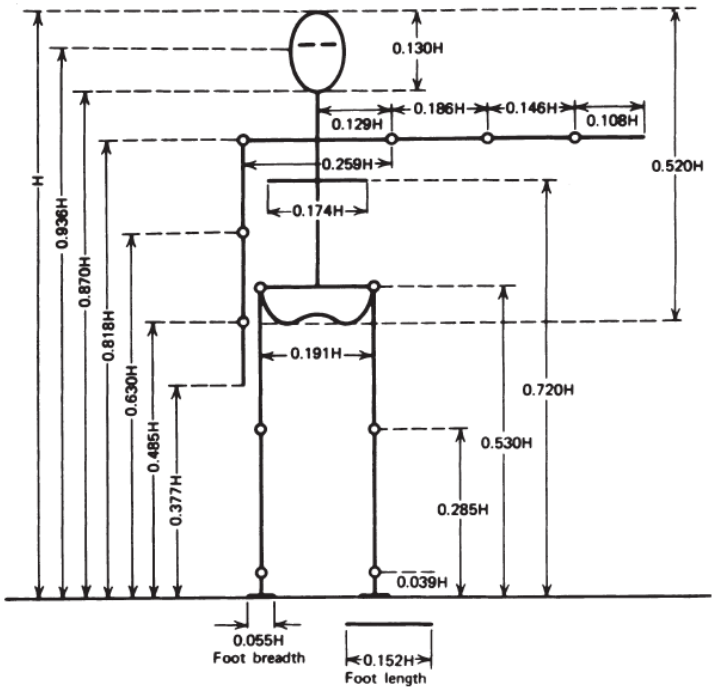

Fig. 3.7. *Body segment lengths expressed as a fraction of body height (H) and developed by Drillis and Contini (1966) [23].*

To build the model, together with the lengths elements, the segment mass have to be defined in order to compute the inertial moments and the centers of mass. To do so, there are different data available. The first option is the results of the measurements done by Drills and Contini regarding the density (Fig. 3.8).

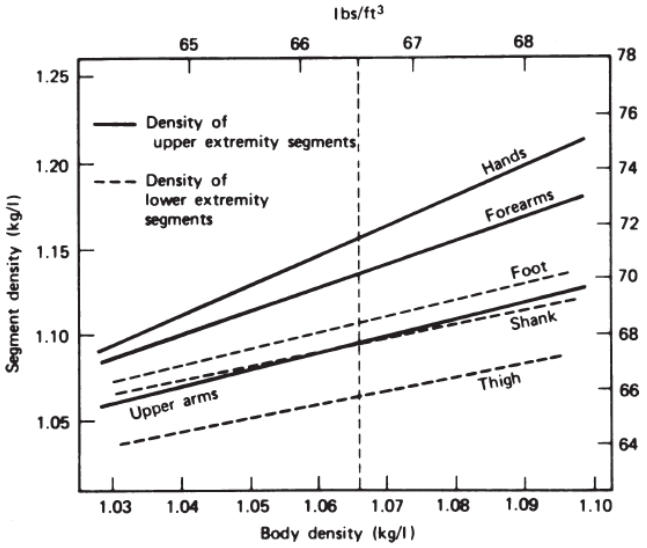

Fig. 3.8. *Density of limb segments as a function of average body density by Drillis and Contini (1966) [23].*

A more direct option is given by the data provided by Dempster. In this case, the anthropometric data was expressed as a portion of the total mass (Table 3.1)

Segment	Definition	Segment Weight/Total Body Weight	Center of Mass/ Segment Length Proximal	Distal	Radius of Gyration/ Segment Length C of G Proximal	Distal	Density
Hand	Wrist axis/knuckle II middle finger	0.006 M	0.506	0.494 P	0.297	0.587	0.577 M	1.16
Forearm	Elbow axis/ulnar styloid	0.016 M	0.430	0.570 P	0.303	0.526	0.647 M	1.13
Upper arm	Glenohumeral axis/elbow axis	0.028 M	0.436	0.564 P	0.322	0.542	0.645 M	1.07
Forearm and hand	Elbow axis/ulnar styloid	0.022 M	0.682	0.318 P	0.468	0.827	0.565 P	1.14
Total arm	Glenohumeral joint/ulnar styloid	0.050 M	0.530	0.470 P	0.368	0.645	0.596 P	1.11
Foot	Lateral malleolus/head metatarsal II	0.0145 M	0.50	0.50 P	0.475	0.690	0.690 P	1.10
Leg	Femoral condyles/medial malleolus	0.0465 M	0.433	0.567 P	0.302	0.528	0.643 M	1.09
Thigh	Greater trochanter/femoral condyles	0.100 M	0.433	0.567 P	0.323	0.540	0.653 M	1.05
Foot and leg	Femoral condyles/medial malleolus	0.061 M	0.606	0.394 P	0.416	0.735	0.572 P	1.09
Total leg	Greater trochanter/medial malleolus	0.161 M	0.447	0.553 P	0.326	0.560	0.650 P	1.06
Head and neck	C7–T1 and 1st rib/ear canal	0.081 M	1.000	— PC	0.495	0.116	— PC	1.11
Shoulder mass	Sternoclavicular joint/glenohumeral axis	—	0.712	0.288	—	—	—	1.04
Thorax	C7–T1/T12–L1 and diaphragm*	0.216 PC	0.82	0.18	—	—	—	0.92
Abdomen	T12–L1/L4–L5*	0.139 LC	0.44	0.56	—	—	—	—
Pelvis	L4–L5/greater trochanter*	0.142 LC	0.105	0.895	—	—	—	—
Thorax and abdomen	C7–T1/L4–L5*	0.355 LC	0.63	0.37	—	—	—	—
Abdomen and pelvis	T12–L1/greater trochanter*	0.281 PC	0.27	0.73	—	—	—	1.01
Trunk	Greater trochanter/glenohumeral joint*	0.497 M	0.50	0.50	—	—	—	1.03
Trunk head neck	Greater trochanter/glenohumeral joint*	0.578 MC	0.66	0.34 P	0.503	0.830	0.607 M	—
Head, arms, and trunk (HAT)	Greater trochanter/glenohumeral joint*	0.678 MC	0.626	0.374 PC	0.496	0.798	0.621 PC	—
HAT	Greater trochanter/mid rib	0.678	1.142	—	0.903	1.456	—	—

*NOTE: These segments are presented relative to the length between the greater trochanter and the glenohumeral joint.
Source Codes: M, Dempster via Miller and Nelson; *Biomechanics of Sport*, Lea and Febiger, Philadelphia, 1973. P, Dempster via Plagenhoef; *Patterns of Human Motion*, Prentice-Hall, Inc. Englewood Cliffs, NJ, 1971. L, Dempster via Plagenhoef from living subjects; *Patterns of Human Motion*, Prentice-Hall, Inc., Englewood Cliffs, NJ, 1971. C, Calculated.

Table 3.1 *Mass fraction of the different bodies by Dempster [23].*

However, the most complete measure of center of mass until 2009 was the 21-marker, 14-segment model, used to determine balance mechanisms during quiet standing by Winter et al. [23]. In the following immage (Fig. 3.9) the location of the markers and the table give the definition of the 14 segments used, along with mass fraction of each segment.

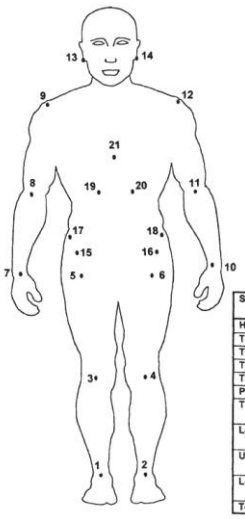

1. R Ankle
2. L Ankle
3. R Knee
4. L Knee
5. R Hip
6. L Hip
7. R Wrist
8. R Elbow
9. R Shoulder
10. L Wrist
11. L Elbow
12. L Shoulder
13. R Ear
14. L Ear
15. R ASIS
16. L ASIS
17. R Iliac Crest
18. L Iliac Crest
19. R Lower Rib
20. L Lower Rib
21. Xiphoid

Segment	Mass Fraction	Definition of Segment COM
Head	0.081	(13 + 14)/2
Trunk 4	0.136	(9 + 12 + 21)/3
Trunk 3	0.078	((19 +20)/2 + 21)/2
Trunk 2	0.065	(17 + 18 + 19 + 20)/4
Trunk 1	0.078	(17 + 18 + 15 + 16)/4
Pelvis	0.142	(15 + 16)/2
Thighs	0.100 (2)	0.433 x 3 + 0.567 x 5 and 0.433 x 4 + 0.567 x 6
Legs & feet	0.060 (2)	0.606 x 1 + 0.394 x 3 and 0.606 x 2 + 0.394 x 4
Upper arms	0.028 (2)	0.436 x 8 + 0.564 x 9 and 0.436 x 11 + 0.564 x 12
Lower arms	0.022 (2)	0.682 x 7 + 0.318 x 8 and 0.682 x 10 + 0.318 x 11
Total	1.00	

Fig. 3.9. *Mass fraction of the different bodies by Winter et al. (1998) [23].*

To compute the center of mass, when dealing with a multisegment system, the following equations have been used:

$$x_0 = \frac{m_1x_1 + m_2x_2 + m_3x_3}{M}$$
$$y_0 = \frac{m_1y_1 + m_2y_2 + m_3y_3}{M} \quad (3.2.)$$

Being $M = m_1 + m_2 + m_3$

m_i, *for i=1..3, the mass of the corresponding segment (i).*

Later on, considering the model as a set of rigid geometrical bodies, the moments of intertia have been computed, using often the Parallel-Axis Theorem (Eq. 3.3.).

$$J = J_0 + m \cdot x^2 \quad (3.3.)$$

$J_0 = moment\ of\ inertia\ about\ the\ center\ of\ mass$
$m = mass\ of\ the\ segment$
$x = distance\ between\ center\ of\ mass\ and\ center\ of\ rotation$

Even though all the needed information has been found in the *"Biomechanicsand Motor Control of Human Movement"* book by David A. [23]. Being it a recap of the different authors named and studied before such as Dempster and Contini. It is worth to analyze the thesis of Hanavan as those approximations gave the best results in the paper *"Determination of Body Segment Parameters and Their Effect in the Calculation of the Position of Center of Pressure During Postural Sway"* [2].

"A Mathematical Model of the Human Body" by Hanavan describes a human body model dividing it in different segments, to later on analyze the model with a computer program. According to this thesis work, the personalized mathematical model is made of 15 simple geometric solids as shown in Fig. 3.10.

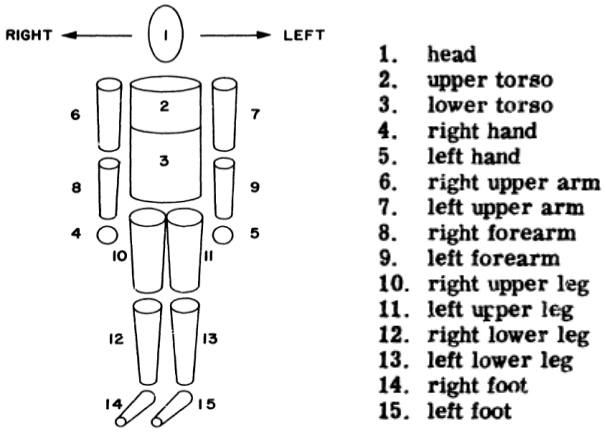

Fig. 3.10. *Body segments by Hanavan [18].*

Hanavan details each of the 15 bodies' geometry and analyses the anthropologic parameters, the center of gravity and the moment of inertia about the three different axes. With all the data acquired by the model, a comparison is made with the experimental data. Reaching the results shown in Table 3.2 and Fig. 3.11.

BODY SEGMENT	MODEL HIGH	MODEL LOW	MODEL AVE	EXPERIMENT[2]
HEAD AND TORSO	73.2	61.3	64.5	60.4
UPPER ARM	49.6	44.6	47.3	43.6
FOREARM	45.0	39.8	42.8	43.0
UPPER LEG	45.3	42.0	43.7	43.3
LOWER LEG	47.6	39.8	41.6	43.3

[1] DISTANCE FROM UPPER END IN % OF SEGMENT LENGTH
[2] FROM REF 5:194

BODY SEGMENT	MODEL HIGH	MODEL LOW	MODEL AVE.	EXPERIMENT[1]
HEAD	1.47	.90	1.15	1.11
UPPER TORSO	1.00	.72	.84	.92
LOWER TORSO	1.10	.80	.92	1.01
HAND	1.72	1.02	1.29	1.17
UPPER ARM	1.22	.79	.97	1.07
FOREARM	1.56	1.04	1.30	1.13
UPPER LEG	1.32	.88	1.13	1.05
LOWER LEG	1.44	.83	1.19	1.09
FOOT	2.14	1.12	1.62	1.09

[1] FROM REF 5:195-196

Table 3.2. *Location of center of gravity (left) and Specific gravity of body segments (right) [18].*

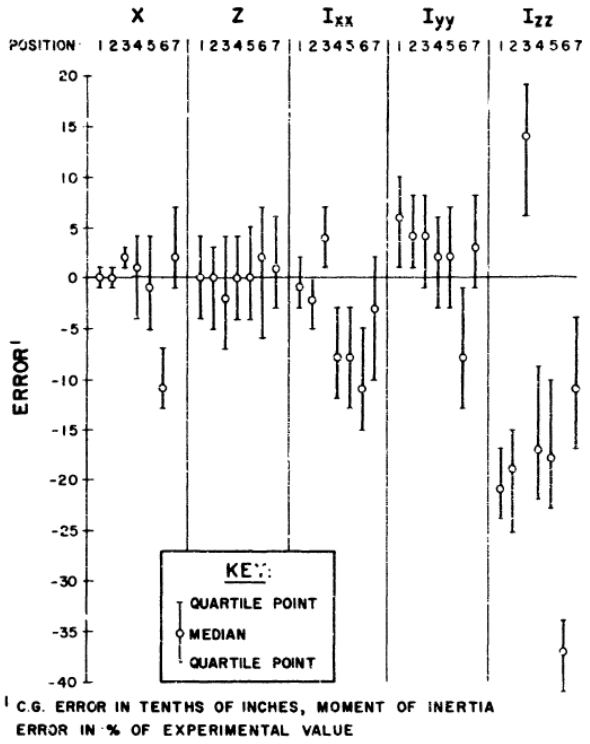

Fig. 3.11. *Error distribution in 7 different positions (66 subjects). Being X and Z the location of the center of gravity, and I_{xx} I_{yy} and I_{zz} the moments of inertia about the named axes [18].*

Even though the data obtained and analyzed in Hanavan's thesis in 1964 was crucial for the development of the field, it is not directly useful for this project, as data such as the lengths of the bodies were measured on the studied subjects.

3.2. Chosen values

3.2.1. Partial mass and length

After analyzing all the data and bibliography stated above, the partial mass and lengths have been computed according to the Table 3.1 and Fig. 3.9 respectively. The following data has been obtained.

Mass		**Height**	
Total	70 Kg	Total	1,75 m
Two legs	32,34 Kg	Legs	0,9275 m
Torso	24,99 Kg	Torso	0,504 m
Head	5,67 Kg	Head	0,225 m
Two arms	7 Kg	Arms	0,99575 m

Table 3.3.*Computed Mass and Length*

3.2.2. Moments of inertia

Regarding the moments of inertia, two different cases will be considered in order to compare the results.

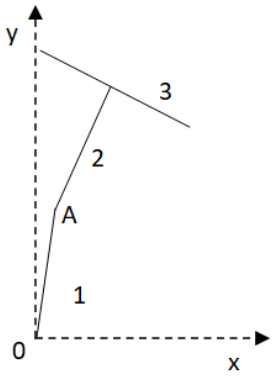

Fig. 3.12.*Body Diagram for the computations*

CASE1. All components as a Slender rod

Using the following information and the data stated before:

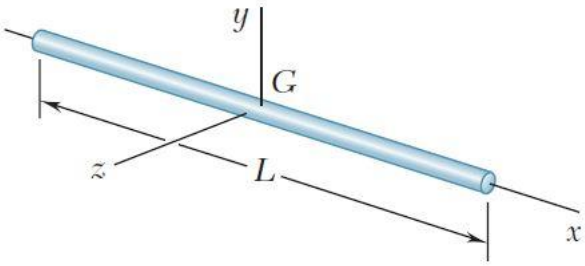

Fig. 3.13. *Slender rot diagram [6]*

$$J_y = J_z = \frac{1}{12} \cdot m \cdot L^2$$

$$\begin{aligned} &where: J_y \text{ and } J_z \text{ are the moments of intertia} \\ &\quad \text{with respect to the corrisponding axis} \\ &\quad m \text{ is the mass} \\ &\quad L \text{ is the length} \end{aligned} \tag{3.4.}$$

BODY 1: Legs

Using the equations above, the moment of inertia with respect to the center of gravity G1 has been computed: J_{G1}= 2,4996 Kg*m^2

Then, applying the parallel axis theorem, the moment of inertia of the first body (legs) with respect to the point 0, has been obtained: J_{01}=9,4548 Kg*m^2

BODY 2 and 3: Torso and Arms

Initially the same procedure is followed for the bodies 2 and 3. First computing the moment of inertia with respect their own center of gravity (J_{G2} and J_{G3}), and then the one with respect to the point A has been obtained for both bodies (J_{A2} and J_{A3}) using the parallel axis theorem. Finally, for the latter, the sum has been performed (J_{A23})as both bodies will be behaving as one.

J_{G2}= 1,28772 Kg·m^2 J_{G3}= 6,97025 Kg·m^2

J_{A2}= 3,23475 Kg·m^2 J_{A3}= 8,748362 Kg·m^2 J_{A23}= J_{A2}+ J_{A3}=11,9831 Kg·m^2

CASE2. Using different geometric shapes.

In order to try to approximate a more realistic case, the arms have been considered slender rods as before, while both the torso and the legs are treated as rectangular prisms (Fig. 3.14).

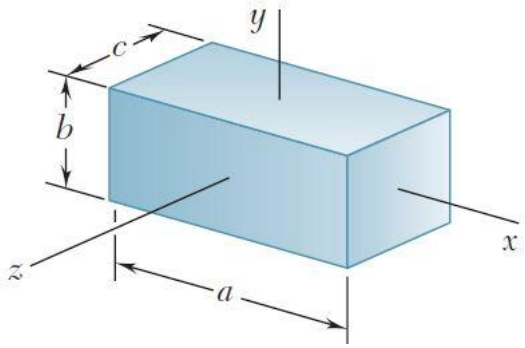

Fig. 3.14. *Rectangular prism diagram [6].*

$$J_x = \frac{1}{12} \cdot m \cdot (b^2 - c^2)$$
$$J_y = \frac{1}{12} \cdot m \cdot (c^2 - a^2)$$
$$J_z = \frac{1}{12} \cdot m \cdot (a^2 - b^2) \qquad (3.5.)$$

where: J_x J_y *and* J_z *are the moments of intertia with respect to the corrisponding axis*
m *is the mass*
a, b, c *are the dimentions of the body*

BODY 1: Legs

Using the equations above, the moment of inertia with respect to the center of gravity G1 has been computed: J_{G1}= 2,6195 Kg*m^2

Then, applying the parallel axis theorem, the moment of inertia of the first body (legs) with respect to the point 0, has been obtained: J_{01}=9,574656 Kg*m^2

BODY 2 and 3: Torso and Arms

In this case, the data regarding the arms has already been computed in Case 1, so only the moments of inertia of the 2nd body are needed. However, they have been computed following the same procedure.

J_{G2}= 1,173899 Kg·m^2 J_{G3}= 6,97025 Kg·m^2

J_{A2}= 3,1209 Kg·m^2 J_{A3}= 8,748362 Kg·m^2 J_{A23}= J_{A2}+ J_{A3}=11,86929 Kg·m^2

Comparison between both cases

	Case 1	**Case 2**
J_{01}	9,4548 Kg·m^2	9,574656 Kg·m^2
J_{A2}	3,23475 Kg·m^2	3,1209 Kg·m^2
J_{A3}	8,748362 Kg·m^2	8,748362 Kg·m^2
J_{A23}	11,9831 Kg·m^2	11,86929 Kg·m^2

Table 3.4. *Comparison between the values of the computed moments of inertia.*

As it can be seen in Table 3.4, the difference between choosing different geometrical bodies to represent the different parts of the body does not imply a huge variation in the values. In this project a really schematized version of the human body is used; so variations in the decimals do not have a significant impact in the results of the model. Therefore, it can be concluded that both options are suitable, but if a more accurate project would be performed the different should not be neglected.

4. Model and methodology

4.1. Introduction

Once all the biomechanical data have been computed, the next step is to proceed to determine the equations that will describe the chosen model.

Following the work of A. Tenerelli a frontal approach has been chosen. In her thesis "*Study of a balance postural control system"* the following model was used (Fig. 4.1).

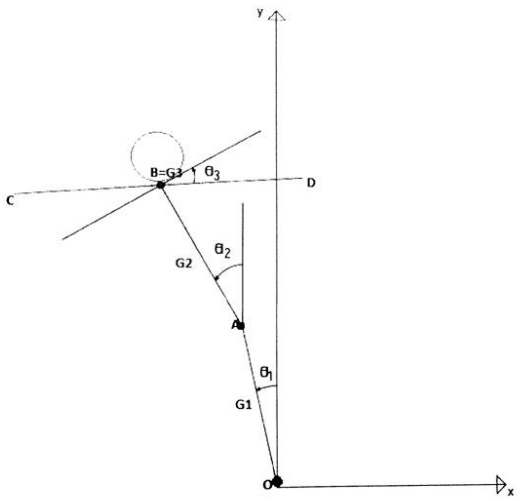

Fig. 4.1. *Schematics of the model used by A.Tenerelli [22].*

The aim of the thesis work [22] was to design a control system that allowed the body to stabilize when a small lateral perturbation was produced. However, after different attempts, the designed controller worked only for a linearized system.

The behavior of the human body, when schematized with such simplicity gets really close to a well known system called Pendubot (Fig. 4.2). It is a two-link open chain robot, with an actuator in one of the links, and then, that same link connected to the second one. Therefore the action applied on the first link will be passed on to the second one by a non-linear relation.

Fig. 4.2. *Pendubot connected to the motor (left), Pendubot fully extended (right) [7].*

In order to focus on the basis of the movement a double pendulum system has been chosen. Therefore, the following model (Fig. 4.3) has been used to develop the equations:

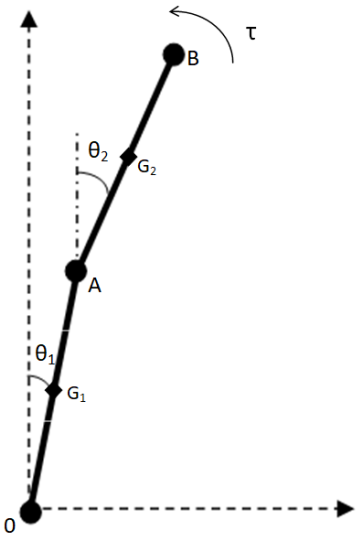

Fig. 4.3. *Diagram of the body balance scheme.*

Regarding the methodology, in the thesis work developed by A. Tenerelli [22] the equations to describe the system where found using Newton-Euler method. However, in this project a different methodology has been followed. Even though it is a simple system, thus using either Newton-Euler or Lagrange should not make a significant difference; in more complex systems the latter is highly recommended. Therefore, in order to use the most extendable methodology, Lagrange has been chosen.

4.2. Non-linear model

According to Lagrange's theory:

$$L(q_i, \dot{q}_i) = E_k - E_p \quad for\ i = 1..n$$

$$\frac{d}{dt}\left(\frac{\partial L}{\partial \dot{q}_i}\right) - \frac{\partial L}{\partial q_i} = \sum Non\ conservative\ \tau \tag{4.1.}$$

where: L is a real − valued function with continuous first partial derivatives
q_i and $\dot{q}_i$ are the function to be found and its derivative respectively
E_K is the kinetic energy
E_P is the potential energy

In order to understand the following computations a few parameters have to be defined according to Fig. 4.3.

J_1, J_2: moment of inertia of bodies 1 and 2

G_1, G_2: center of gravity of bodies 1 and 2

m_1, m_2: mass of bodies 1 and 2

l_{G1}: distance from point 0 to G_1

l_1, l_2: length of bodies 1 and 2

l_{G2}: distance from point A to G_2

Kinetic Energy

$$E_{k1} = \frac{1}{2} \cdot J_1 \cdot \dot{\theta}_1^2 \tag{4.2.}$$

$$E_{k2} = \frac{1}{2} \cdot J_2 \cdot \dot{\theta}_2^2 + \frac{1}{2} \cdot m_2 \cdot |\overrightarrow{v_{G2}}|^2 \tag{4.3.}$$

Where $\overrightarrow{v_{G2}}$ states the velocity of G_2, therefore: $\overrightarrow{v_{G2}} = \frac{d\overrightarrow{OG_2}}{dt}$, with:

$$\overrightarrow{OG_2} = (l_1 \cdot \sin(\theta_1) + l_{G2} \cdot \sin(\theta_2)) \cdot \hat{\imath} + (l_1 \cdot \cos(\theta_1) + l_{G2} \cdot \cos(\theta_2)) \cdot \hat{\jmath} \tag{4.4.}$$

After computing the proper calculations:

$$|\overrightarrow{v_{G2}}|^2 = l_1^2 \cdot \dot{\theta}_1^2 + l_{G2}^2 \cdot \dot{\theta}_2^2 + 2 \cdot l_1 \cdot l_2 \cdot \dot{\theta}_1 \cdot \dot{\theta}_2 \cdot \cos(\theta_1 - \theta_2) \tag{4.5.}$$

Finally getting the total kinetic energy:

$$E_k = E_{k1} + E_{k2} =$$

$$= \frac{1}{2} \cdot J_1 \cdot \dot{\theta}_1^2 + \frac{1}{2} \cdot J_2 \cdot \dot{\theta}_2^2 + \frac{1}{2} \cdot m_2 \cdot (l_1^2 \cdot \dot{\theta}_1^2 + l_{G2}^2 \cdot \dot{\theta}_2^2 + 2 l_1 l_2 \dot{\theta}_1 \dot{\theta}_2 \cos(\theta_1 - \theta_2)) \quad (4.6.)$$

Potential Energy

$$E_{p1} = m_1 \cdot g \cdot l_{G1} \cdot \cos(\theta_1) \quad (4.7.)$$

$$E_{p2} = m_2 \cdot g \cdot (l_1 \cos(\theta_1) + l_{G2} \cos(\theta_2)) \quad (4.8.)$$

$$E_p = E_{p1} + E_{p2} =$$

$$= m_1 \cdot g \cdot l_{G1} \cdot \cos(\theta_1) + m_2 \cdot g \cdot (l_1 \cos(\theta_1) + l_{G2} \cos(\theta_2)) \quad (4.9.)$$

Applying Lagrange

$$L(\theta_1, \theta_2, \dot{\theta}_1, \dot{\theta}_2) = E_k - E_p \quad (4.10.)$$

The different derivatives need to be computed. For more commodity two of them will be renamed like follows:

$\frac{\partial L}{\partial \dot{\theta}_1} = A(\theta_1, \theta_2, \dot{\theta}_1, \dot{\theta}_2)$ and $\frac{\partial L}{\partial \dot{\theta}_2} = B(\theta_1, \theta_2, \dot{\theta}_1, \dot{\theta}_2)$

Then the partial derivatives are computed:

$$\frac{\partial A}{\partial t}(\theta_1, \theta_2, \dot{\theta}_1, \dot{\theta}_2) = \frac{\partial A}{\partial \theta_1} \cdot \dot{\theta}_1 + \frac{\partial A}{\partial \theta_2} \cdot \dot{\theta}_2 + \frac{\partial A}{\partial \dot{\theta}_1} \cdot \ddot{\theta}_1 + \frac{\partial A}{\partial \dot{\theta}_2} \cdot \ddot{\theta}_2 = \quad (4.11.)$$

$$= -m_2 l_1 l_{G2} \sin(\theta_1 - \theta_2) \dot{\theta}_1 \dot{\theta}_2 + m_2 l_1 l_{G2} \sin(\theta_1 - \theta_2) \dot{\theta}_2^2 + (J_1 + m_2 l_1^2) \ddot{\theta}_1 +$$

$$+ m_2 l_1 l_{G2} \cos(\theta_1 - \theta_2) \ddot{\theta}_2$$

$$\frac{\partial B}{\partial t}(\theta_1, \theta_2, \dot{\theta}_1, \dot{\theta}_2) = \frac{\partial B}{\partial \theta_1} \cdot \dot{\theta}_1 + \frac{\partial B}{\partial \theta_2} \cdot \dot{\theta}_2 + \frac{\partial B}{\partial \dot{\theta}_1} \cdot \ddot{\theta}_1 + \frac{\partial B}{\partial \dot{\theta}_2} \cdot \ddot{\theta}_2 = \quad (4.12.)$$

$$= -m_2 l_1 l_{G2} \sin(\theta_1 - \theta_2) \dot{\theta}_1^2 + m_2 l_1 l_{G2} \sin(\theta_1 - \theta_2) \dot{\theta}_1 \dot{\theta}_2 + m_2 l_1 l_{G2} \cos(\theta_1 - \theta_2) \ddot{\theta}_1 +$$

$$+ (J_2 + m_2 l_{G2}^2) \ddot{\theta}_2$$

Finally the derivatives with respect to the angles are computed.

$$\frac{\partial L}{\partial \theta_1} = -m_2 l_1 l_{G2} \sin(\theta_1 - \theta_2)\dot{\theta}_1 \dot{\theta}_2 + (m_1 l_{G1} + m_2 l_1) g \sin(\theta_1) \tag{4.13.}$$

$$\frac{\partial L}{\partial \theta_2} = m_2 l_1 l_{G2} \sin(\theta_1 - \theta_2)\dot{\theta}_1 \dot{\theta}_2 + m_2 l_{G2} g \sin(\theta_2) \tag{4.14.}$$

With the last four equations, it is possible to write Lagrange's equations.

$$0 = \frac{d}{dt}\left(\frac{\partial L}{\partial \dot{\theta}_1}\right) - \frac{\partial L}{\partial \theta_1} = \frac{\partial A}{\partial t} - \frac{\partial L}{\partial \theta_1} \tag{4.15.}$$

$$\tau = \frac{d}{dt}\left(\frac{\partial L}{\partial \dot{\theta}_2}\right) - \frac{\partial L}{\partial \theta_2} = \frac{\partial B}{\partial t} - \frac{\partial L}{\partial \theta_2} \tag{4.16.}$$

4.2.1. State space equations

In order to simplify the equations above a set of constants have been defined, leading to the following equations:

$$0 = A_1 \ddot{\theta}_1 + A_2 \ddot{\theta}_2 \cos(\theta_1 - \theta_2) + A_3 \dot{\theta}_2^2 \sin(\theta_1 - \theta_2) - A_4 \sin(\theta_1) \tag{4.17.}$$

$$\tau = B_1 \ddot{\theta}_1 \cos(\theta_1 - \theta_2) + B_2 \ddot{\theta}_2 - B_3 \dot{\theta}_1^2 \sin(\theta_1 - \theta_2) - B_4 \sin(\theta_2) \tag{4.18.}$$

Where the constants have the values below:

$$A_1 = J_1 + m_2 l_1^2 \qquad B_1 = m_2 l_1 l_{G2}$$

$$A_2 = m_2 l_1 l_{G2} \qquad B_2 = J_2 + m_2 l_{G2}^2$$

$$A_3 = A_2 = m_2 l_1 l_{G2} \qquad B_3 = m_2 l_1 l_{G2}$$

$$A_4 = (m_1 l_{G1} + m_2 l_1) g \qquad B_4 = m_2 l_{G2} g$$

Isolating $\ddot{\theta}_1$ from equation 4.17,

$$\ddot{\theta}_1 = \frac{1}{-A_1}\left(A_2 \ddot{\theta}_2 \cos(\theta_1 - \theta_2) + A_3 \dot{\theta}_2^2 \sin(\theta_1 - \theta_2) - A_4 \sin(\theta_1)\right) \tag{4.19.}$$

Then substituting it in equation 4.18, the relation for $\ddot{\theta}_2$is obtained.

$$\ddot{\theta}_2 = \frac{-\frac{B_1 A_3}{A_1}\dot{\theta}_2^2 \sin(\theta_1-\theta_2)\cos(\theta_1-\theta_2) + \frac{B_1 A_4}{A_1}\sin(\theta_1)\cos(\theta_1-\theta_2)}{\frac{B_1}{A_1}A_2\cos^2(\theta_1-\theta_2) - B_2} \ldots$$

$$\ldots \frac{-B_3\dot{\theta}_1^2 \sin(\theta_1-\theta_2) - B_4\sin(\theta_1) - \tau}{\frac{B_1}{A_1}A_2\cos^2(\theta_1-\theta_2) - B_2} \tag{4.20.}$$

The same procedure is followed to obtain the last relationship ($\ddot{\theta}_1$).

$$\ddot{\theta}_2 = \frac{1}{-A_2\cos(\theta_1-\theta_2)}\left(A_1\ddot{\theta}_1 + A_3\dot{\theta}_2^2\sin(\theta_1-\theta_2) - A_4\sin(\theta_1)\right) \tag{4.21.}$$

Finally,

$$\ddot{\theta}_1 = \frac{B_2A_3\dot{\theta}_2^2\sin(\theta_1-\theta_2) - B_2A_4\sin(\theta_1) + B_3A_2\dot{\theta}_1^2\sin(\theta_1-\theta_2)\cos(\theta_1-\theta_2)}{B_1A_2\cos^2(\theta_1-\theta_2) - B_2A_1} \ldots \tag{4.22.}$$

$$\ldots \frac{+B_4A_2\sin(\theta_2)\cos(\theta_1-\theta_2) + A_2\cos(\theta_1-\theta_2)\tau}{B_1A_2\cos^2(\theta_1-\theta_2) - B_2A_1}$$

At this point the system is in a state-space form.

$$\dot{X} = F\left(\theta_1, \theta_2, \dot{\theta}_1, \dot{\theta}_2\right) + G(\tau) \tag{4.23.}$$

$$F\left(\theta_1, \theta_2, \dot{\theta}_1, \dot{\theta}_2\right) = \begin{bmatrix} 0 & 0 & 1 & 0 \\ 0 & 0 & 0 & 1 \\ f_1(\theta_1, & \theta_2, & \dot{\theta}_1, & \dot{\theta}_2) \\ f_2(\theta_1, & \theta_2, & \dot{\theta}_1, & \dot{\theta}_2) \end{bmatrix} \tag{4.24.}$$

$$G(\tau) = \begin{bmatrix} 0 \\ 0 \\ g_1(\tau) \\ g_2(\tau) \end{bmatrix} \tag{4.25.}$$

The non-linear model is ready to be implemented; however, in order to solve the control system the linearization is needed.

4.3. Linear model

In order to continue with the project, a linear model is needed for the design of the LQR controller. There are different linearization techniques, while A. Tenerelli decided to use equivalences such as $\cos(\theta) = 1$ or $\sin(\theta) = \theta$ assuming small angles values, in this project Taylor's expansion will be used.

$$\dot{X} = \dot{X}_{eq} + A \cdot \Delta X + B \cdot \Delta U \tag{4.26.}$$

With A and B defined as the Jacobian of matrixes F and G respectively as stated in equations 4.24 and 4.25.

$$A = \begin{bmatrix} 0 & 0 & 1 & 0 \\ 0 & 0 & 0 & 1 \\ \frac{\partial f_1}{\partial \theta_1} & \frac{\partial f_1}{\partial \theta_2} & \frac{\partial f_1}{\partial \dot{\theta}_1} & \frac{\partial f_1}{\partial \dot{\theta}_2} \\ \frac{\partial f_2}{\partial \theta_1} & \frac{\partial f_2}{\partial \theta_1} & \frac{\partial f_2}{\partial \dot{\theta}_1} & \frac{\partial f_2}{\partial \dot{\theta}_2} \end{bmatrix}_{[\theta_{1eq}, \theta_{2eq}, \dot{\theta}_{1eq}, \dot{\theta}_{2eq}]^T} \tag{4.27.}$$

$$B = \begin{bmatrix} 0 \\ 0 \\ \frac{\partial g_1}{\partial \tau} \\ \frac{\partial g_2}{\partial \tau} \end{bmatrix}_{\tau_{eq}} \tag{4.28.}$$

According to the chosen model the equilibrium state ($\dot{X}_{eq}$) would be null both angles and velocities, therefore the term with the equilibrium condition can be deleted leading to the final expression in equation 4.27.

$$\dot{X} = A \cdot \Delta X + B \cdot \Delta U \tag{4.29.}$$

As the computations are complexes, all the partial derivatives have been performed with Maple16, including the evaluation in the equilibrium point. The full computations can be found in the Annex D with all the results.

4.4. Linear Quadratic Regulation

To design the controller, the Linear-quadratic regulator (LQR) i used. It is also known as the optimal control as its algorithms reduce the amount of work performed by the control system. It is a feedback controller and an important part of the solution to the Linear-quadratic-Gaussian problem.

The name itself states its use; linear because the main idea is to regulate a dynamic system described by a set of linear differential equations and quadratic because the cost is described by a quadratic function. This situation itself is called the LQ problem. The cost function is the following:

$$\frac{1}{2}\int_{t_0}^{t_f}(x^T Q\ x + u^T R\ u)\ d\tau \tag{4.30.}$$

Where: x is the state vector
u is the input vector
Q is a non-negative defined matrix
R is a positive defined matrix

To use the Matlab function LQR,the matrixes *Q* and *R* have to be defined. This definition has to be performed depending on the kind of control that is wanted. However, their values will have major consequences in the control. A large value of *Q* will translate into a quick stabilitzation, while if the values of *R* are the ones accentuated then the effect of the controller will be smaller, and therefore it will be a small realimentazion. Different parameters will lead to different results. Once, all the data is defined, the Matlab function will retourn a vector (K), equivalent to the weights of the function that will be implemented in the controller.

4.5. Force Analysis

In order to get a full analysis of the movement, the forces between the body 0-A and the floor are computed (Fig. 4.4).

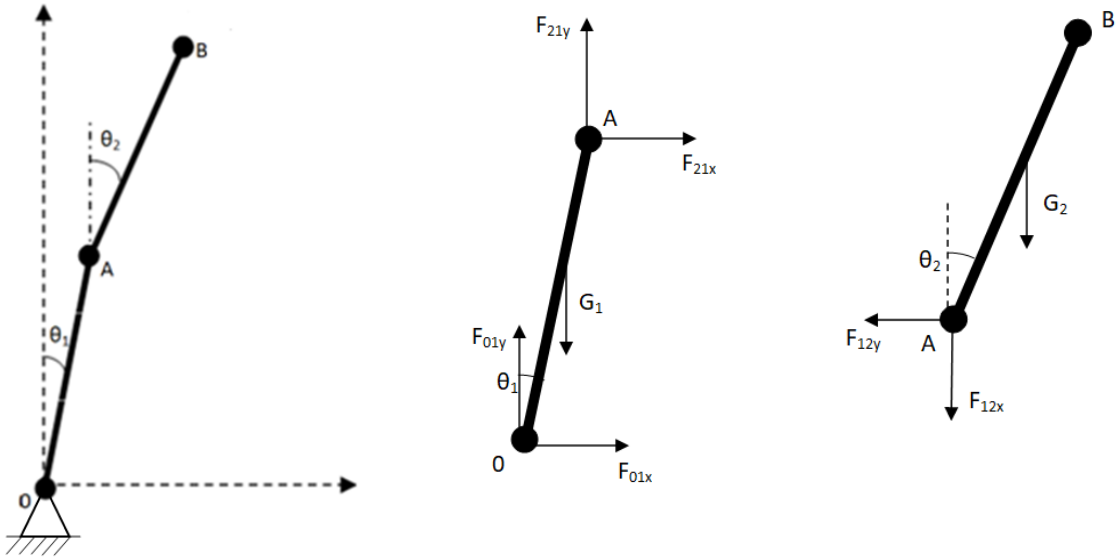

Fig. 4.4. *Diagram of the model (left), body 0-A force analysis (center) and body A-B force analysis (right).*

Kinematics

First, the body 0-A is analyzed leading to the following position, velocity and acceleration vectors:

Position

$$r_{G1} = x_{G1} \cdot \hat{\imath} + y_{G1} \cdot \hat{\jmath}$$

$$x_{G1} = l_{G1} \cdot \sin(\theta_1) \qquad (4.31.)$$

$$y_{G1} = l_{G1} \cdot \cos(\theta_1)$$

Velocity

$$v_{G1} = \dot{r}_{G1} = \dot{x}_{G1} \cdot \hat{\imath} + \dot{y}_{G1} \cdot \hat{\jmath}$$

$$\dot{x}_{G1} = l_{G1} \cdot \dot{\theta}_1 \cos(\theta_1) \qquad (4.32.)$$

$$\dot{y}_{G1} = -l_{G1} \cdot \dot{\theta}_1 \sin(\theta_1)$$

Acceleration

$$a_{G1} = \ddot{r}_{G1} = \ddot{x}_{G1} \cdot \hat{\imath} + \ddot{y}_{G1} \cdot \hat{\jmath}$$

$$\ddot{x}_{G1} = l_{G1}\ddot{\theta}_1 \cos(\theta_1) - l_{G1}\dot{\theta}_1^2 \sin(\theta_1) \qquad (4.33.)$$

$$\ddot{y}_{G1} = -l_{G1}\ddot{\theta}_1 \sin(\theta_1) - l_{G1}\dot{\theta}_1^2 \cos(\theta_1)$$

Then the second body A-B is analyzed like follows:

Position

$$r_{G2} = x_{G2} \cdot \hat{\imath} + y_{G2} \cdot \hat{\jmath}$$

$$x_{G2} = l_1 \cdot \sin(\theta_1) + l_{G2} \cdot \sin(\theta_2) \quad (4.34.)$$

$$y_{G2} = l_1 \cdot \cos(\theta_1) + l_{G2} \cdot \cos(\theta_1)$$

Velocity

$$v_{G2} = \dot{r}_{G2} = \dot{x}_{G2} \cdot \hat{\imath} + \dot{y}_{G2} \cdot \hat{\jmath}$$

$$\dot{x}_{G2} = l_1 \cdot \dot{\theta}_1 \cdot \cos(\theta_1) + l_{G2} \cdot \dot{\theta}_2 \cdot \cos(\theta_1) \quad (4.35.)$$

$$\dot{y}_{G2} = -l_1 \cdot \dot{\theta}_1 \cdot \sin(\theta_1) - l_{G2} \cdot \dot{\theta}_2 \cdot \sin(\theta_2)$$

Acceleration

$$a_{G2} = \ddot{r}_{G2} = \ddot{x}_{G2} \cdot \hat{\imath} + \ddot{y}_{G2} \cdot \hat{\jmath}$$

$$\ddot{x}_{G2} = l_1\ddot{\theta}_1 \cos(\theta_1) - l_1\dot{\theta}_1^2 \sin(\theta_1) + l_{G2}\ddot{\theta}_2 \cos(\theta_2) - l_{G2}\dot{\theta}_2^2 \sin(\theta_2) \quad (4.36.)$$

$$\ddot{y}_{G2} = -l_1\ddot{\theta}_1 \sin(\theta_1) - l_1\dot{\theta}_1^2 \cos(\theta_1) - l_{G2}\ddot{\theta}_2 \sin(\theta_2) - l_{G2}\dot{\theta}_2^2 \cos(\theta_2)$$

Once the position, velocity and acceleration vectors have been obtained for both bodies the relationship between both of them can be obtained:

Link 1: $$m_1 \cdot a_{G1} = F_{01} + F_{21} + G_1$$

x-axis: $$m_1 \cdot \ddot{x}_{G1} = F_{01x} + F_{21x} \quad (4.37.)$$

y-axis: $$m_1 \cdot \ddot{y}_{G1} = F_{01y} + F_{21y} - m_1 g$$

Link 2: $$m_2 \cdot a_{G2} = F_{12} + G_2$$

x-axis: $$m_2 \cdot \ddot{x}_{G2} = -F_{12x} \rightarrow m_2 \cdot \ddot{x}_{G2} = F_{21x} \quad (4.38.)$$

y-axis: $$m_2 \cdot \ddot{y}_{G2} = -F_{12y} - m_2 g \rightarrow m_2 \cdot \ddot{y}_{G2} = F_{21y} - m_2 g$$

As the variables $\theta_1, \theta_2, \dot{\theta}_1, \dot{\theta}_2$ are already known and computed by the Matlab program (Annex A), it is a linear system of equations. In order to add it to the program, it is solved for both F_{01x} and F_{01y}

$$F_{01x} = m_1 \cdot \ddot{x}_{G1} - F_{21x} = m_1 \cdot \ddot{x}_{G1} - m_2 \cdot \ddot{x}_{G2} \quad (4.39.)$$

$$F_{01y} = m_1 \cdot \ddot{y}_{G1} - F_{21y} + m_1 g = m_1 \cdot \ddot{y}_{G1} - m_2 \cdot \ddot{y}_{G2} - m_2 g + m_1 g \quad (4.40.)$$

4.6. Updating the model

Once the controller is implemented with the chosen biomechanical parameters, a new step forward is taken. A more realistic model is designed by incorporating an elastic or stiffness element equivalent to the hip joint. To do so, a new background check has been done on all the joints, to try to find the more appropriate value for the elasticity constant.

4.6.1. Background

In 1997 R. Riener and T. Edrich wrote their paper on "*Passive elastic joint moments in the lower extremity"* [14] focusing on the passive elastic joint properties while taking into account the influence of other joints. As joints' behavior depends on the muscles and other tissues' mechanical properties, a non-linear elastic relationship was taken into account and approximated by an exponential function of joint angles. [14] In this case, measurements were performed at the ankle, knee and hip joint with the set up shown in Fig. 4.5.

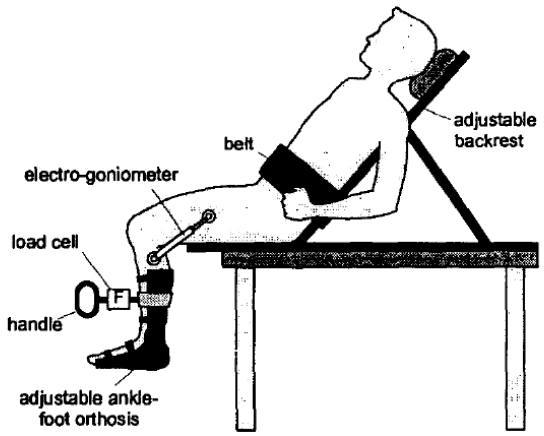

Fig. 4.5. *Experimental setup for knee measurements with defined ankle and hip joint positions. [18]*

Different measurements were performed in health subjects. The total joint moment can be divided in different components; the passive elastic joint moment (M_{elast}), the dissipative passive moment (M_{diss}), the influence of active force (M_{act}), the gravitational moment (M_{grav}) and finally, the dynamic moment (M_{dyn}) [14].

$$M_{tot} = M_{elast} + M_{diss} + M_{act} + M_{grav} + M_{dyn} \quad (4.41.)$$

However, by following the proper methodology the effects of some of them were neglected. For example, by moving the subject's leg quasi-statically, both the dynamic and dissipative moments were neglected. As the study focuses on the passive component, the subject was not allowed to take an active role, and therefore the active moment could also be neglected, leading to equation 4.42.

$$M_{tot} = M_{elast} + M_{grav} \rightarrow M_{elast} = M_{tot} - M_{grav} \quad (4.42.)$$

Following the example of previous research, exponential functions were used to approximate the elastic moment. However, Riener and Edrich took into consideration the influence of other joints leading to the following equation that considers the coupling effects.

$$M_{elast} = \exp\left(c_1 + c_2\varphi + c_3\varphi_{prox} + c_4\varphi_{dist}\right) - \quad (4.43.)$$

$$\exp\left(c_5 + c_6\varphi + c_7\varphi_{prox} + c_8\varphi_{dist}\right) + c_9$$

where: φ is the joint angle
φ_{prox} is the angle of the proximal joint
φ_{dist} is the angle of the distal joint
$c_1 - c_9$ are constants determined with an iterative least square procedure

After analyzing the results, different observations could be made. The results leaded to the fact that the knee joint is not significantly influenced by the ankle, while the hip angle has a strong effect on it. Looking to the results of the hip joint, it could be seen that due to the existence of the hip flexors and extensors, the knee joint angle had a huge influence on it.

All this information allows putting into perspective the project itself. In this project the knee joint is blocked, as legs are considered as a single bloc, and due to the simplicity of the model, the approximation is performed by the product of a constant and the relative angle of the joint.

In 1999, R. Aissaoui and J. Dausereau reviewed the existent literature regarding the analysis of sit-to-stand task in their paper "*Biomechanical analysis and modelling of sit to stand task: a literature review"*. The purpose was to do an overview of the state of the art at that point focusing in the sit-to-stand transfer in elderly population.

Sitting and standing are two tasks that are often done without paying attention, but as the population ages the mobility is usually reduced. There is a wide range of reasons that may cause difficulties in this apparently simple task such as progressive conditions like arthritis. Along all the literature the sit-to-strand process (also known as STS) has been defined and divided in different

phases. The first studies identified it in two distinct phases, to move later on to three phases; the initiation phase, the seat unloading phase and the lift. However, in 1997, Kralk, A., Jaeger, R.J. and Munih, M. defined the movement in five different phases as explained in their paper "*Analysis of standing up and sitting down in humans: definitions and normative data presentation"* (Fig. 4.6).

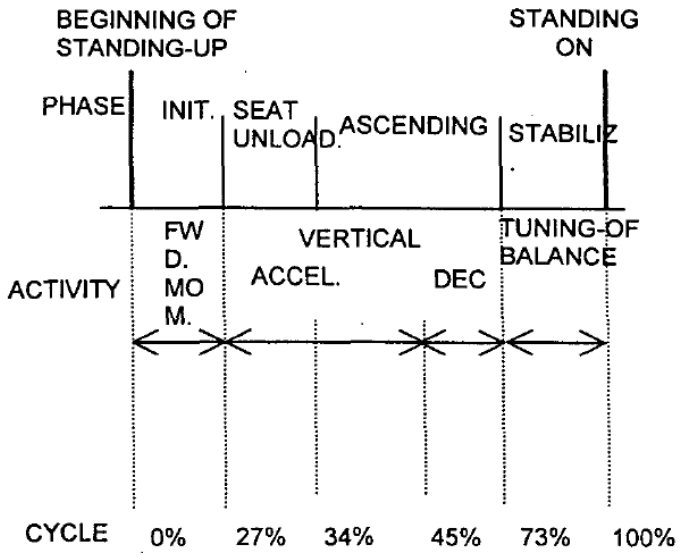

Fig. 4.6. *Sit to stand cycle phase diagram [1].*

This kind of terminology allows defining each stage; the beginning (0%) states for the ground reaction force, then the 27% is the starting of the standing face that leads to an acceleration and deceleration periods (45% and 73% respectively). Finally the last stage (100%) is the stabilization in standing position.

Different strategies of transferring from sit-to-stand are studied and reviewed, but the review done by Aissaoui and Dansereau does not include constant values for the approximation of the joint behavior. Therefore, even if it is important to understand how the movement works, the data reliable for the project is not stated.

In 2003 a team formed by J. Van der Spek, P. Veltink, H. Hermens, B. Koopman and H.Boom published their research on the influence of supplementary hip joint stiffness and a stabilizing model for paraplegic subjects. On the one hand in the article "*Static and Dynamic Evaluation of the Influence of Supplementary Hip-joints Stiffness on Crutch-Supported Paraplegic Stance"* [11] and on the other hand, "*A model-Based Approach to Stabilizing Crutch Supported Paraplegic Standing by Artificial Hip Joint Stiffness"* [10]. Both articles give a significant amount of information regarding the stiffness of the hip-joint and its effects when testing its value following the procedure in Fig. 4.7.

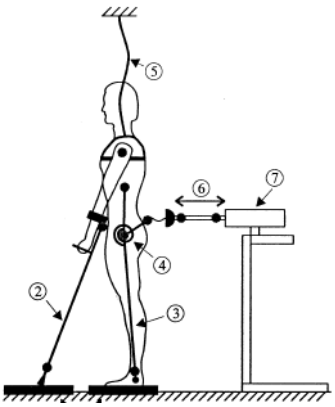

Fig. 4.7. *Schematic representation of the experimental setup [11].*

When testing different values for the stiffness coefficient, different springs were tested with the following values:

Spring	Stiffness [$^{Nm}/_{rad}$]
K_0	0
K_1	41
K_2	68
K_3	126
K_4	208
K_5	313

Table 4.1. *Values of the stiffness of each spring [11]*

After testing five different subjects with each spring, the minimum level of stiffness necessary to enable each subject to stand was found. In average, the level needed was 68 N.m/rad and therefore the spring number 2 (K_2).

In the second article the double inverted pendulum model was modified to add the crutches, as it is the assistance tool needed by the paraplegic subjects (Fig. 4.8).

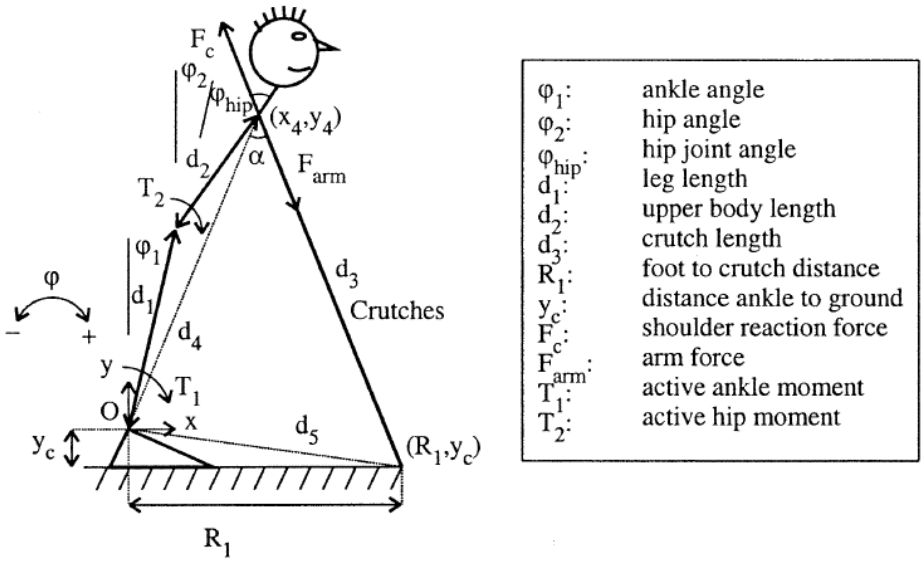

Fig. 4.8. *Schematic representation of the model [11].*

By using Lagrange's method, the mathematical model was obtained and it allowed to compare the hip stiffness to the ankle one.

Both articles give information regarding the hip stiffness importance and influence. However, a sagittal plane approach was followed, while a frontal approach is being studied in this project. Therefore, the values used by the research cannot be directly used.

In 2005 the team from the Institute for Rehabilitation of Slovenia formed by A. Olensek and Z. Matjacic shared their study "*Further Steps Toward More Human-like Passive Bipedal Walking Robots*" in the International Conference on Robotics and Automation. In the paper a two-legs mechanical structure is described. The model incorporates the basic joints; ankle, knee and hip. The implemented model is capable of having a stable walking performance with null or reduced energy consumption.

Even though some researchers have always avoided lateral stability issues by designing a mechanism where the outer legs function as crutches, in this case, a human-like mechanism was designed. Three hinged joints are present (ankle, knee and hip) resulting in a three pieces leg-design.

First of all, the gait cycle is the sequence of movement corresponding to taking two steps. Therefore it starts with one foot that was in contact to the ground lifts, until that same foot goes back to the foot.

In the following picture (Fig. 4.9), the drawing of the design is shown, and so it is a picture of the model already built.

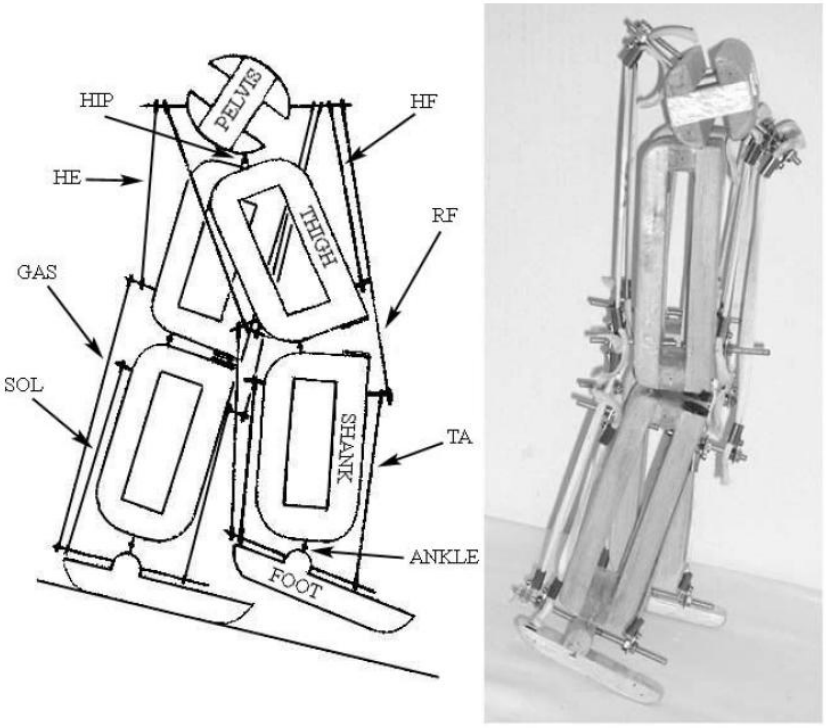

Fig. 4.9. *Schematics and photograph of a biped physical model [20].*

Regarding the elastic components, Olensek and Matjacic state that the gait cycle elastic strings have to ensure gait stability. Therefore, they have to offer support during stance and leg advancement during swing, but also they have to maintain stable lateral swaying. It is important to understand that for a natural step movement elastic elements are critical. Therefore, in the appropriate extent they should be included when designing a model equivalent to the human body. However, no specific parameters are given during the article.

In 2008, the team conducted by S.Pejhan, F.Farahmand and M.Parnianpour wrote their paper in "*Design Optimization of an Above-Knee Prosthesis Based on the Kinematics of Gait*". A mathematical modeling approach was used to analyze the dynamics of an above-knee prosthesis during the complete gait cycle. Regarding the method, it included three rigid segments; thigh, shank and food, equivalent to a two-dimensional model of an amputee leg with prosthesis. Each component was connected with revolute joints at the knee and angle (Fig. 4.10).

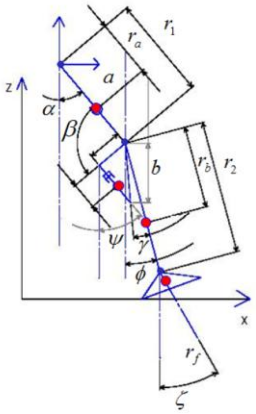

Fig. 4.10. *Model of amputee leg system [17].*

The mathematical model was developed, putting strong attention to the bond between foot and floor. Therefore, a penetration contact model considering two contact points; heel and mid point, was used. The main parameters can be found in Table 4.2

Parameter	Value
Spring coefficient	2× e+6 (N/m)
Spring exponent	2.2
Damping coefficient	1500 (Ns/m)
Damping penetration	1 (mm)
Friction coefficient	0.4

Table 4.2. *Foot-ground contact model parameters [17].*

On the other hand, the knee elastic controller was designed as a spring in the proper configuration (Fig. 4.11).

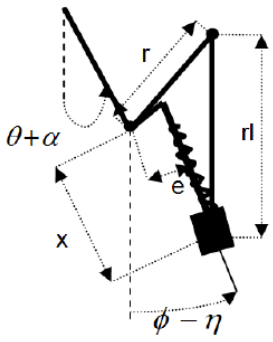

Fig. 4.11. *Knee elastic controller [17.]*

The knee moment produced by the designed controller follows was given by the following set of mathematical relations. [17]

$$
\begin{aligned}
&K1 = \{r_r \sin(\xi - \theta - \alpha + \phi - \eta) - [e - r_r \sin(\xi - \theta - \alpha + \phi - \eta)]r_r \\
&\cos(\xi - \theta - \alpha + \phi - \eta) / R\}kx \\
&where \\
&R = [r_l^2 - [\theta - r_r \sin(\xi - \theta - \alpha + \phi - \eta)]^2 \\
&x = -r_r \cos(\xi - \theta - \alpha + \phi - \eta)R - l_0 \\
&l_0 = l + unstretched \;\; length
\end{aligned}
\qquad (4.44.)
$$

Being the different constants and parameters defined in Table 4.3:

Parameter	Value	Unit
Angle between Hip-knee and crank of spring mechanism : ξ	80	deg
Length of the spring mechanism coupler: r_l	18	mm
Length of the spring mechanism crank: r_r	40	mm
Offset of the spring mechanism: e	0.04	
Distance from upper attachment point of the controller of the knee joint	3.1	mm
Distance from lower attachment point of the controller of the knee joint	2.1	mm
Angle between knee-ankle and knee- shank cg: γ	0	deg
Angle between hip-knee and knee- upper attachment point: β	π/2	deg
Distance from upper attachment point to cm of controller: r_c	10.2	mm
Mass of the controller	0.6	Kg
Moment of inertia about center of mass	0.0085	Kg/m^3

Table 4.3. *Biomechanical parameters [17].*

Regarding the results, the optimum values for stiffness of the elastic controller weas found to be 1980 N/m, while the damping coefficient of the hydraulic controller of prosthetic knee obtained was 0.7 Kg/s. Moreover, for the ankle joint, the torsion stiffness and damping coefficient were 5,35 Kg/s and 10,5 N·cm/rad, respectively [17].

Recent research conducted by the New Jersey Institute of Technology University Heights focused on identifying values for the non-linear passive knee joint stiffness. In their article "*Assessment of Passive Knee Stiffness and Set Point"* the Wartenberg Pendulum Knee Test was used. The passive stiffness moment is defined by the product of the passive stiffness constant (K_p) and the relative angle of the

joint. After the experiment and modeling was performed the values differed significantly from subject to subject (Table 4.4).

#	Age (Year)	Sex	Weight (Kg)	Height (cm)	K_P (N-m)/rad Mid-range	K_P (N-m)/rad Extremes	θ_p rad
1	30	M	64.4	175.3	**5.2**	**13.1**	**0.31**
2	26	F	44.5	157.5	**1.9**	**3.5**	**0.19**
3	21	M	99.8	168.9	**2.1**	**4.9**	**0.33**
4	20	M	92.9	171.5	**6.7**	**11.2**	**0.31**
5	27	M	83.7	180.3	**1.7**	**3.5**	**0.25**

Table 4.4. *Values of K_p of the knee and physical characteristics of the subjects [3].*

The authors explained the significant differences between the stiffness coefficients with the physiological differences between the subjects of the study. However, they conclude that the stiffness value does not follow a linear behavior.

In 2013 a team of researchers of the Purdue University in the USA performed a study in "*Dynamic stability of a human standing on a balance board".* In it a sagittal approach was followed.

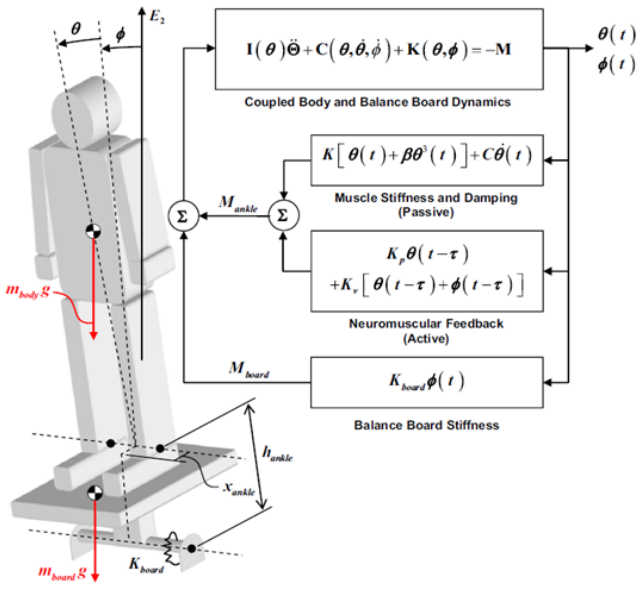

Fig. 4.12. *Diagram of posture on a !-DOF balance board with forces and correlating moments (left). Block diagram of the postural control system (right). [12]*

To design the model, different biomechanical parameters were used. Regarding the moment at the ankle it was determined as a function of time, depending also on the angles and different coefficients as shown below:

$$M_{ankle}\ (t) = K[\theta(t) + \beta\theta^3(t)] + C\dot{\theta}(t) \tag{4.45.}$$

where: K is the linear muscle stiffness
β is the ratio of passive cubic nonlinear muscle stiffness to passive linear muscle stiffness
C is the linar muscle damping

As it has been seen this far with the review of all the different studies, there is a wide range of values, a short example of some of them is given in the article as follows (Table 4.5).

Author	K^{cr} [N m]	k $[\frac{\text{N m}}{\text{rad}}]$	C $[\frac{\text{N m s}}{\text{rad}}]$
Asai et al.(2009)	588.60	470.88	4.00
Maurer and Peterka(2005)	648.64	584.43	171.89
Peterka (2002)	732.19	91.67	24.64
Vette et al. (2010)	713.81	521.00	5.00
This Paper	659.92	593.93	131.98

Table 4.5. *Commonly used postural parameters for similar models [12]*

After analyzing the state of the art regarding the stiffness of the different joints, it can be said that values differ from model to model and subject to subject, however all research follow a sagittal plane approach. Therefore, the parameters found cannot be applied to the project directly, but they are useful to approximate the chosen value.

The chosen value has been obtained with both an approximation taking into account the range of motion of the hip-joint in a frontal approach and an empirical research when simulating the model finding the maximum value for the elastic coefficient that allowed the system to work properly.

4.6.2. Computations

To obtain the new equations that describe the model, Lagrange's method has been used again. In this case a momentum has been also added to the hip joint (Fig. 4.13).

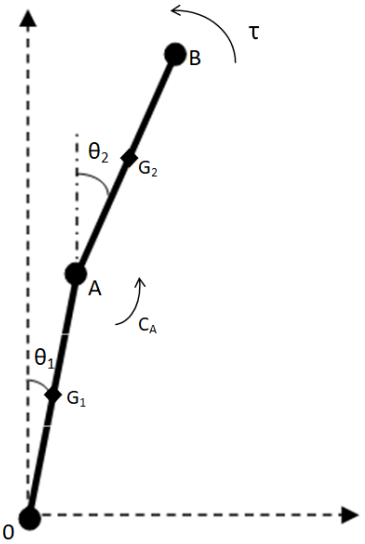

Fig. 4.13. *Model analyzed with the momentum in the hip joint due to the elastic component (C_A)*

Lagrange's equations are the following:

$$C_A = \frac{d}{dt}\left(\frac{\partial L}{\partial \dot{\theta}_1}\right) - \frac{\partial L}{\partial \theta_1} = \frac{\partial A}{\partial t} - \frac{\partial L}{\partial \theta_1} \tag{4.46.}$$

$$\tau = \frac{d}{dt}\left(\frac{\partial L}{\partial \dot{\theta}_2}\right) - \frac{\partial L}{\partial \theta_2} = \frac{\partial B}{\partial t} - \frac{\partial L}{\partial \theta_2} \tag{4.47.}$$

Being the derivatives, the same ones used for the initial model, C_A the torque in the hip and τ the external perturbation.

In order to simplify the equations above a new set of constants have been defined leading to equations 4.48 and 4.49.

$$C_A = A_1\ddot{\theta}_1 + A_2\ddot{\theta}_2\cos(\theta_1 - \theta_2) + A_3\dot{\theta}_2^2\sin(\theta_1 - \theta_2) - A_4\sin(\theta_1) \tag{4.48.}$$

$$\tau = B_1\ddot{\theta}_1\cos(\theta_1 - \theta_2) + B_2\ddot{\theta}_2 - B_3\dot{\theta}_1^2\sin(\theta_1 - \theta_2) - B_4\sin(\theta_2) \tag{4.49.}$$

Where the constants have the following values:

$$A_1 = I_1 + m_2 l_1^2 \qquad B_1 = m_2 l_1 l_{G2}$$

$$A_2 = m_2 l_1 l_{G2} \qquad B_2 = I_2 + m_2 l_{G2}^2$$

$$A_3 = A_2 = m_2 l_1 l_{G2} \qquad B_3 = m_2 l_1 l_{G2}$$

$$A_4 = (m_1 l_{G2} + m_2 l_1) g \qquad B_4 = m_2 l_{G2} g$$

Isolating $\ddot{\theta}_1$ from equation 4.38.

$$\ddot{\theta}_1 = \frac{1}{-A_1}\left(A_2 \ddot{\theta}_2 \cos(\theta_1 - \theta_2) + A_3 \dot{\theta}_2^2 \sin(\theta_1 - \theta_2) - A_4 \sin(\theta_1) - C_A\right) \tag{4.50.}$$

Then substituting it in equation 4.39, $\ddot{\theta}_2$is obtained.

$$\ddot{\theta}_2 = \frac{-\frac{B_1 A_3}{A_1}\dot{\theta}_2^2 \sin(\theta_1 - \theta_2)\cos(\theta_1 - \theta_2) + \frac{B_1 A_4}{A_1}\sin(\theta_1)\cos(\theta_1 - \theta_2)}{\frac{B_1}{A_1}A_2 \cos^2(\theta_1 - \theta_2) - B_2} \ldots$$

$$\ldots \frac{-B_3 \dot{\theta}_1^2 \sin(\theta_1 - \theta_2) - B_4 \sin(\theta_1) - \tau - \frac{B_1}{A_1} C_A \cos(\theta_1 - \theta_2)}{\frac{B_1}{A_1}A_2 \cos^2(\theta_1 - \theta_2) - B_2} \tag{4.51.}$$

The same procedure is followed to obtain the last state equation ($\ddot{\theta}_1$).

$$\ddot{\theta}_2 = \frac{1}{-A_2 \cos(\theta_1 - \theta_2)}\left(A_1 \ddot{\theta}_1 + A_3 \dot{\theta}_2^2 \sin(\theta_1 - \theta_2) - A_4 \sin(\theta_1) - C_A\right) \tag{4.52.}$$

Finally,

$$\ddot{\theta}_1 = \frac{B_2 A_3 \dot{\theta}_2^2 \sin(\theta_1 - \theta_2) - B_2 A_4 \sin(\theta_1) + B_3 A_2 \dot{\theta}_1^2 \sin(\theta_1 - \theta_2)\cos(\theta_1 - \theta_2)}{B_1 A_2 \cos^2(\theta_1 - \theta_2) - B_2 A_1} \ldots \tag{4.53.}$$

$$\ldots \frac{+B_4 A_2 \sin(\theta_2)\cos(\theta_1 - \theta_2) + A_2 \cos(\theta_1 - \theta_2)\tau - B_2 C_A}{B_1 A_2 \cos^2(\theta_1 - \theta_2) - B_2 A_1}$$

Once the non-linear model is obtained, the linearization is performed using Taylor's method in order to design the new controller.

$$\dot{X} = \dot{X}_{eq} + A \cdot \Delta X + B \cdot \Delta U \tag{4.54.}$$

$$A = \begin{bmatrix} 0 & 0 & 1 & 0 \\ 0 & 0 & 0 & 1 \\ \frac{\partial f_1}{\partial \theta_1} & \frac{\partial f_1}{\partial \theta_2} & \frac{\partial f_1}{\partial \dot{\theta}_1} & \frac{\partial f_1}{\partial \dot{\theta}_2} \\ \frac{\partial f_2}{\partial \theta_1} & \frac{\partial f_2}{\partial \theta_1} & \frac{\partial f_2}{\partial \dot{\theta}_1} & \frac{\partial f_2}{\partial \dot{\theta}_2} \end{bmatrix}_{[\theta_{1eq}, \theta_{2eq}, \dot{\theta}_{1eq}, \dot{\theta}_{2eq}]^T} \tag{4.55.}$$

$$B = \begin{bmatrix} 0 \\ 0 \\ \frac{\partial g_1}{\partial \tau} \\ \frac{\partial g_2}{\partial \tau} \end{bmatrix}_{\tau_{eq}} \tag{4.56.}$$

The derivatives have been computed with Maple16 and can be found in the Annex D.

4.7. Non-linear control

In order to reach a wider understanding on the control system a new approach is followed. A non-linear control is developed based on an energy approach and the passivity properties of the system [16]. By using a non-linear control law there is no need for the linearization as LQR method is avoided.

Fantoni, I., Lozano, R. and Spong, M.W. studied a non-linear controller for a Pendubut system. Instead of using partial feedback linearization techniques and the linear quadratic regulator, an energy balance based controller was studied. Applying the methodology to our initial system, the following controller is obtained.

4.7.1. Computations

Using the already existing original system, the following matrixes and constants are defined:

$$D(\theta)\ddot{\theta} + C\left(\theta, \dot{\theta}\right)\dot{\theta} + g(\theta) = \tau \tag{4.57.}$$

$$D(\theta) = \begin{bmatrix} Q_1 & Q_2 \cdot \cos(\theta_1 - \theta_2) \\ Q_2 \cdot \cos(\theta_1 - \theta_2) & Q_4 \end{bmatrix} \tag{4.58.}$$

$$C\left(\theta, \dot{\theta}\right) = Q_2 \cdot \sin(\theta_1 - \theta_2) \begin{bmatrix} 0 & \dot{\theta}_2 \\ \dot{\theta}_2 & 0 \end{bmatrix} \tag{4.59.}$$

$$g(\theta) = \begin{bmatrix} -Q_3 \cdot g \cdot \sin(\theta_1) \\ -Q_5 \cdot g \cdot \sin(\theta_2) \end{bmatrix} \tag{4.60.}$$

$$\ddot{\theta} = \begin{bmatrix} \ddot{\theta}_1 \\ \ddot{\theta}_2 \end{bmatrix} \qquad \dot{\theta} = \begin{bmatrix} \dot{\theta}_1 \\ \dot{\theta}_2 \end{bmatrix} \qquad \tau = \begin{bmatrix} 0 \\ \tau \end{bmatrix} \tag{4.61.}$$

$$Q_1 = A_1 = J_1 + m_2 \cdot l_1^2$$

$$Q_2 = A_2 = A_3 = B_1 = B_3 = m_2 \cdot l_1 \cdot l_{G2}$$

$$Q_3 = \frac{A_4}{g} = m_1 \cdot l_{G1} + m_2 \cdot l_1 \qquad (4.62.)$$

$$Q_4 = B_2 = J_2 + m_2 \cdot l_{G2}^2$$

$$Q_5 = \frac{B_4}{g} = m_2 \cdot l_{G2}$$

The total kinetic (E_{KT}) and potential (E_{PT}) energy is defined as follows:

$$E_{KT} = \frac{1}{2} \cdot J_1 \cdot \dot{\theta}_1^2 + \frac{1}{2} \cdot J_2 \cdot \dot{\theta}_2^2 + \frac{1}{2} \cdot m_2 \cdot \left(l_1^2 \cdot \dot{\theta}_1^2 + l_{G2}^2 \cdot \dot{\theta}_2^2 + 2 \cdot l_1 \cdot l_{G2} \cdot \dot{\theta}_1 \cdot \dot{\theta}_2 \cdot \cos(\theta_1 - \theta_2)\right) =$$

$$= \frac{1}{2} \cdot \dot{\theta}_1^2 \cdot (J_1 + m_2 \cdot l_1^2) + \frac{1}{2} \cdot \dot{\theta}_2^2 \cdot (J_2 + m_2 \cdot l_{G2}^2) + m_2 \cdot l_1 \cdot l_{G2} \cdot \dot{\theta}_1 \cdot \dot{\theta}_2 \cdot \cos(\theta_1 - \theta_2) = \qquad (4.63.)$$

$$= \frac{1}{2} \cdot Q_1 \cdot \dot{\theta}_1^2 + \frac{1}{2} \cdot Q_4 \cdot \dot{\theta}_2^2 + Q_2 \cdot \dot{\theta}_1 \cdot \dot{\theta}_2 \cdot \cos(\theta_1 - \theta_2)$$

$$E_{PT} = m_1 \cdot l_{G1} \cdot g \cdot \cos(\theta_1) + m_2 \cdot l_1 \cdot g \cdot \cos(\theta_1) + m_2 \cdot l_{G2} \cdot g \cdot \cos(\theta_2) = \qquad (4.64.)$$

$$= Q_3 \cdot g \cdot \cos(\theta_1) + Q_5 \cdot g \cdot \cos(\theta_2)$$

For the stabilization control law, the following conditions are assumed:

i. $\dot{\theta}_2 = 0$
ii. $E(\theta, \dot{\theta}) = E_{top}$

Applying condition (i) and developing the condition (ii) the equation 4.65 is obtained.

$$E(\theta, \dot{\theta}) = Q_3 \cdot g \cdot \cos(\theta_1) + Q_5 \cdot g \cdot \cos(\theta_2) = (Q_3 + Q_5) \cdot g = E_{top} \qquad (4.65.)$$

If a third condition is applied:

iii. $\theta_2 = 90º$

Then a homoclinic orbit is obtained.

$$\frac{1}{2}\cdot Q_1 \cdot \dot{\theta}_1^2 + Q_3 \cdot g \cdot \cos(\theta_1) = Q_3 \cdot g \;\rightarrow\; \frac{1}{2}\cdot Q_1 \cdot \dot{\theta}_1^2 = \; Q_3 \cdot g \cdot (1 - \cos(\theta_1)) \tag{4.66.}$$

Defining the following parameters:

$$\tilde{E} = E - E_{top}$$

$$\tilde{\theta}_2 = \theta_2 - \theta_{2eq} = \theta_2$$

The next Lyapunov function is chosen.

$$V(\theta, \dot{\theta}) = \frac{K_E}{2}\cdot \tilde{E}(\theta, \dot{\theta})^2 + \frac{K_D}{2}\cdot \dot{\theta}_2^2 + \frac{K_P}{2}\cdot \tilde{\theta}_2 \tag{4.67.}$$

Performing the derivative,

$$\dot{V}(\theta, \dot{\theta}) = K_E \cdot \tilde{E}(\theta, \dot{\theta}) \cdot \dot{E}(\theta, \dot{\theta}) + K_D \cdot \dot{\theta}_2 \cdot \ddot{\theta}_2 + K_P \cdot \tilde{\theta}_2 \cdot \dot{\theta}_2 \tag{4.68.}$$

Knowing that:

$$\dot{E}(\theta, \dot{\theta}) = \dot{\theta}^T \cdot \tau = [\dot{\theta}_1 \quad \dot{\theta}_2] \cdot \begin{bmatrix} 0 \\ \tau \end{bmatrix} = \dot{\theta}_2 \cdot \tau \tag{4.69.}$$

The derivative of the Lyapunov function becomes the following:

$$\dot{V}(\theta, \dot{\theta}) = K_E \cdot \tilde{E}(\theta, \dot{\theta}) \cdot \dot{\theta}_2 \cdot \tau + K_D \cdot \dot{\theta}_2 \cdot \ddot{\theta}_2 + K_P \cdot \tilde{\theta}_2 \cdot \dot{\theta}_2 \tag{4.70.}$$

In order to continue with the computations, the value of $\ddot{\theta}_2$ is needed. Therefore isolating $\ddot{\theta}$ from the motion equation 4.57. the next formula is obtained.

$$\begin{bmatrix} \ddot{\theta}_1 \\ \ddot{\theta}_2 \end{bmatrix} = D(\theta)^{-1} \cdot \left[\tau - C(\theta, \dot{\theta}) \cdot \dot{\theta} - g(\theta)\right] \tag{4.71.}$$

After performing all the computations (Annex D) the following value for $\ddot{\theta}_2$ is reached:

$$\ddot{\theta}_2 = \frac{1}{Q_1 \cdot Q_4 - Q_2^2 \cdot \cos^2(\theta_1 - \theta_2)} \cdot \left[Q_1 \cdot \tau + Q_2^2 \cdot \cos(\theta_1 - \theta_2) \cdot \sin(\theta_1 - \theta_2) \cdot \dot{\theta}_2^2 - Q_2 \cdot Q_3 \cdot g \cdot \cos\theta 1 - \theta 2 \cdot \sin\theta 1 + Q1 \cdot Q2 \cdot \sin\theta 1 - \theta 2 \cdot \theta 12 + Q1 \cdot Q5 \cdot g \cdot \sin\theta 2 = \right.$$

$$= \frac{1}{Q_1 \cdot Q_4 - Q_2^2 \cdot \cos^2(\theta_1 - \theta_2)} \cdot \left[Q_1 \cdot \tau + F(\theta, \dot{\theta}) \right] \tag{4.72.}$$

Now, putting $\ddot{\theta}_2$ into $\dot{V}$'s equation:

$$\dot{V}(\theta, \dot{\theta}) = K_E \cdot \tilde{E}(\theta, \dot{\theta}) \cdot \dot{\theta}_2 \cdot \tau + K_D \cdot \dot{\theta}_2 \cdot \frac{1}{Q_1 \cdot Q_4 - Q_2^2 \cdot \cos^2(\theta_1 - \theta_2)} \cdot \left\{ Q_1 \cdot \tau + F(\theta, \dot{\theta}) \right\} + K_P \cdot \tilde{\theta}_2 \cdot \dot{\theta}_2 =$$

$$= \dot{\theta}_2 \cdot \left[\tau \cdot \left(K_E \cdot \tilde{E}(\theta, \dot{\theta}) + \frac{K_D \cdot Q_1}{Q_1 \cdot Q_4 - Q_2^2 \cdot \cos^2(\theta_1 - \theta_2)} \right) + \frac{K_D \cdot F(\theta, \dot{\theta})}{Q_1 \cdot Q_4 - Q_2^2 \cdot \cos^2(\theta_1 - \theta_2)} + K_P \cdot \tilde{\theta}_2 \right] \tag{4.73.}$$

If $\dot{V}(\theta, \dot{\theta}) = -\dot{\theta}_2^2$, then:

$$-\dot{\theta}_2 = \tau \cdot \left(K_E \cdot \tilde{E}(\theta, \dot{\theta}) + \frac{K_D \cdot Q_1}{Q_1 \cdot Q_4 - Q_2^2 \cdot \cos^2(\theta_1 - \theta_2)} \right) + \frac{K_D \cdot F(\theta, \dot{\theta})}{Q_1 \cdot Q_4 - Q_2^2 \cdot \cos^2(\theta_1 - \theta_2)} + K_P \cdot \tilde{\theta}_2 \tag{4.74.}$$

Finally, isolating τ the control law is obtained.

$$\tau = \frac{-\left(Q_1 \cdot Q_4 - Q_2^2 \cdot \cos^2(\theta_1 - \theta_2)\right) \cdot \left(\dot{\theta}_2 + K_P \cdot \tilde{\theta}_2\right) - K_D \cdot F(\theta, \dot{\theta})}{K_E \cdot \tilde{E}(\theta, \dot{\theta}) \cdot \left(Q_1 \cdot Q_4 - Q_2^2 \cdot \cos^2(\theta_1 - \theta_2)\right) + K_D \cdot Q_1} \tag{4.75.}$$

More detailed computations are available on the Annex D

5. Implementation and results

5.1. Initial model

The project has been performed in phases. The first is the design and implementation of original or initial model, it is the most basic one designed. The second phase, consists on adding the stiffness element. Finally, the third one is the design of a non-linear controller to regulate the original system.

The use of Matlab/Simulink allows to solve differential equation systems by simulation. Therefore, the system does not need to be solved and allows studying different cases by using different parameters. All Matlab scripts and Simulink schemes used can be found in Annex A, B and C.

In order to test if the system was able to stabilize, the initial conditions were changed from null to different values, which means that either θ_1 or θ_2 were different from zero. The schemes for both the linear and non-linear system can be seen in Fig. 5.1 and Fig. 5.2, respectively.

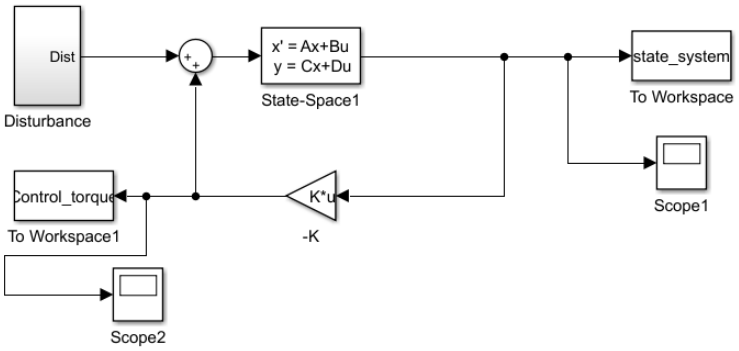

Fig. 5.1. *Simulink diagram of the linear system.*

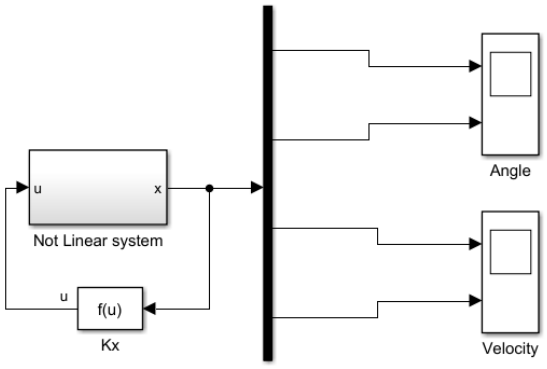

Fig. 5.2. *Simulink diagram for the simple non-linear system.*

5.1.1. Different perturbations

The first case is the study of the system when the same perturbation is produced in either θ_1 or θ_2 and if both of them have a non-null initial value.

As the values of the parameters do not change in either case, it is only the value of the initial conditions, the control parameters are the same in all three cases. They can be found in Table 5.1.

$\lambda = \begin{bmatrix} 4{,}0839 \\ 2{,}4656 \\ -4{,}0839 \\ -2{,}4656 \end{bmatrix}$
$C_o = \begin{bmatrix} 0 & -0{,}0196 & 0 & -0{,}4454 \\ 0 & 0{,}0785 & 0 & 0{,}8675 \\ -0{,}0196 & 0 & -0{,}4454 & 0 \\ 0{,}0785 & 0 & 0{,}8675 & 0 \end{bmatrix}$
$K = 10^3 \cdot [-4{,}7080 \quad -0{,}0264 \quad -1{,}3400 \quad -0{,}1632]$

Table 5.1. *Control parameters for the initial model.*

Regarding how the linear system reacts to each perturbation the results are the following (Fig. 5.3 and Fig. 5.4):

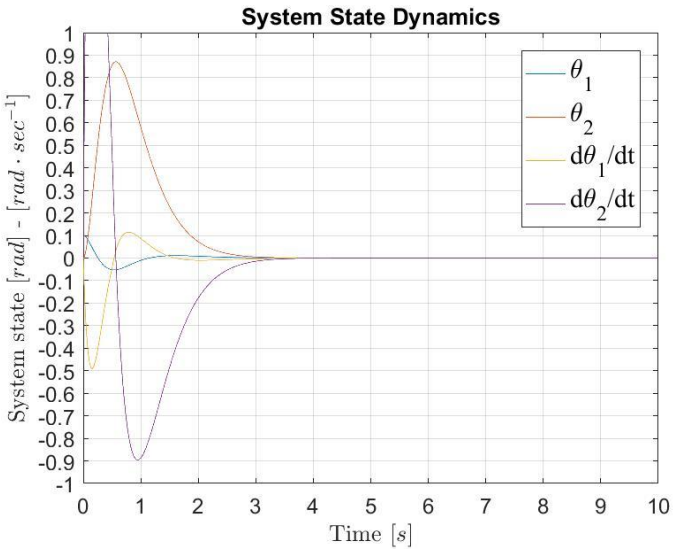

Fig. 5.3. *Response of the linear system for a initial perturbation of θ_1=0,1 rad.*

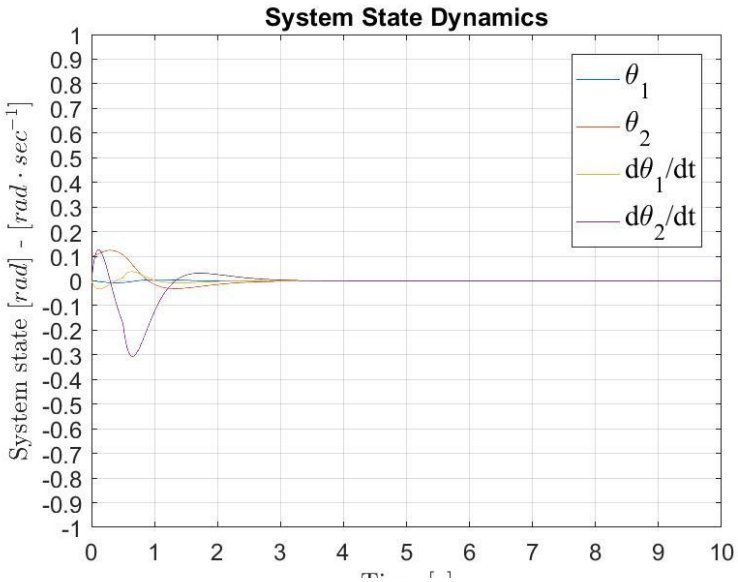

Fig. 5.4. *Response of the linear system for a initial perturbation of θ_2=0,1 rad.*

As it can be seen in the figures above, there is a huge difference in the linear system between having the same initial perturbation in θ_1 or θ_2. In the former case, the system stabilizes in 3,5 s with θ_2 reaching a maximum value of 0,88 rad. The latter, stabilizes much faster, at 3 s. And the angle values belong to a much shorter range.

Regarding the non linear values, the results are the following:

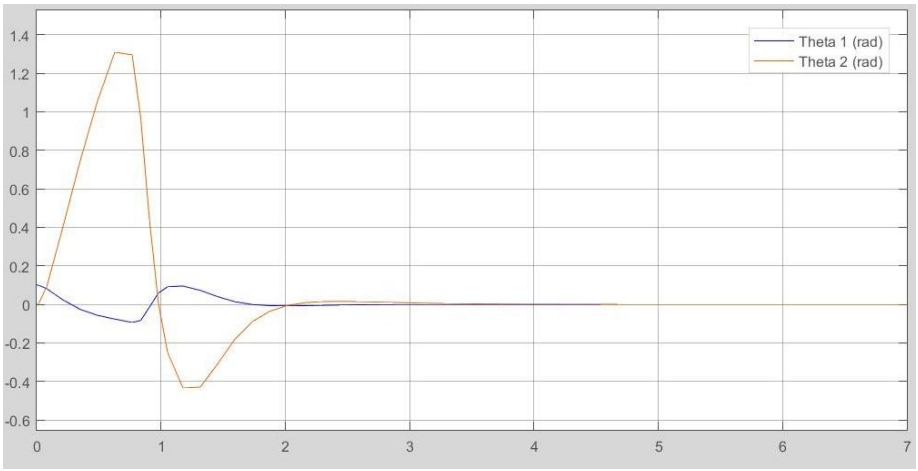

Fig. 5.5. *Response of the non-linear system for a initial perturbation of θ_1=0,1 rad.*

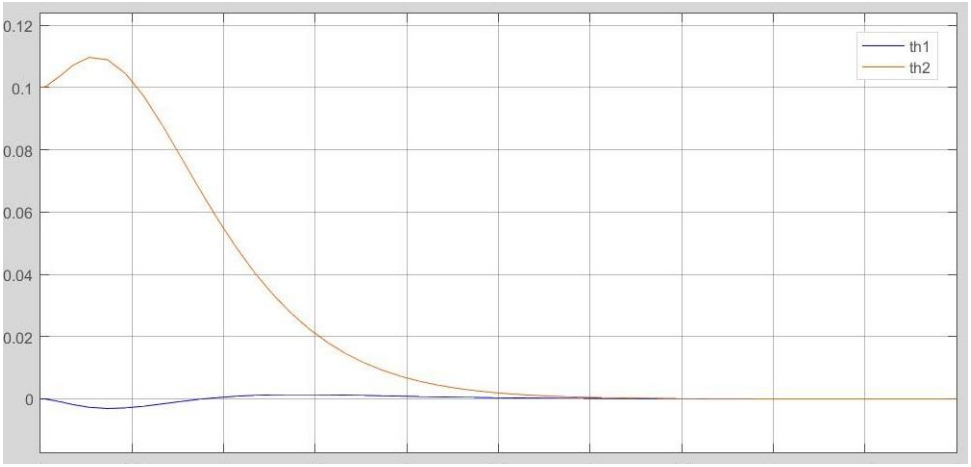

Fig. 5.6. *Response of the non-linear system for a initial perturbation of θ_2=0,1 rad.*

The figures above (Fig. 5.5 and Fig. 5.6) show the response of the non-linear system with the LQR control method. The tendency followed is the same than for the linear system. The stabilization time for an initial perturbation in θ_1 is 3.5 s and therefore higher than for θ_2 that is 3 s. The main difference between the linear and non-linear results are the angle range in the latter. In this case, for the first perturbation (θ_1= 0,1 rad) the angle θ_2 reaches the maximum value of 1,3 rad.

When there is an initial perturbation in both angles, the system does not hold a big range of angles. For example, for an initial perturbation of θ_1= 0,1 rad, the system does not stabilize for θ_2 = 0,1 rad. Therefore the following simulations have been performed for an initial perturbation of: θ_1 = 0,1 rad and θ_2= 0,01 rad. The results for the linear system can be seen in Fig. 5.7 and the non-linear systen corresponds to Fig. 5.8.

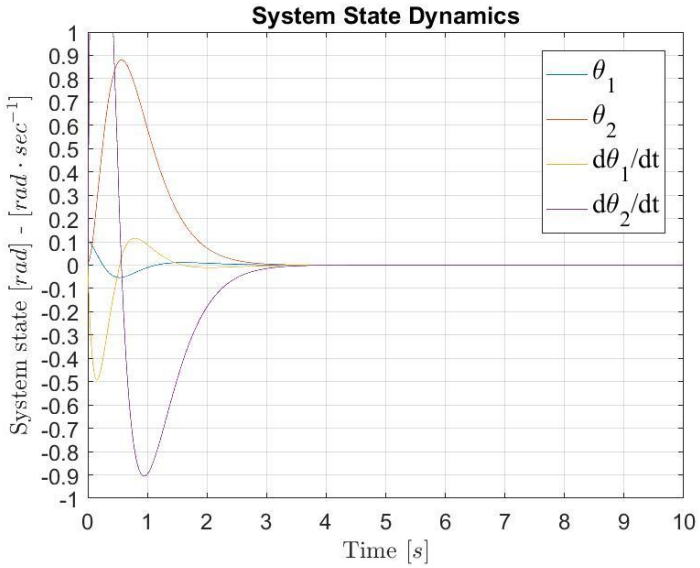

Fig. 5.7. *Response of the linear system for a initial perturbation of θ_1=0,1 rad and θ_2=0,01 rad.*

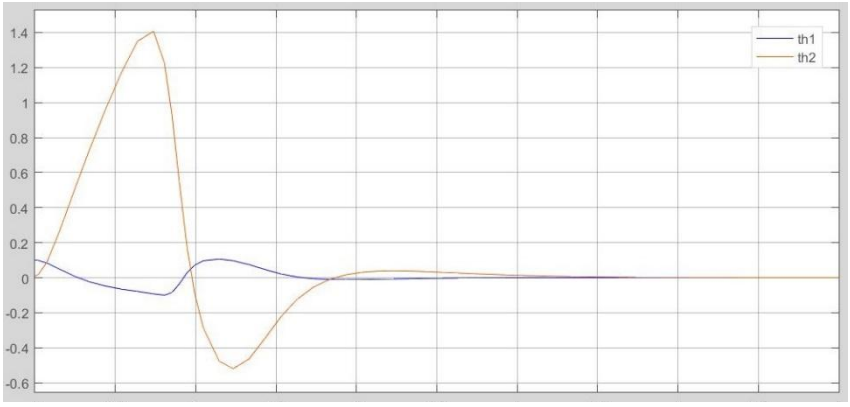

Fig. 5.8. *Response of the linear system for a initial perturbation of θ_1=0,1 rad and θ_2=0,01 rad.*

As it can be seen, in the figures above, the results for a double perturbation are really similar to the behavior for the single biggest perturbation. However the system is still more unstable, reaching a higher value for $\boldsymbol{\theta_2}$.

5.1.2. Different moments of inertia

As it was explained in the biomechanical chapter, two different sets of moments of inertia have been computed. On the one hand, all the bodies were approximated as slender rods. While, on the other hand, the arms were considered slender rods but both the torso and the legs were approximated as rectangular prism.

The obtained values have been the following (Table 5.2):

	Case 1	**Case 2**
J_{01}	9,4548 Kg·m^2	9,574656 Kg·m^2
J_{A2}	3,23475 Kg·m^2	3,1209 Kg·m^2
J_{A3}	8,748362 Kg·m^2	8,748362 Kg·m^2
J_{A23}	11,9831 Kg·m^2	11,86929 Kg·m^2

Table 5.2. *Comparison between the values of the computed moments of inertia.*

In this case, as the parameters values are different, the values for the control system are also different. As slender rods, the obtained values are the following:

$\lambda = \begin{bmatrix} 4{,}0839 \\ 2{,}4656 \\ -4{,}0839 \\ -2{,}4656 \end{bmatrix}$
$C_o = \begin{bmatrix} 0 & -0{,}0196 & 0 & -0{,}4454 \\ 0 & 0{,}0785 & 0 & 0{,}8675 \\ -0{,}0196 & 0 & -0{,}4454 & 0 \\ 0{,}0785 & 0 & 0{,}8675 & 0 \end{bmatrix}$
$K = 10^3 \cdot [-4{,}7080 \quad -0{,}0264 \quad -1{,}3400 \quad -0{,}1632]$

Table 5.3. *Control parameters for moment of inertia as slender rods.*

While the values for the control system when the torso is approximated as a rectangular prism but both the arms and the legs are slender rods, are the following:

$\lambda = \begin{bmatrix} -4{,}0863 \\ -2{,}4710 \\ 4{,}0863 \\ 2{,}4710 \end{bmatrix}$
$C_o = \begin{bmatrix} 0 & -0{,}0197 & 0 & -0{,}4488 \\ 0 & 0{,}0791 & 0 & 0{,}8811 \\ -0{,}0197 & 0 & -0{,}4488 & 0 \\ 0{,}0791 & 0 & 0{,}8811 & 0 \end{bmatrix}$
$K = 10^3 \cdot [-4{,}6945 \quad -0{,}0263 \quad -1{,}3381 \quad -0{,}1630]$

Table 5.4. *Control parameters for moment of inertia as slender rods and rectangular prisms.*

Comparing the results for the linear system both conditions behave the same. As it can be seen in Fig. 5.9 and Fig. 5.10, in order to compare the effects of the different moments of inertia the system has been simulated with the same perturbation. The chosen initial perturbation has been θ_1=0,1 rad.

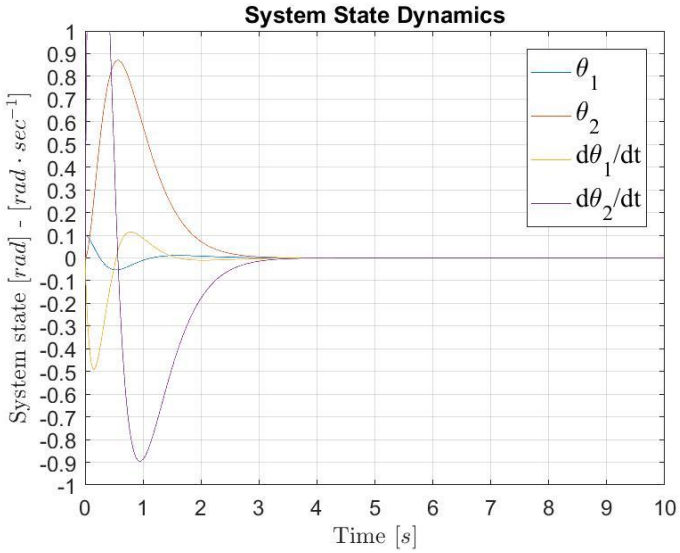

Fig. 5.9. *Response of the linear system for moment of inertia as slender rod and initial perturbation θ_1 = 0,1 rad.*

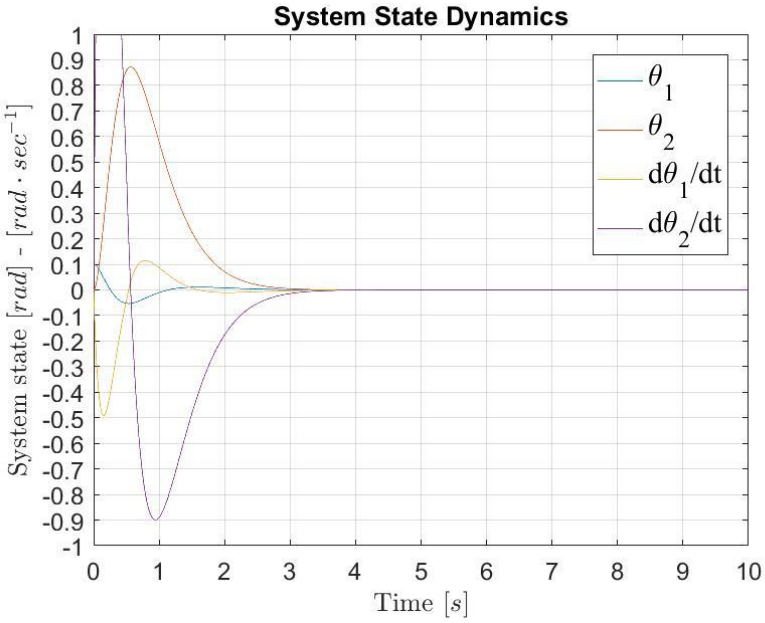

Fig. 5.10. *Response of the linear system for moment of inertia as slender rod and rectangular prism and initial perturbation θ_1 = 0,1 rad.*

The same situation is repeated for the non-linear systems (Fig. 5.11 and Fig. 5.12). The changes in the parameters are so subtle that they do not report the effects in the behavior of the system.

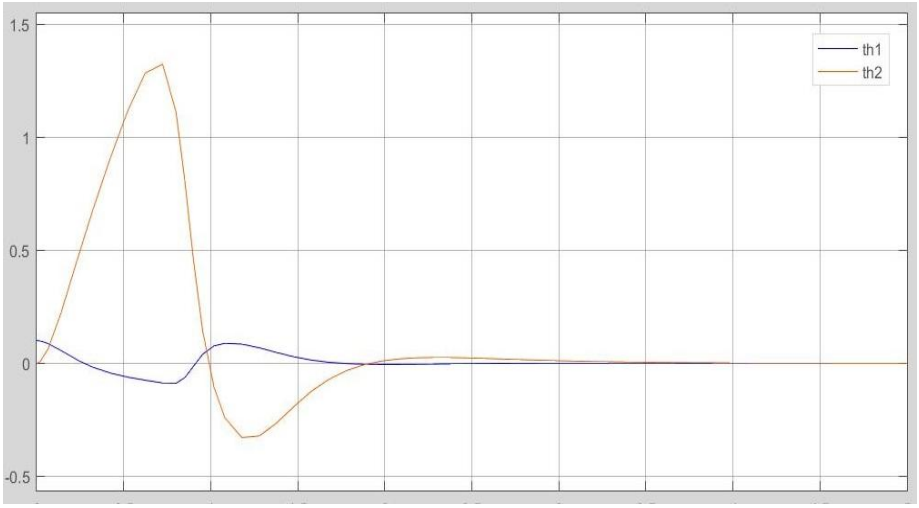

Fig. 5.11. *Response of the linear system for moment of inertia as slender rod and initial perturbation θ_1= 0,1 rad.*

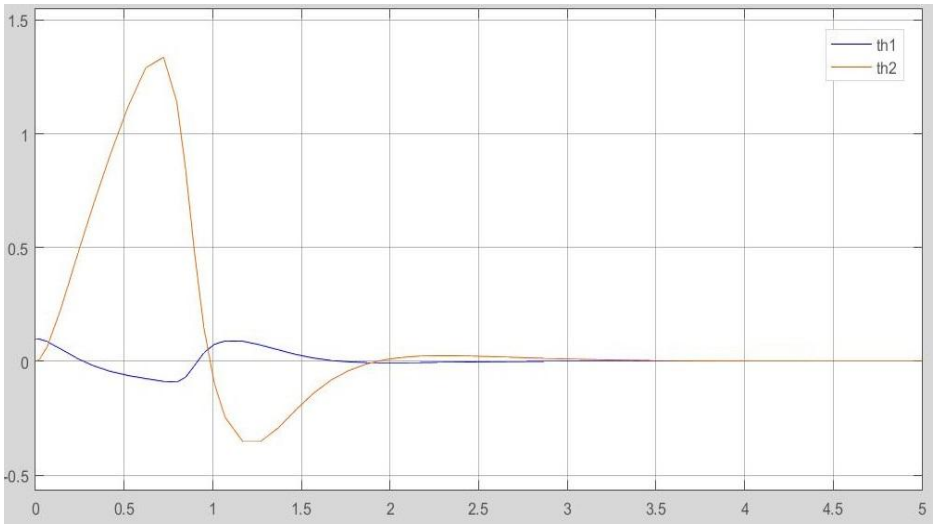

Fig. 5.12. *Response of the non-linear system for moment of inertia as slender rod and rectangular prism and initial perturbation θ_1=0,1 rad.*

Seeing the null effects of the small variations in the moments of inertia, even if it translates into different control parameters, it can be concluded that it is not significant and therefore the approximations hold.

5.1.3. Forces

In order to have the data to perform a more accurate analysis of the whole system, the forces exchanged between the feet and the floor, have been computed using Matlab.

For the horizontal force the Simulink scheme can be seen in Fig. 5.13.

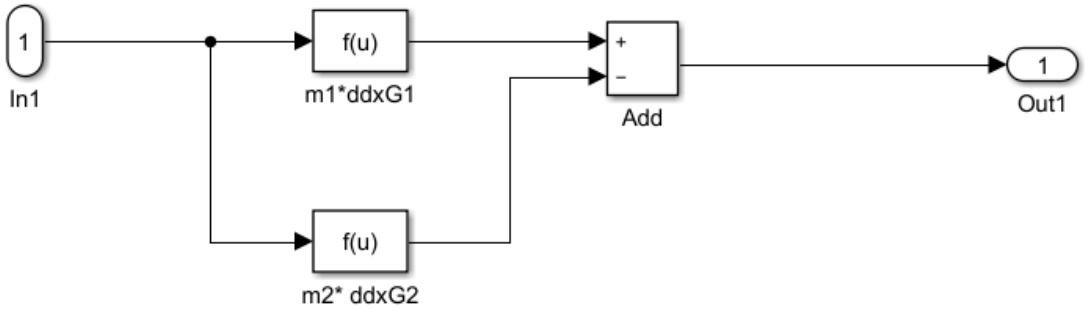

Fig. 5.13. *Simulink diagram to compute the lateral force exchanged between the feet and the floor (F_{01x}).*

While for the vertical one it is the following (Fig. 5.14):

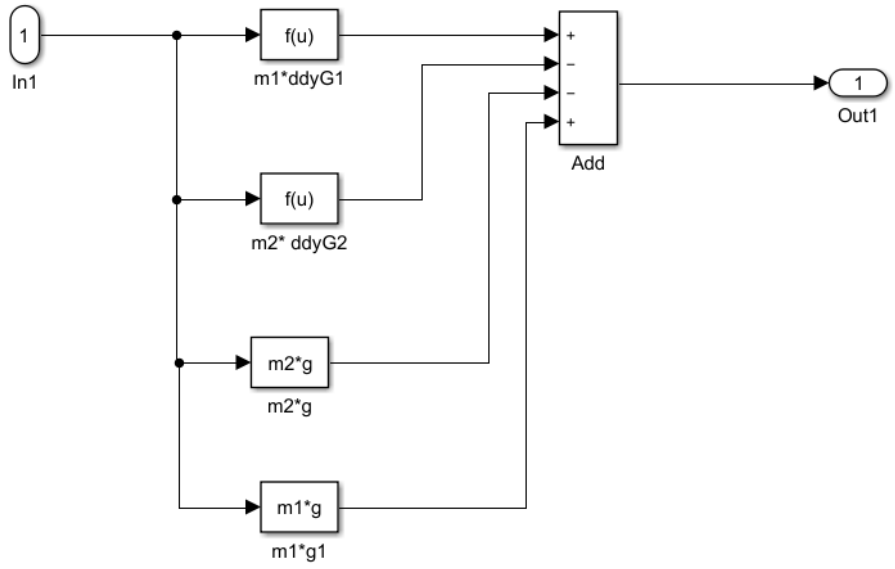

Fig. 5.14. *Simulink diagram to compute the vertical force exchanged between the feet and the floor (F_{01x}).*

When simulating the behavior of the system for an initial perturbation of θ_1=0.1 rad the following results have been obtained:

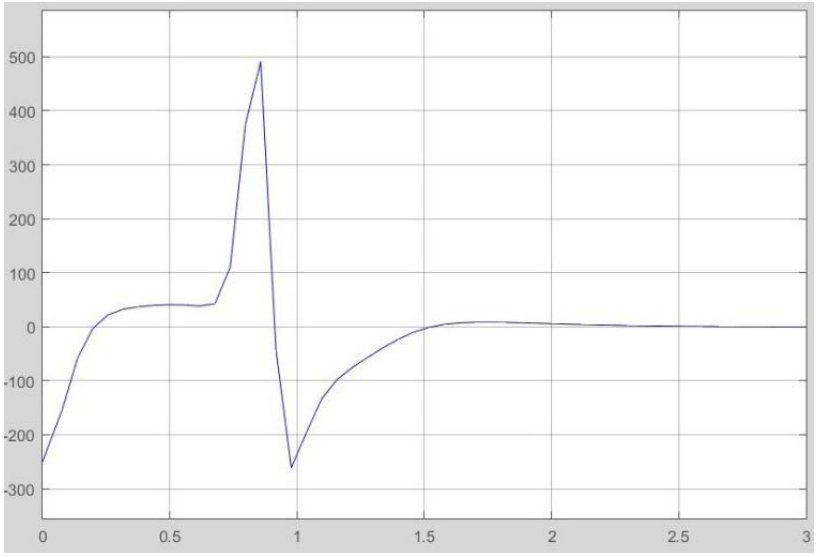

Fig. 5.15. *Horizontal force in 0. F_{01x}(Units: N) for an initial angle θ_1 =0.1 rad.*

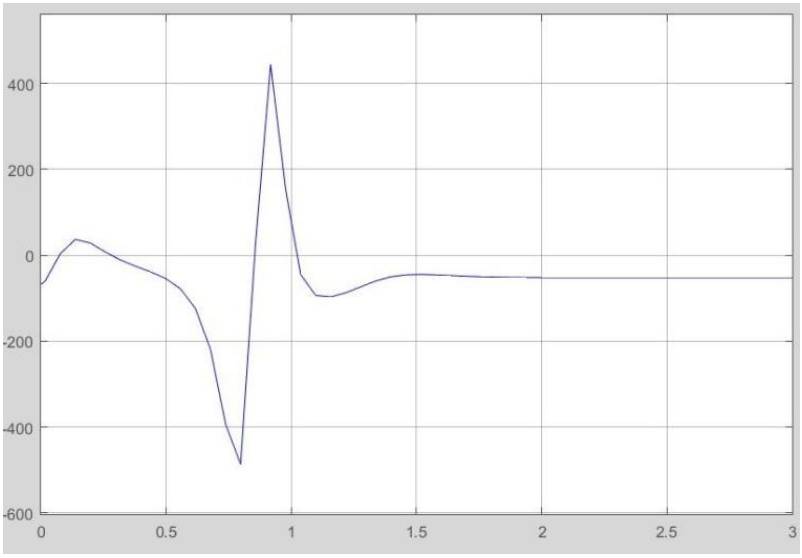

Fig. 5.16. *Vertical force in 0. F_{01y} (Units: N) for an initial angle θ_1 =0.1 rad.*

As it can be clearly seen in the vertical axis the forces asked for the system to stabilize are impossible to reach as the reaction forces of the floor can not be controlled. Therefore having positive values indicates that it is not a realistic situation. Given this situation, a new simulation has been made with a smaller initial perturbation: θ_1=0.1 rad.

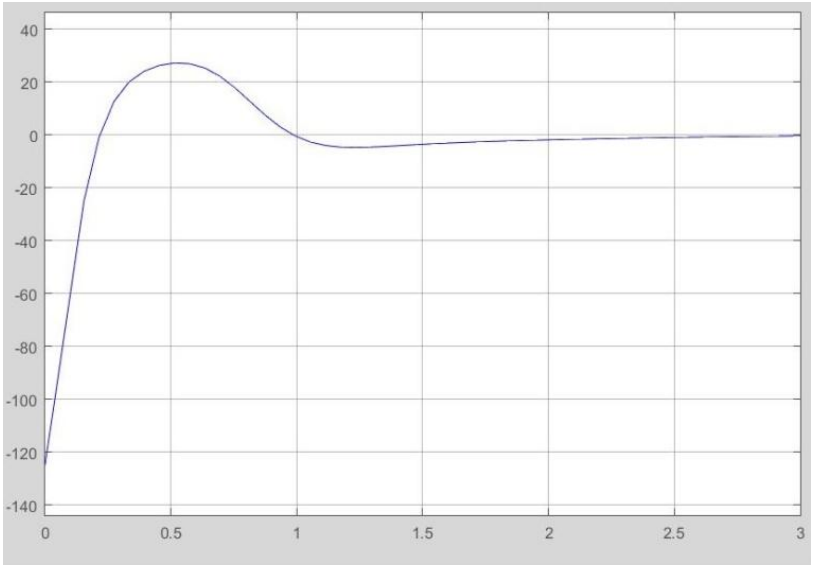

Fig. 5.17. *Horizontal force in 0. F_{01x} (Units: N) for an initial angle θ_1 = 0,05 rad.*

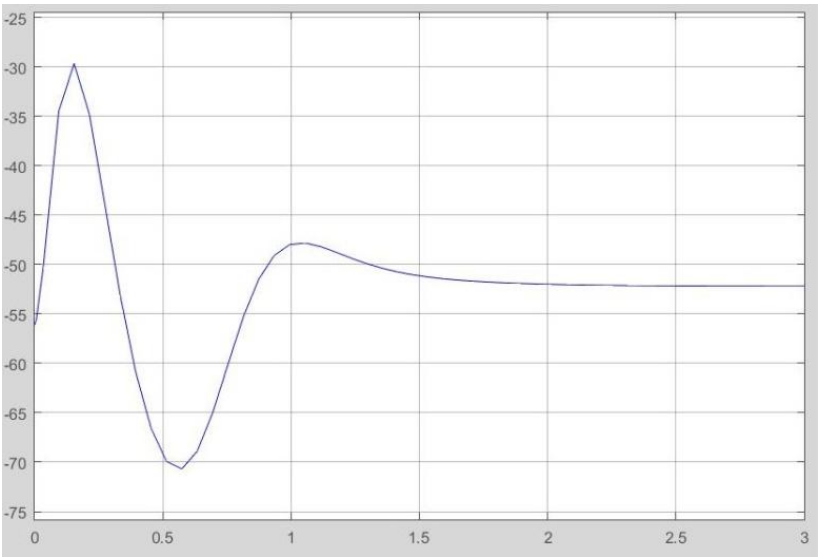

Fig. 5.18. *Vertical force in 0. F_{01y} (Units: N) for an initial angle θ_1 = 0,05 rad.*

In this case not only the magnitude of the results is reduced but also the sign and therefore the direction of the force required. Therefore, they are plausible.

Finally to check the limitations of the system, the force analysis has been performed for a perturbation in the second angle: θ_2 = 0,1 rad.

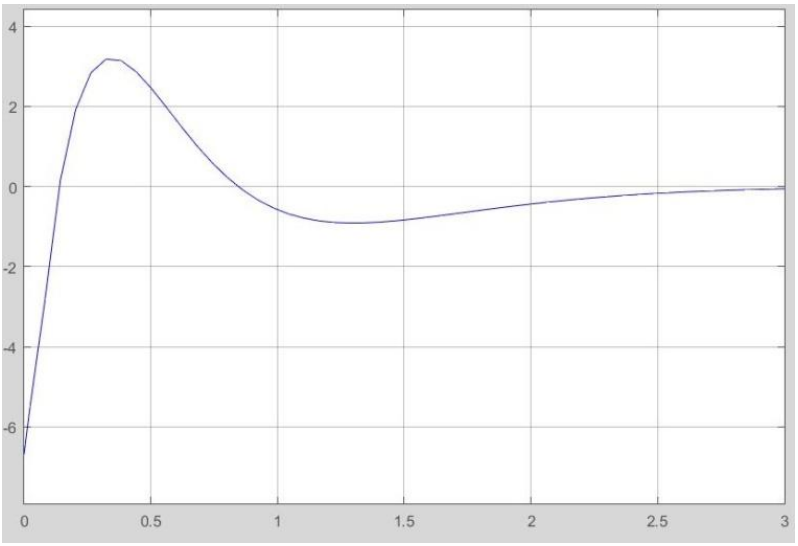

Fig. 5.19. *Horizontal force in Point 0. F_{01x} (Units: N) for an initial angle θ_2 =0.1 rad.*

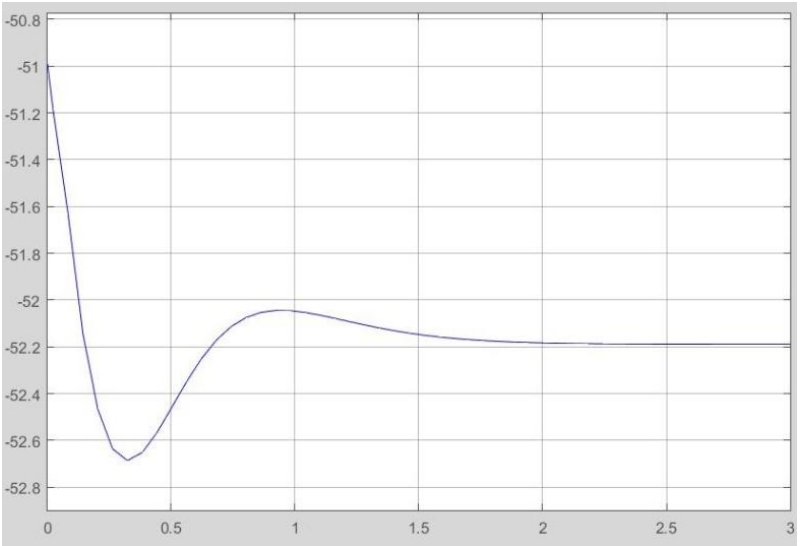

Fig. 5.20. *Vertical force in Point 0. F_{01y} (Units: N) for an initial angle θ_2 =0.1 rad.*

The importance of analyzing the exchange of forces between the feet and the floor is because mathematically the system can require a force impossible to perform or control in reality. Therefore a proper study of the force exchange leads to a better understanding of the system and its limitations.

5.2. Updated model

Once the original model has been analyzed, a step forward is taken by including an elastic component equivalent to the hip joint. Adding this parameter leads toward a more realistic system.

Again, the use of Matlab allows to solve the differential equation systems that otherwise would be extremely difficult. The modifications needed to update the model are in both the Matlab Script and the Simulink file. On the one hand, the results of the linearization using Matlab have changed and therefore the control system has changed too. While, on the other hand, some terms need to be added to the non-linear system of equations. All details can be found in the Annexes.

In order to test if the system was able to stabilize, the same procedure has been followed, the initial conditions are changed from null to different values, which means that either θ_1 or θ_2 become different than zero.

Regarding the chosen elastic component, as it has been discussed in the background chapter, there are no values in the literature for a frontal approach of the problem. Therefore, the value has been chosen to be as coherent as possible to the relationship between the mobility range to the elastic or stiffness coefficient form the studies performed in the different joints with a sagittal approach.

5.2.1. Different perturbations

The first case of study is again what happens to the system when the same perturbation is produced only in θ_1, only in θ_2 or both at the same time.

As the values of the parameters do not change in either case, it is only the value of the initial conditions, the control parameters are the same in all three cases:

$\lambda = \begin{bmatrix} -4{,}0977 \\ -2{,}4623 \\ 4{,}0977 \\ 2{,}4623 \end{bmatrix}$
$C_o = \begin{bmatrix} 0 & -0{,}0196 & 0 & -0{,}4511 \\ 0 & 0{,}0785 & 0 & 0{,}8714 \\ -0{,}0196 & 0 & -0{,}4511 & 0 \\ 0{,}0785 & 0 & 0{,}8714 & 0 \end{bmatrix}$
$K = 10^3 \cdot [-4{,}6465 \quad -0{,}0074 \quad -1{,}3192 \quad -0{,}1577]$

Table 5.5. *Control parameters for the system with an elastic element.*

As it can be seen the obtained values are different from the ones without the elastic element in the hip-joint.

Regarding how the system reacts to each perturbation the results are the following:

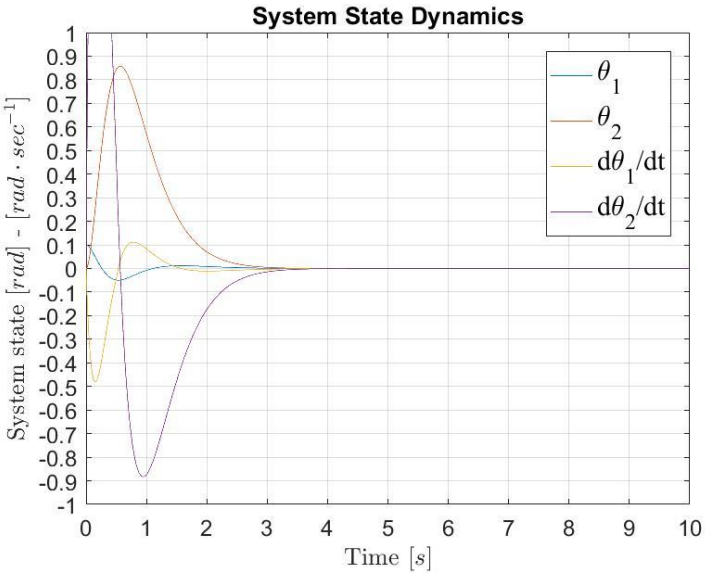

Fig. 5.21. *Response of the linear system for a initial perturbation of θ_1=0,1 rad.*

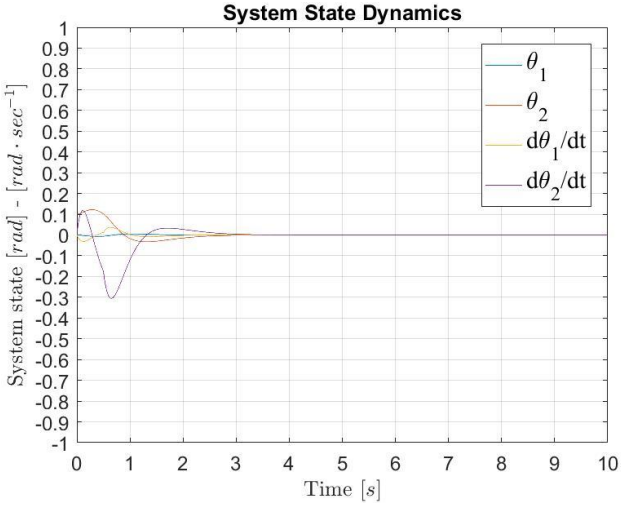

Fig. 5.22. *Response of the linear system for a initial perturbation of θ_2=0,1 rad.*

As it can be seen in the figures above, there is a huge difference in the linear system between having the same initial perturbation in θ_1 or θ_2. In the former case, the system stabilizes in 3,25 s with θ_2 reaching a maximum value of 0,86 rad. The latter, stabilizes much faster, at 2,85 s. And the angle values belong to a much shorter range.

Regarding the non linear values, the results are the following:

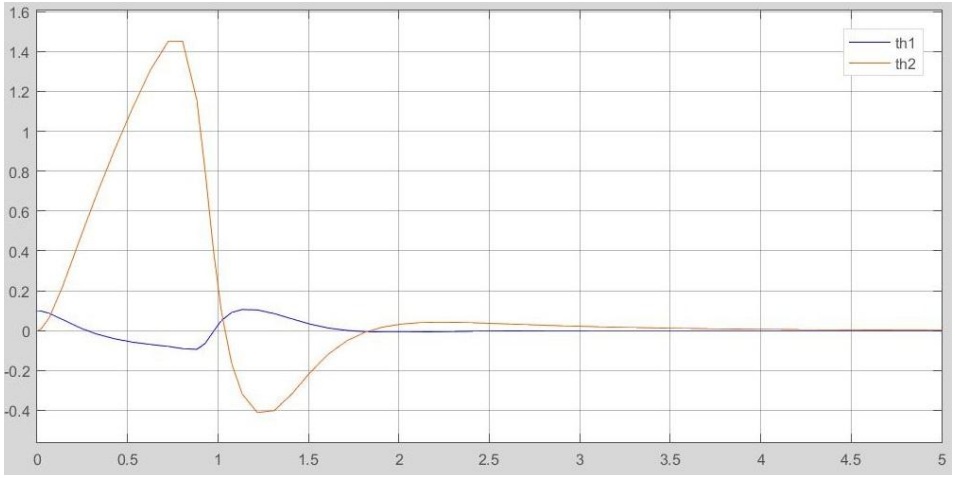

Fig. 5.23. *Response of the non-linear system for a initial perturbation of θ_1=0,1 rad.*

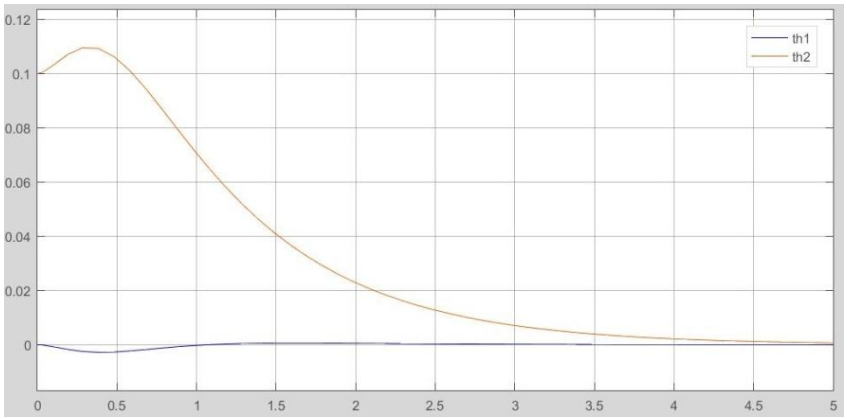

Fig. 5.24. *Response of the non-linear system for a initial perturbation of θ_2.=0,1 rad.*

The figures above show the response of the non-linear system with the control designed with the LQR method. The tendency followed is the same than for the linear system. However, there is an extremly important difference. Now, in the non-linear system it is the second case (initial perturbation in θ_2) that takes longer to stabilize reaching the 5 s. While the former stabilizes around 3.5 s. This case it is clearly related to the elastic element that now links both elements of the model.

When there is an initial perturbation in both angles, the system does not hold a big range of angles. For example, for an initial perturbation of θ_1 = 0,1 rad, the system does not stabilize for θ_2 = 0,1 rad. In the previos chapter, when no stiffness element was considered it was possible to simulate the system for an initial perturbation of: θ_1 = 0,1 rad and θ_2 = 0,01 rad. However, now, taking into account the elastic element it is impossible to stabilize the non-linear system for those values, even

though the linear one does stabilize. Taking that fact into consideration the values have been reduced to: θ_1 = 0,05 rad and θ_2 = 0,01 rad.

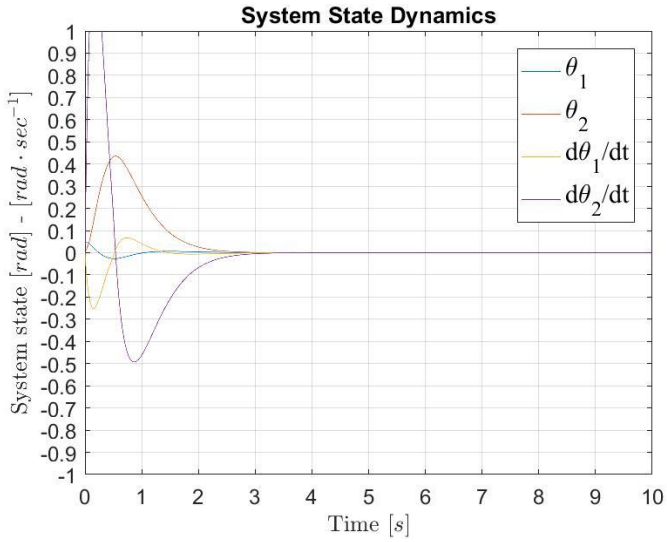

Fig. 5.25. *Response of the linear system for a initial perturbation of θ_1=0,05 rad and θ_2=0,01 rad.*

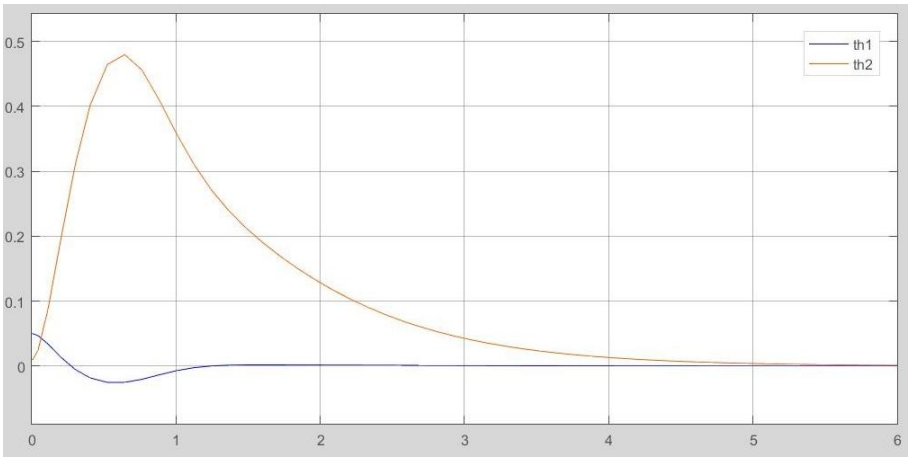

Fig. 5.26. *Response of the linear system for a initial perturbation of θ_1= 0,05 rad and θ_2=0,01 rad.*

As it can be seen, in the figures above, the results for a double perturbation are really similar to the behavior for the single biggest perturbation.

5.2.2. Different moments of inertia

As it has been done for the original system the different values for the moment of inertia will be tested to see if now that there is a stiffness element their influence is stronger. The two cases for the moments of inertia are the following:

	Case 1	**Case 2**
J_{01}	9,4548 Kg·m^2	9,574656 Kg·m^2
J_{A2}	3,23475 Kg·m^2	3,1209 Kg·m^2
J_{A3}	8,748362 Kg·m^2	8,748362 Kg·m^2
J_{A23}	11,9831 Kg·m^2	11,86929 Kg·m^2

Table 5.6. *Comparison between the values of the computed moments of inertia*

In the Case 1 all bodies have been considered as slender rods. While the Case 2 corresponds to different geometrical shapes depending on the body part; the torso as a rectangular prism and the legs and arms as slender rods.

As slender rods, the obtained values are the following:

$$\lambda = \begin{bmatrix} -4{,}0977 \\ -2{,}4623 \\ 4{,}0977 \\ 2{,}4623 \end{bmatrix}$$
$$C_o = \begin{bmatrix} 0 & -0{,}0196 & 0 & -0{,}4511 \\ 0 & 0{,}0785 & 0 & 0{,}8714 \\ -0{,}0196 & 0 & -0{,}4511 & 0 \\ 0{,}0785 & 0 & 0{,}8714 & 0 \end{bmatrix}$$
$$K = 10^3 \cdot [-4{,}6465 \quad -0{,}0074 \quad -1{,}3192 \quad -0{,}1577]$$

Table 5.7. *Control parameters for the system with an elastic element for inertia Case 1*

While the values for the control system when the torso is approximated as a rectangular prism but both the arms and the legs are slender rods, are the following:

$\lambda = \begin{bmatrix} -4{,}1001 \\ -2{,}4677 \\ 4{,}1001 \\ 2{,}4677 \end{bmatrix}$
$C_o = \begin{bmatrix} 0 & -0{,}0197 & 0 & -0{,}4545 \\ 0 & 0{,}0791 & 0 & 0{,}8850 \\ -0{,}0197 & 0 & -0{,}4545 & 0 \\ 0{,}0791 & 0 & 0{,}8850 & 0 \end{bmatrix}$
$K = 10^3 \cdot [-4{,}6329 \quad -0{,}0075 \quad -1{,}3172 \quad -0{,}1575]$

Table 5.8. *Control parameters for the system with an elastic element for inertia Case 2.*

As it can be seen both sets of values differ slightly. They are also different from the ones obtained for the original model.

Comparing the results for the linear system both conditions behave exactly the same, like it had happened for the original model.

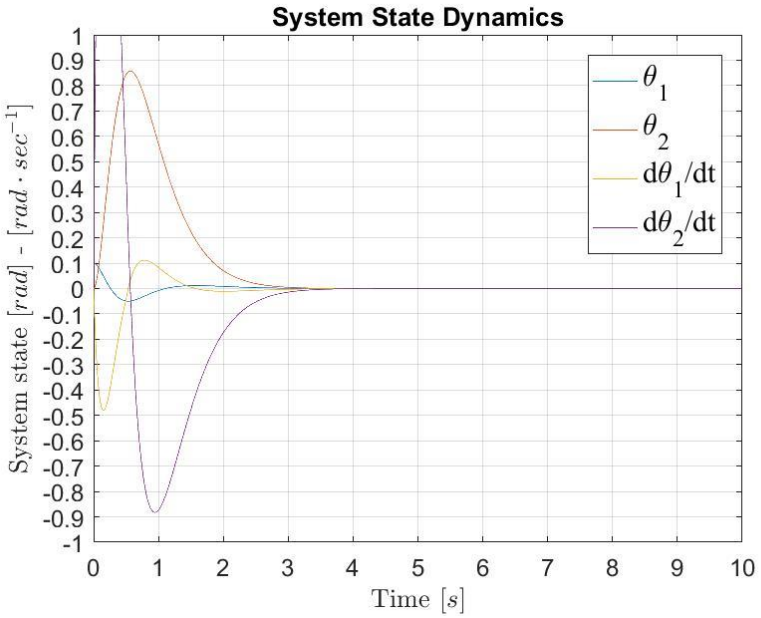

Fig. 5.27. *Response of the linear system for moment of inertia as slender rod and initial perturbation θ_1=0,1 rad.*

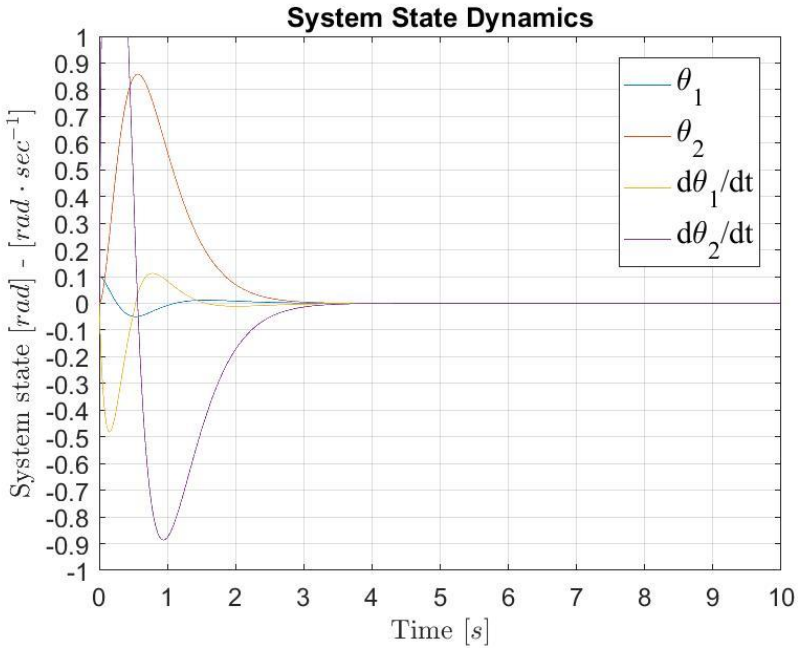

Fig. 5.28. *Response of the linear system for moment of inertia as slender rod and rectangular prism and initial perturbation θ_1=0,1 rad.*

The same situation is repeated for the non-linear system. The changes in the parameters are so subtle that they do not report the effects in the behavior of the system.

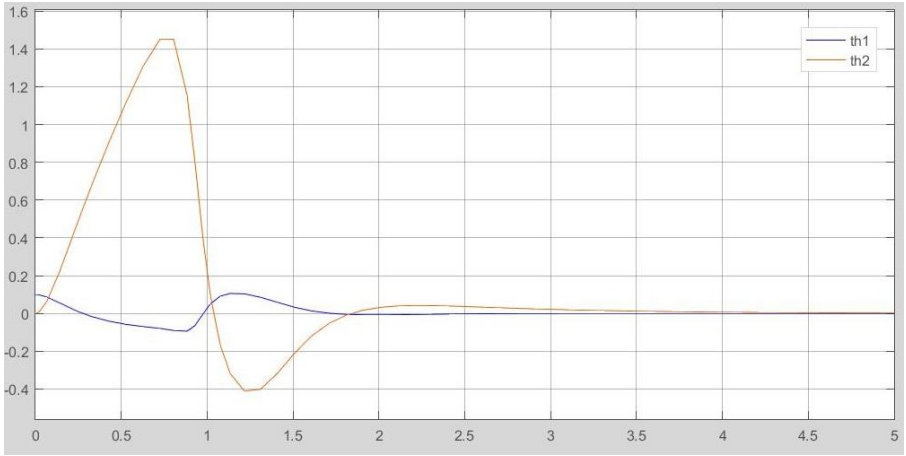

Fig. 5.29. *Response of the linear system for moment of inertia as slender rod and initial perturbation θ_1=0,1 rad.*

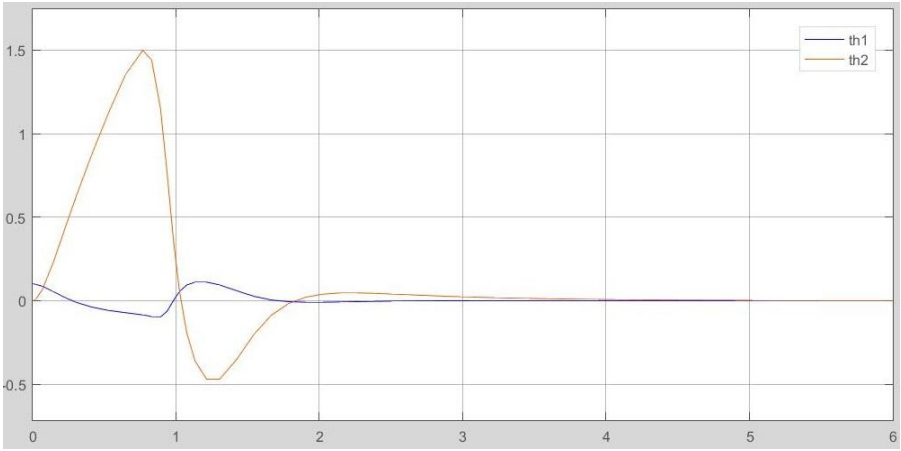

Fig. 5.30. *Response of the non-linear system for moment of inertia as slender rod and rectangular prism and initial perturbation θ_1= 0,1 rad.*

Seeing the null effects of the small variations in the moments of inertia, even if it translates into different control parameters, it can be concluded that it is not significant and therefore the approximations hold for both the original model and the updated one.

5.2.3. Forces

Using the same Simulink design than for the original model, the forces have been computed reaching the following results:

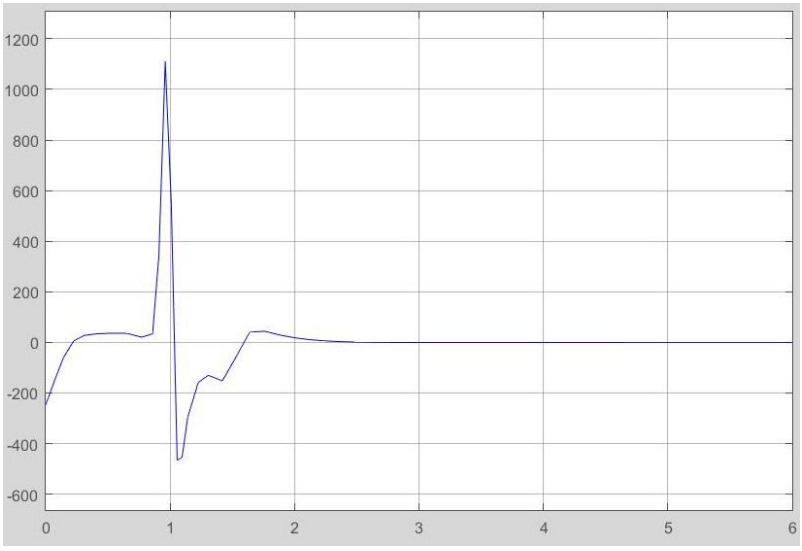

Fig. 5.31. *Horizontal force in Point 0. $F_{01x.}$(Units: N) For an initial perturbation θ_1=0,1 rad.*

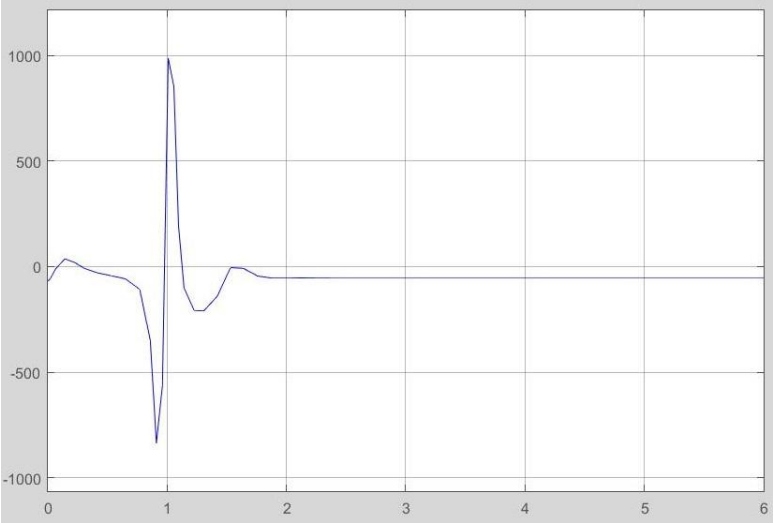

Fig. 5.32. *Vertical force in Point 0. F_{01y} (Units: N) For an initial perturbation θ_1=0,1 rad.*

As it can be seen, compared to the original model the situation is the same even if the values are bigger. It is still an impossible situation. Following the same procedure as before, in order to understand better the results a new simulation has been performed with a smaller angle.

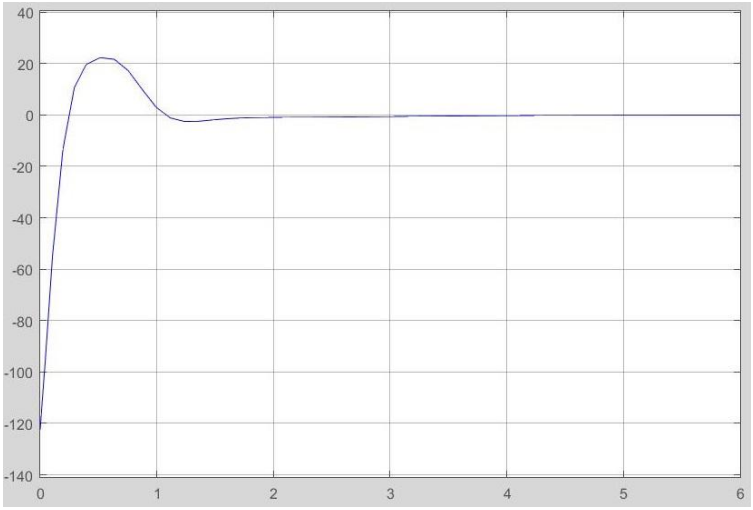

Fig. 5.33. *Horizontal force in Point 0. $F_{01x.}$ (Units: N) For an initial perturbation θ_1=0,05 rad.*

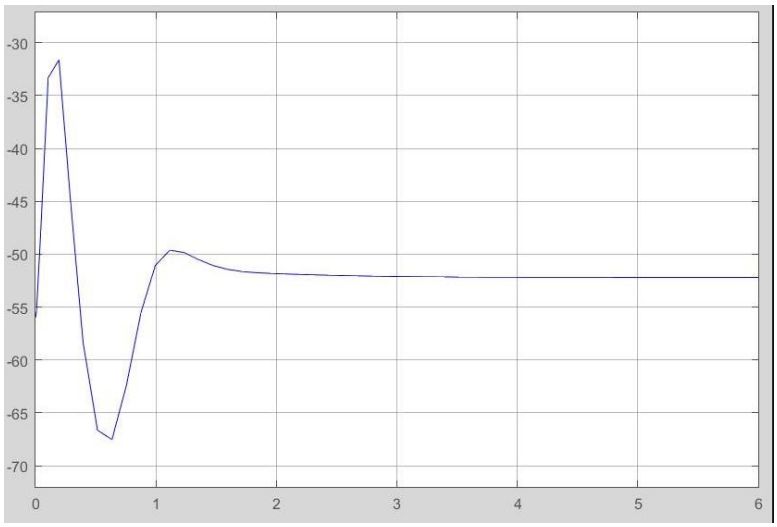

Fig. 5.34. *Vertical force in 0. F_{01y} (Units: N) For an initial perturbation θ_1==0,05 rad.*

In this case, the results are like expected, not only the magnitudes of the forces have been reduced but also the sign leading to a viable situation.

Finally, a simulation with a non null initial value for the second angle has been performed.

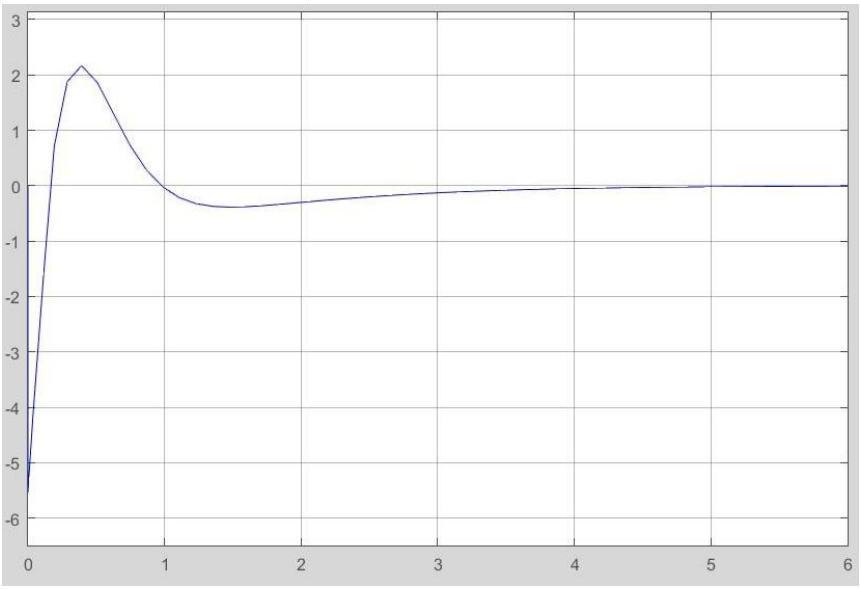

Fig. 5.35. *Horizontal force in Point 0. $F_{01x.}$ (Units: N) For an initial perturbation θ_2=0,1 rad.*

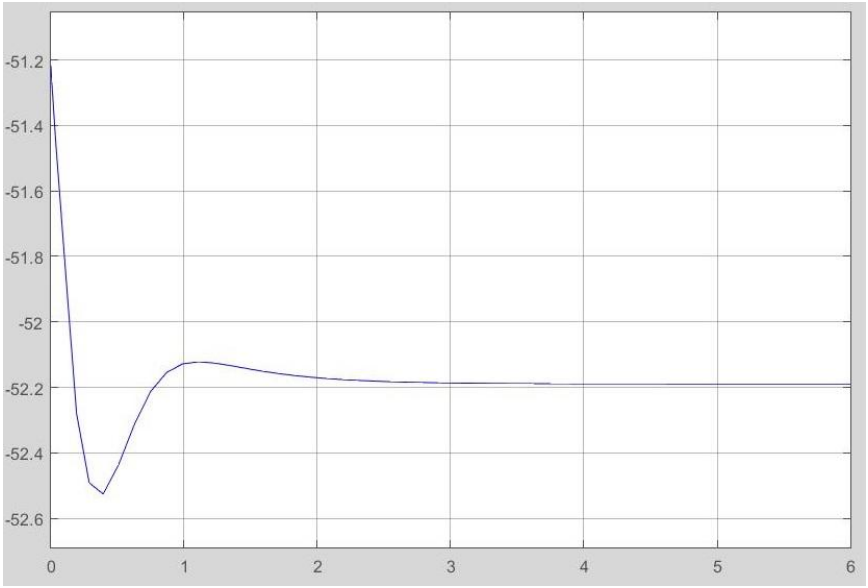

Fig. 5.36. *Vertical force in Point 0. F_{01y} (Units: N) For an initial perturbation θ_2=0,1 rad.*

Again, the results were the expected ones, following also the same tendency than for the initial model.

5.3. Non-linear controller system

The non-linear control law has been implemented in the Simulink file for the initial system. However, when the simulation was performed the system did not stabilize. After checking all the computations and the implementation no solution has been found. However, the following are the results.

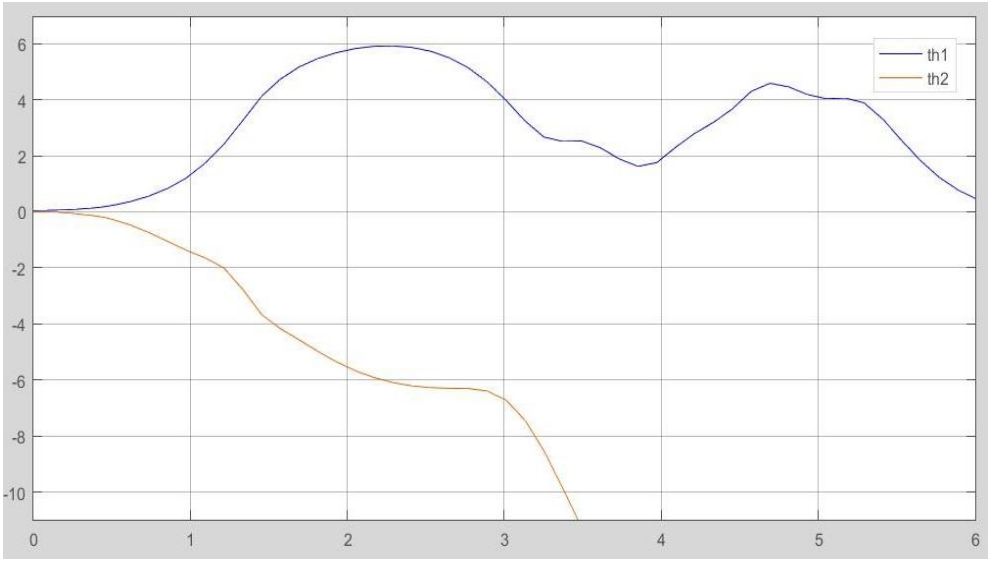

Fig. 5.37. *Response of the non-linear system for a initial perturbation of θ_1=0,05 rad.*

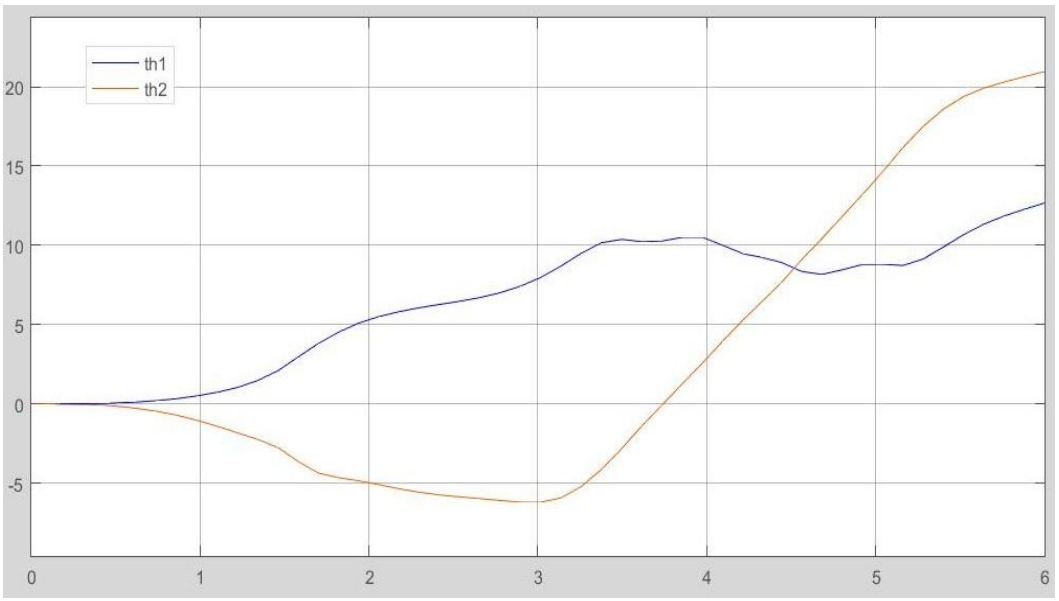

Fig. 5.38. *Response of the non-linear system for a initial perturbation of θ_2=0,05 rad.*

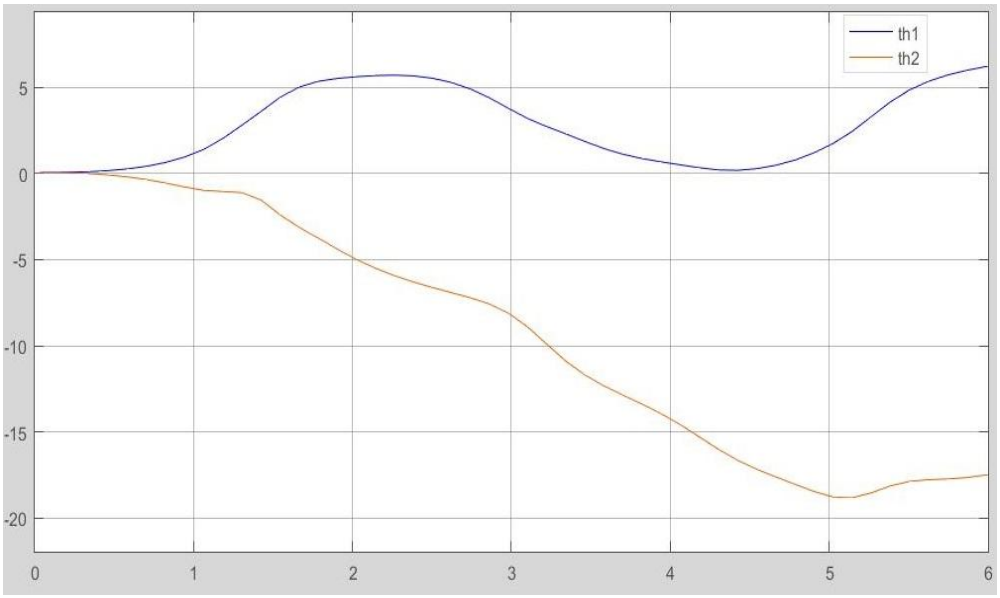

Fig. 5.39. *Response of the non-linear system for a initial perturbation of θ_1=0,05 rad and θ_2=0,05 rad.*

6. Conclusions

In this thesis a study and design of a balance postural control system with a frontal approach has been made. It has been a transversal study as it has involved numerous engineering fields which have presented numerous difficulties along the way, but all of them have been properly solved by performing an extensive research in the literature regarding each particular topic. Not only the initial expectations have been met, but also an update on the model has been performed in order to design a more realistic model by including an elastic element.

The first step has been a research on the existing literature on biomechanical data. While analyzing the state of the art in such a topic, it has been clear that the recent research focuses in specific goals and parameters instead of performing a statistical approach to determine the average values for partial masses and lengths for the different body components. Therefore, in order to obtain the necessary values for the model, older investigations have been analyzed leading to authors like Hanavan (1964), Drillis and Contini (1966), Dempster (1973) or Winter et al. (1998). These focused in a wider field by using different techniques to obtain the main anthropometric parameters of the human body.

In order to perform a more accurate project, different moments of inertia have been computed by approximating the different body parts with various geometrical shapes. By obtaining these values and through the simulation of the system it has been confirmed that the difference in the results is so subtle that can be completely neglected. Therefore, it can be confirmed that in such basic models the shape in which the body components are approximated is not relevant.

Regarding the non-linear model, after considering the different techniques available, Lagrange's equations have been chosen as it is a more useful method when the system gets more complex. By performing the basic modeling already using the techniques that would be used in a more extensive future research, the bases are properly set and allow a direct comparison. Moreover, this method can be easily transported to any computation software allowing faster and saver results.

When dealing with the necessity of a linear model different approaches have been considered. However, Taylor's technique offers the best results and provides a structured methodology to linearize the equations. As this method implies the calculation of numerous partial derivatives external software; Maple16, had been used. The implementation in Maple16 has implied a more extensive knowledge on the software, but also a reliable source to ensure proper results. Moreover, providing a tool easy to modify when any change or update had to be made.

Another key element of the project has been the design and implementation of a control system. To do so, the Linear Quadratic Regulation (LQR) method has been chosen as it allowed the regulation of the system while letting some parameters up to the design so more or less weight could be given to its parameters. Translating into a faster stabilization thanks to a high control action or a slower regulation but with a lower control action.

Moreover, in order to make a full analysis of the system and the results, the exchanged forces between the floor and the subject during the whole stabilization process have been computed and implemented on Matlab. The obtained results lead to a wider understanding as showed the limitations of the system when depending on the perturbation they required an implausible force value and direction. However, values have been found where the required forces to stabilize the system were performed in a plausible sense and direction.

Once the initial objective of designing and implementing a controller for a balance system with a frontal approach had been accomplished new ways of improving the model have been discussed. The natural step, though, was to implement an elastic parameter in order to simulate the hip joint. In order to do so, an extended bibliographical research has been done. After analyzing numerous studies that dealt with values for damping and stiffness coefficients regarding the different joints, it can be concluded that there is a lack of research for a frontal approach. All studies focused on a sagittal study of movement, and even in this case the values for elastic coefficients differed significantly from subject to subject. However, all the research has been crucial to understand the behavior of the joints and be able to approximate a value taking into account the mobility range of the hip joint in the frontal plane.

Finally, the study of a non-linear control law allowed a different approach to the case of study itself. Leading to a wider understanding of the field of control and regulation even though the results were not the expected ones, but it set a start point for future projects.

Overall, the use of powerful software such as Matlab and its graphical programming environment; Simulink, has allowed avoiding the necessity to solve the system of differential equations by simulating the system itself. It has been a key element, as only by obtaining the simulations of the different scenarios it has been possible to compare the results and reach all the conclusions stated above.

Regarding where a future research could be focused on, it would be really interesting to approximate the elastic component of the joints with an exponential function instead of a linear one. Moreover, in order to get a more precise research, it would be better to follow a sagittal approach as there is more literature about it and more precise values could be used. Also a more extent study on non-linear controllers could be performed leading to more complex regulating systems.

Bibliography

[1] Aissaoui, R., Dausereau, J. (1999). *Biomechanical analysis and modeling of sit to stand task: a literature review.* Systems, Man, and Cybernetics. IEEE SMC '99 Conference Proceedings. IEEE International Conference.

[2] Anand, V.V., Lipson, H., Saxena, A., Vaero-Cuevas, F.J. (2007). *Beyond Parameter Estimation: Extending Biomechanical Modeling by the Explicit Exploration of Model Topology.* Transactions on biomedical engineering, Vol. 54, n.11, p.1951-1964. IEEE Publications.

[3] Androwis, G.J., Foulds, R.A., Simon, D. (2012). *Assessment of passive knee stiffness and set point.* Bioengineering Conference (NEBEC). IEEE 38th Annual Northeast.

[4] Andrysek, J., Cleghorn, W., Naumann S. (2004). *Design characteristics of pediatric prosthetic knees.* Transactions on Neural Systems and Rehabilitation Engineering Vol.12, n.4, p.369-378. IEEE Publications.

[5] Becke, M., Schlegl, T. (2011). *Toward an experimental method for evaluation of biomechanical joint behavior under high variable load conditions.* Robotics and Automation (ICRA). IEEE International Conference.

[6] Beer, F.P., Johnston, E.R. Jr., Mazurek, D.F., Eisenberg, R.E. (2009) *Vector Mechanics for Engineers.* 9th Edition. Mc.GrawHill.

[7] Blanquer, E., Dufour, A., Henriksson, E., Mairesse, B., Riback, J. (2006). *Pendubot.* Final Report. KTH.

[8] Block, D. J. (1991). *Mechanical design and control of the pendubot*. Final Thesis. University of Illinois.

[9] Bonnet, V., Fraisse, P., Joukov, V., Kulic, D. Ramdani, N., Venture, G. (2016). *Monitoring of hip and knee joint angles using a single inertial measurement unit during lower limb rehabilitation*. IEEE Sensors Journal Vol.16, n. 6, p1557-1764. IEEE Publications.

[10] Boom, H.B.K., Hermens, H.J., Hoopman, B., Van der Spek, J.H., Veltink, P.H. (2003). *A model-based approach to stabilizing crutch supported paraplegic standing by artifictial hip joint stiffness.* IEEE Transactions on Neural Systems and Rehabilitation Engineering Vol.11, n. 4, p.443-451. IEEE Publications.

[11] Boom, H.B.K., Hermens, H.J., Hoopman, B., Van der Spek, J.H., Veltink, P.H. (2003). *Static and dynamic evaluation of the influence of supplementary hip-joint stiffness on crutch-supported paraplegic stance.* IEEE Transactions on Neural Systems and Rehabilitation Engineering Vol.11, n. 4, p.452-462. IEEE Publications.

[12] Chadges, J.R., Haddad, J.M., Raman, A., Rietdyk, S., Zelaznik, H.N. (2013). *Dynamic stability of a human standing on a balance board*. Journal of Biomechanics Vol. 46, p2593-2602. ElSevier.

[13] Duerk, J., Koozekanani, S.H. (1985). *Determination of Body Segment Paramters and Their Effectinte Calculation of the Position of Center of Pressure During Postural Sway.* Transactions on Biomedical Engineering, Vol. BME-32, n.1, p.67-69. IEEE Publications.

[14] Edrich, T., Riener, R. (1997). *Passive elastic joint moments in the lower extremity.* Engineering in Medicine and Biology Society, 1997. IEEE 19th Annual International Conference.

[15] El Hafi, F., Gorce, P. (1998). *Biomechanical modeling of human body control scheme in stepping motion over an obstacle.* Engineering in Medicine and Biology Society, Vol. 20, n.5. IEEE 20th International Conference.

[16]Fantoni, I., Lozano, R.,Spong, M. . (2000). *Engergy Based Control of the Pendubot.* Transactions on automatic control. Vol. 45, n.4, p.725-729. IEEE Publications.

[17]Farahmand, F., Parnianpour, M., Pejhan, S. (2008). *Design optimization of an above-knee prosthesis based on kinematics of gait.* Engineering in Medicine and Biology Society. EMBS 2008. IEEE 30th Annual International Conference.

[18]Hanavan, E.P., Caotain, JR. (1964). *A Mathematical model of the human body.* USAF.

[19]Leonhardt, S., Lüken, M., Misgeld, B. J.E. (2016). *Identification of isolated biomechanical parameters with a wireless body sensor network.* Wearable and Implantable Body Sensor Networks. IEEE 13th International Conference.

[20]Matjacic, Z., Olensek, A. (2005). *Further steps toward more human-like passive bipedal walking robots.* Robotics and Automation. IEEE International Conference.

[21] Silver-Thorn, B., Tönük, E. (2003). *Nonlinear elastic material property estimation of lower extremity residual limb tissues.* Transactions on Neural Systems and Rehabilitation EngineeringVol.11, n.1, p.43-45. IEEE Publications.

[22]Tenerelli, A. (2016)*Study of a Balance Postural Control System.*Politecnico di Bari.

[23] Winter, D.A. (2009). *Biomechanics and motor control of human movement.*4th Edition. John Wiley & Sons, INC.

ANNEXES

Annex A

In this Annex all the Matlab detailed files for the original model can be found.

A1. Matlab Script

Matlab Script of the initial model, both linear and non-linear

```
clear all
close all

%DATI
m1=32.34;
l1=0.9275;
lG1=l1/2;
m2=30.66+7; %taking into acount the arms (m2+m3)
l2=0.504;
lG2=(319/538)*l2;
g=9.81;

%Moments of inertia --> Body 1 and Body 23 as Slender rods
J1=9.4548;
J2=11.9831;

%Moments of inertia --> Body 1 as rectangular prism,
%and Body 23 as a composition of a rectangular prism and a slender rod
% J1=9.574656;
% J2=11.86929;


%P.Equilibrio
x0=[0.1 0 0 0];

%%%%%
%LINEARE

f11=-(J2+m2*lG2^2)*(m1*lG1+m2*l1)*g/(m2^2*l1^2*lG2^2-(J2+m2*lG2^2)*(J1+m2*l1^2));
f12=m2^2*g*lG2^2*l1/(m2^2*l1^2*lG2^2-(J2+m2*lG2^2)*(J1+m2*l1^2));
f13=0;
f14=0;

f21=m2*l1*lG2*(m1*lG1+m2*l1)*g/((J1+m2*l1^2)*(m2^2*l1^2*lG2^2/(J1+m2*l1^2)-J2-m2*lG2^2));
f22=-m2*g*lG2/(m2^2*l1^2*lG2^2/(J1+m2*l1^2)-J2-m2*lG2^2);
f23=0;
f24=0;

g11=m2*l1*lG2/(m2^2*l1^2*lG2^2-(J2+m2*lG2^2)*(J1+m2*l1^2));
g22=-1/(m2^2*l1^2*lG2^2/(J1+m2*l1^2)-J2-m2*lG2^2);

A=[0 0 1 0 ;0 0 0 1 ; f11 f12 f13 f14; f21 f22 f23 f24;]
B=[0;0;g11;g22;]
```

```
44
45      %Non c'era nella versione originale del matlab, ma si nella tesis
46 -    lambda=eig(A)
47 -    Co=ctrb(A,B)
48 -    n=rank(Co)
49      %%%
50
51      %disturbo di Coppia:
52 -    ampiezza_dist=20;
53 -    t_dist=(0.5);
54
55 -    C = [1 0 0 0;0 1 0 0 ;0 0 1 0; 0 0 0 1];
56 -    D = [0;0;0;0];
57 -    Q = C'*C;
58 -    Q(1,1) = 500;
59 -    Q(2,2) = 6500;
60 -    Q(3,3)=0;
61 -    Q(4,4)=0;
62 -    R = 1;
63 -    K = lqr(A,B,Q,R)
64
65      %PLOT
66 -    sim('Poleplc8.slx')
67
68 -    fsa     = 12;           % fontsize axis 14
69 -    fsl     = 15;           % fontsize labels 18
70 -    fsc     = 11;           % fontsize commenti
71 -    font    = 'Times';
72
73 -    close all
74
75
76 -    figure(1),plot(state_system)
77 -    title('System State Dynamics')
78          xlabel('Time $$[s]$$','fontsize',fsl,'FontName', font, 'Interpreter',
79          'Latex')
80          ylabel('System state $$[rad]$$ - $$[rad \cdot sec^{-1}]$$','fontsize',
81          fsl,'FontName', font, 'Interpreter', 'Latex')
82 -        set(gca,'fontsize',fsa)        % dimensioni del testo sugli assi
83 -        grid on
84 -        set(gca,'xlim',[0 10],'ylim',[-.5 .5])
85 -        set(gca,'XTick', 0:1:10, 'YTick', -.5:.05:.5)
86 -        legend('\theta_1','\theta_2', 'd\theta_1/dt','d\theta_2/dt')
87 -        legend('boxon')
88 -        set(legend, 'FontName', font, 'FontSize', fsl)
89 -        print('-depsc','-tiff','-r300','SState')
90
```

```
91
92
93      %NON LINEARE %u(1)=x1;u(2)=x2;u(3)=x3;u(4)=x4;u(5)=CM3
94 -    A1=J1+m2*l1^2;
95 -    A2=m2*l1*lG2;
96 -    A3=m2*l1*lG2;
97 -    A4=(m1*lG1+m2*l1)*g;
98 -    B1=m2*l1*lG2;
99 -    B2=J2+m2*lG2^2;
100 -   B3=m2*l1*lG2;
101 -   B4=m2*g*lG2;
102
103     %%%%%%%%%%%%%%%%%%%%
104 -   sim('Nonlineare8.slx')
105
106 -   fsa     = 12;           % fontsize axis 14
107 -   fsl     = 15;           % fontsize labels 18
108 -   fsc     = 11;           % fontsize commenti
109 -   font    = 'Times';
```

A2. Simulink Linear system

Simulink model of the linear system.

The file is called Poleplc, from pole placement.

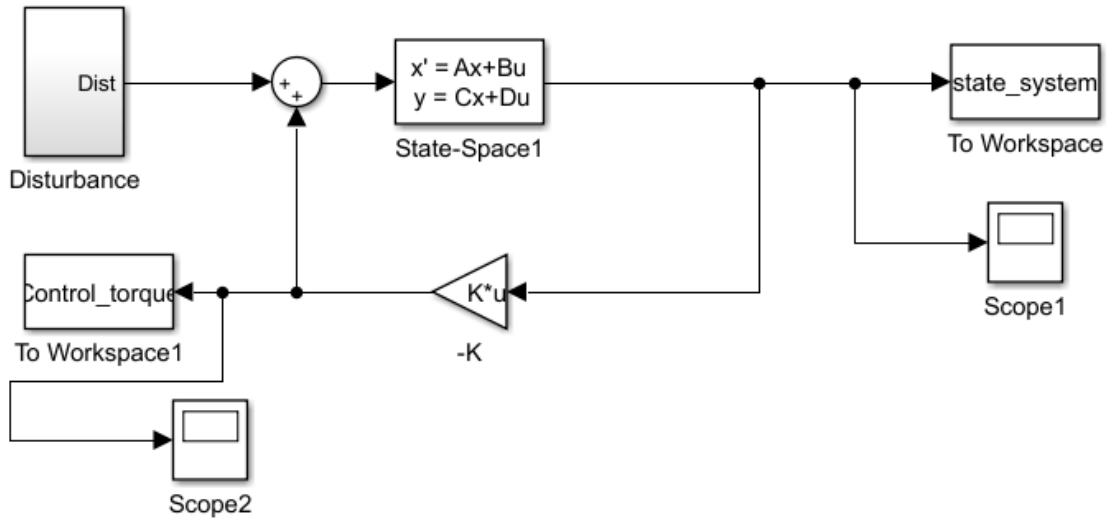

A3. Simulink Non-Linear system

Simulink model of the non-linear system

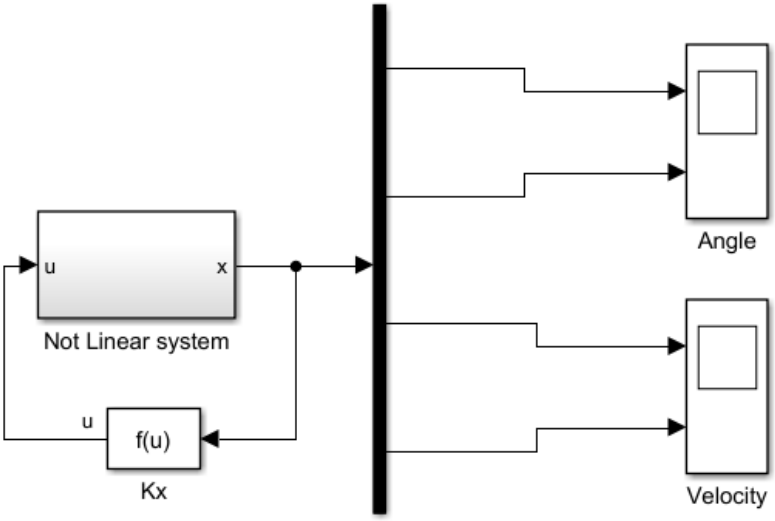

Inside the “Non linear system block”:

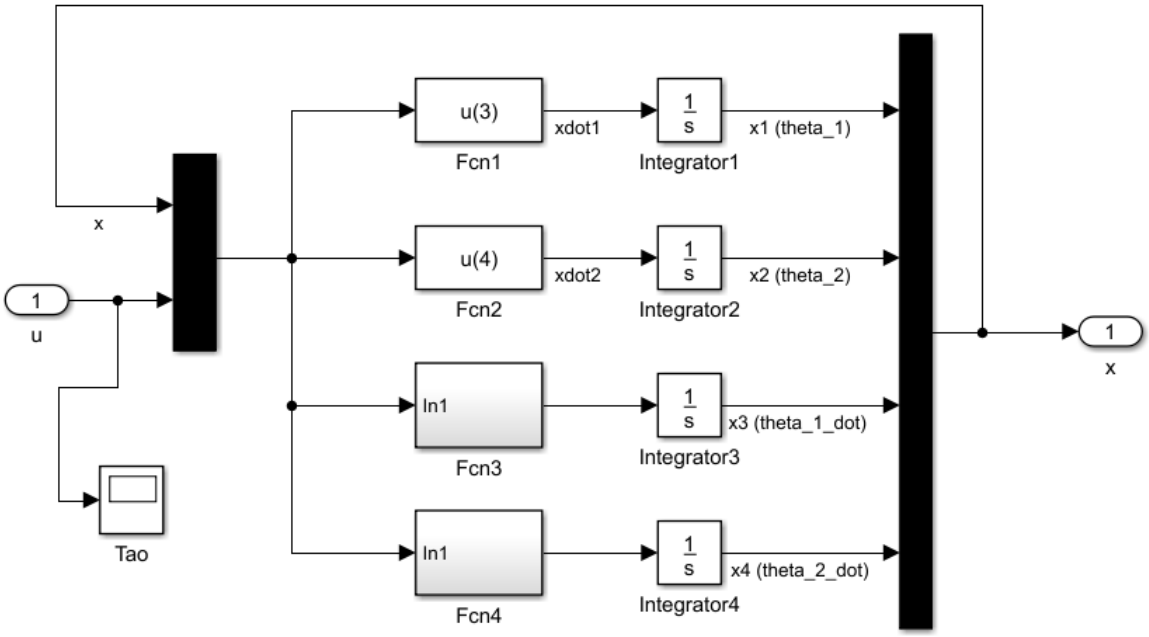

In order to make it easy to find typing mistakes the functions have been divided in different blocs

Inside view of the bloc “Fcn3”

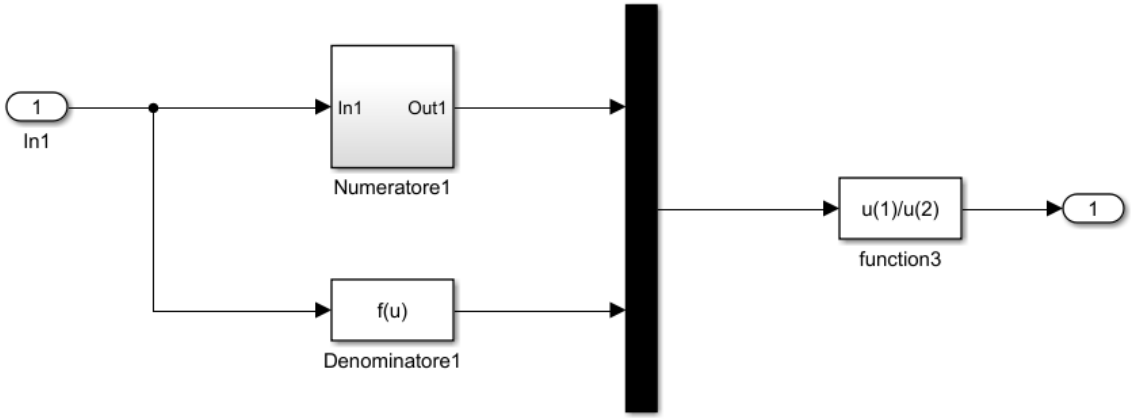

The “Denominatore1” having the following value:

Denominatore1: B1*A2*(cos(u(1)-u(2)))^2-B2*A1

While the inside view of the “Numeratore1” bloc is the following:

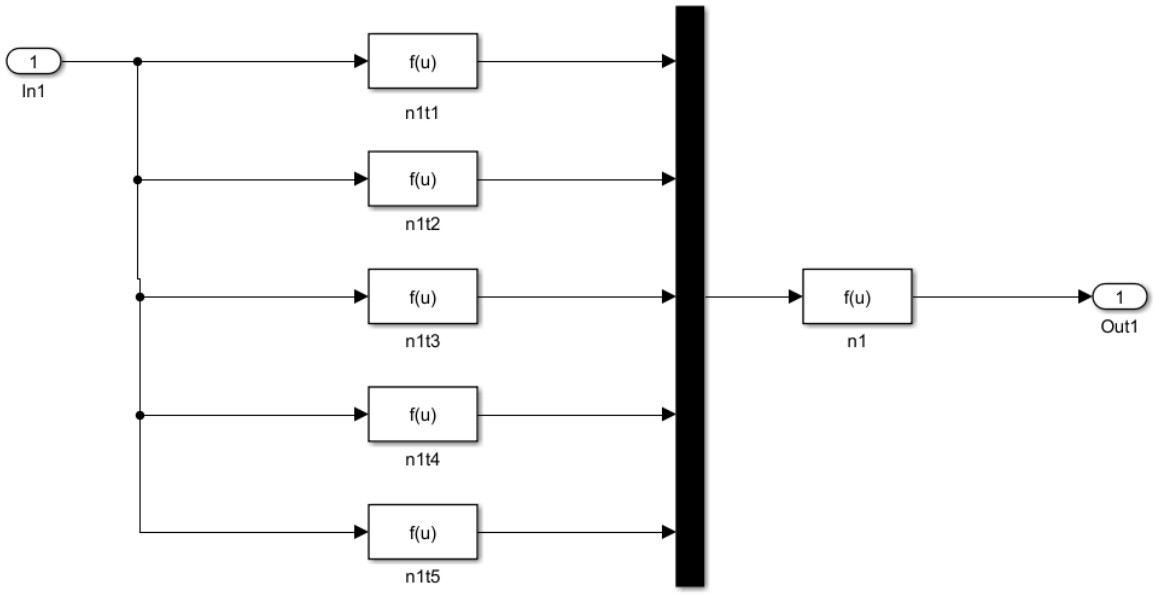

As it can be seen, the numerator has been divided in each different term for an easier control of mistakes, leading to the following values:

n1t1: B2*A3*u(4)^2*sin(u(1)-u(2))

n1t2: B2*A4*sin(u(1))

n1t3: B3*A2*u(3)^2*sin(u(1)-u(2))*cos(u(1)-u(2))

n1t4: B4*A2*sin(u(2))*cos(u(1)-u(2))

n1t5: A2*cos(u(1)-u(2))*u(5)

n1: u(1)-u(2)+u(3)+u(4)+u(5)

Inside view of the block "Fnc4"

The same structure has been followed for the last equation

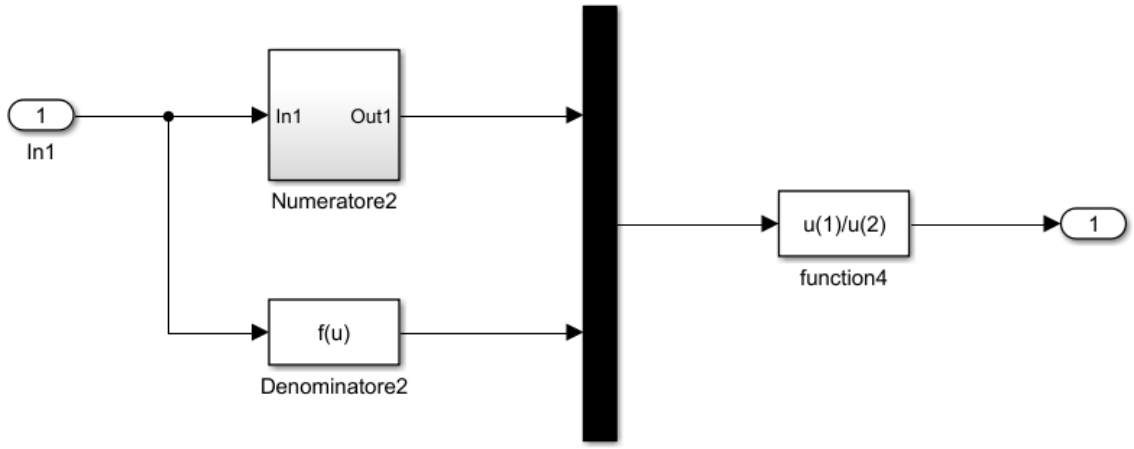

The "Denominatore2" having the following value:

Denominatore2: ((B1*A2)/A1)*(cos(u(1)-u(2)))^2-B2

While the inside view of the "Numeratore2" bloc is the following:

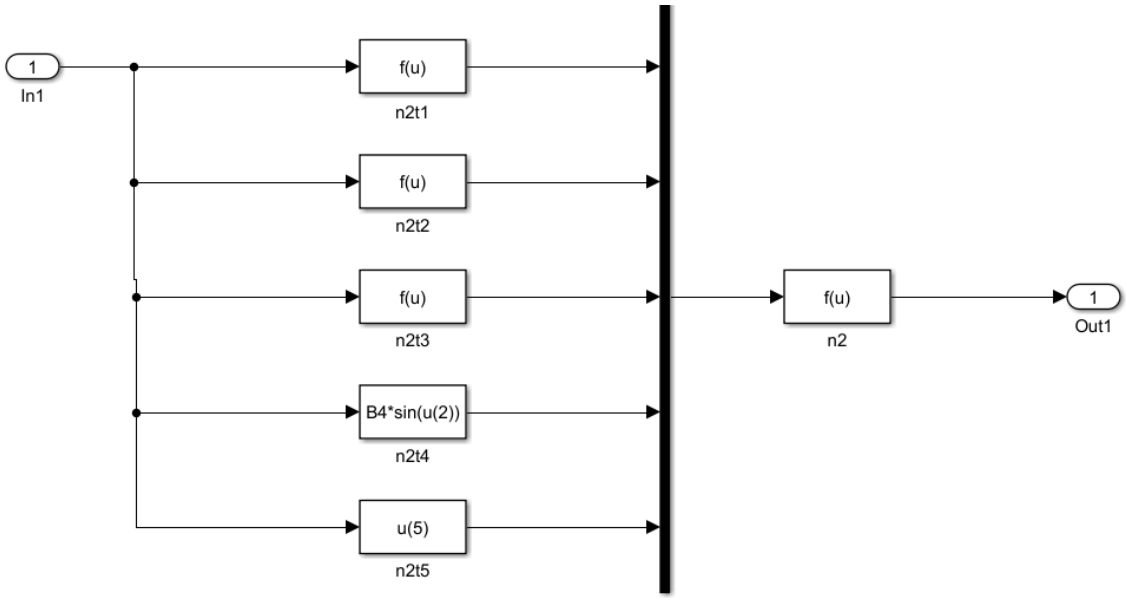

As it can be seen, the numerator has been divided in each different term for an easier control of mistakes, leading to the following values:

n2t1: (B1*A3/A1)*u(4)^2*sin(u(1)-u(2))*cos(u(1)-u(2))

n2t2: (B1*A4/A1)*sin(u(1))*cos(u(1)-u(2))

n2t3: B3*u(3)^2*sin(u(1)-u(2))

n2t4: B4*sin(u(2))

n2t5: u(5)

n2: -u(1)+u(2)-u(3)-u(4)-u(5)

A4. Simulink Non-Linear system with forces

To study how plausible the results were, the forces between the body and the floor have been simulated, meaning the addition of some blocks to the Simulink system while keeping the “Non linear system” the same.

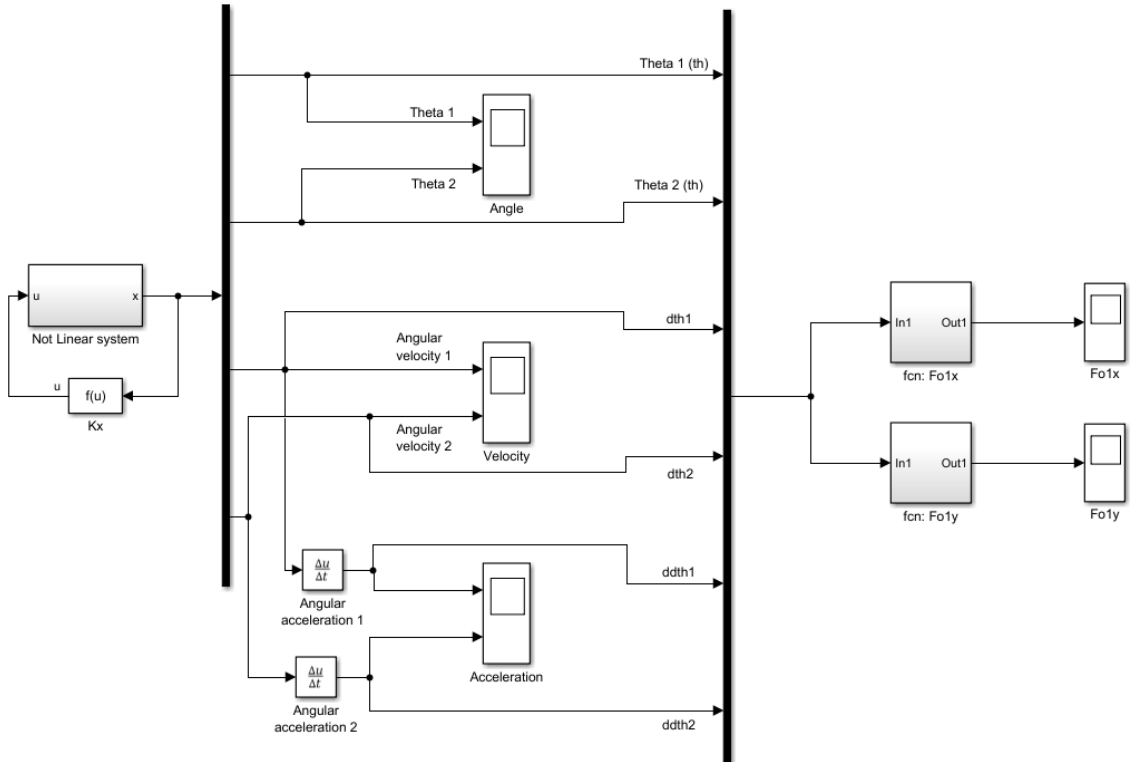

Where the block “fcn:Fo1x” has the following structure and values

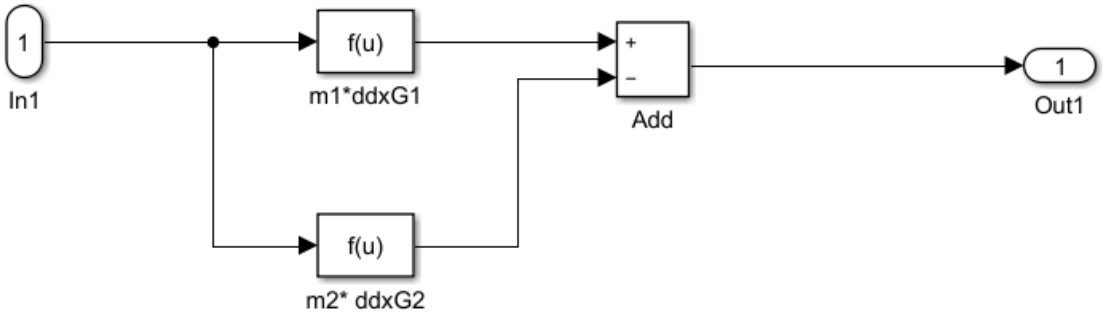

m1*ddxG1: m1*(lG1*u(5)*cos(u(1))-lG1*(u(3))^2*sin(u(1)))

m2*ddxG2: m2*(l1*u(5)*cos(u(1))-l1*(u(3))^2*sin(u(1))+lG2*u(6)*cos(u(2))-lG2*(u(4))^2*sin(u(2)))

And the block “fcn:Fo1y” has the following structure and values

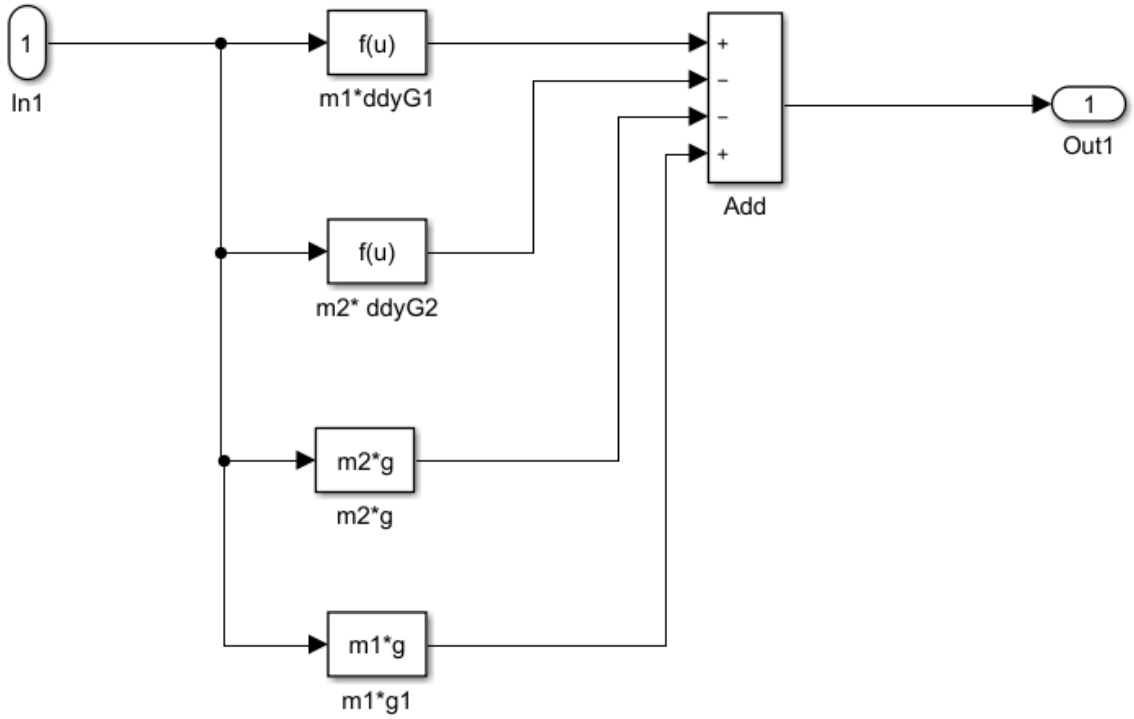

m1*ddyG1: m1*(-lG1*u(5)*sin(u(1))-lG1*(u(3))^2*cos(u(1)))

m2*ddyG2: m2*(-l1*u(5)*sin(u(1))-l1*(u(3))^2*cos(u(1))-lG2*u(6)*sin(u(2))-lG2*(u(4))^2*cos(u(2)))

m2g: m2*g

m1g: m1*g

Annex B

In this Annex the modifications performed to the original Matlab files can be found in order to adapt them to the updated model including an elastic element equivalent to the hip joint.

B1. Matlab script for the updated model

```
clear all
close all
%DATI
m1=32.34;
l1=0.9275;
lG1=l1/2;
m2=30.66+7; %taking into acount the arms (m2+m3)
l2=0.504;
lG2=(319/538)*l2;
g=9.81;

%Elastic coefficient hip frontal plane
Kelas=2.7;

%Moments of inertia --> Body 1 and Body 23 as Slender rods
J1=9.4548;
J2=11.9831;

%Moments of inertia --> Body 1 as rectangular prism,
%and Body 23 as a composition of a rectangular prism and a slender rod
% J1=9.574656;
% J2=11.86929;


%P.Equilibrio
x0=[0.1 0 0 0];

%%%%%
%LINEARE

f11=(-(J2+m2*lG2^2)*(m1*lG1+m2*l1)*g-(J2+m2*lG2^2)*Kelas)/(m2^2*l1^2*lG2^2-
(J2+m2*lG2^2)*(J1+m2*l1^2));
f12=(m2^2*g*lG2^2*l1+(J2+m2*lG2^2)*Kelas)/(m2^2*l1^2*lG2^2-(J2+m2*lG2^2)*
(J1+m2*l1^2));
```

```
f13=0;
f14=0;

f21=(m2*l1*lG2*(m1*lG1+m2*l1)*g/(J1+m2*l1^2)+m2*l1*lG2*Kelas/(J1+m2*l1^2))/
(m2^2*l1^2*lG2^2/(J1+m2*l1^2)-J2-m2*lG2^2);
f22=(-m2*g*lG2-m2*l1*lG2*Kelas/(J1+m2*l1^2))/(m2^2*l1^2*lG2^2/(J1+m2*l1^2)
-J2-m2*lG2^2);
f23=0;
f24=0;

g11=m2*l1*lG2/(m2^2*l1^2*lG2^2-(J2+m2*lG2^2)*(J1+m2*l1^2));
g22=-1/(m2^2*l1^2*lG2^2/(J1+m2*l1^2)-J2-m2*lG2^2)

A=[0 0 1 0 ;0 0 0 1 ; f11 f12 f13 f14; f21 f22 f23 f24;]
B=[0;0;g11;g22;]

%Non c'era nella versione originale del matlab, ma si nella tesis
lambda=eig(A);
Co=ctrb(A,B);
n=rank(Co);
%%%

%disturbo di Coppia:
ampiezza_dist=20;
t_dist=(0.5);

C = [1 0 0 0;0 1 0 0 ;0 0 1 0; 0 0 0 1];
D = [0;0;0;0];
Q = C'*C;
Q(1,1) = 500;
Q(2,2) = 6500;
Q(3,3)=0;
Q(4,4)=0;
R = 1;
K = lqr(A,B,Q,R);

%PLOT
sim('Poleplc10.slx')

fsa     = 12;           % fontsize axis 14
fsl     = 15;           % fontsize labels 18
fsc     = 11;           % fontsize commenti
font    = 'Times';

close all
```

```
figure(1),plot(state_system)
title('System State Dynamics')
    xlabel('Time $$[s]$$','fontsize',fsl,'FontName', font, 'Interpreter',
    'Latex')
    ylabel('System state $$[rad]$$ - $$[rad \cdot sec^{-1}]$$','fontsize',
    fsl,'FontName', font, 'Interpreter', 'Latex')
    set(gca,'fontsize',fsa)        % dimensioni del testo sugli assi
    grid on
    set(gca,'xlim',[0 10],'ylim',[-1 1])
    set(gca,'XTick', 0:1:10, 'YTick', -1:.1:1)
    legend('\theta_1','\theta_2', 'd\theta_1/dt','d\theta_2/dt')
    legend('boxon')
    set(legend, 'FontName', font, 'FontSize', fsl)
    print('-depsc','-tiff','-r300','SState')

%NON LINEARE
%States var: u(1)=x1;u(2)=x2;u(3)=x3;u(4)=x4;u(5)=CM3
%Force var: u(1)=theta1;u(2)=theta2;u(3)=ang.vel.1;u(4)=ang.vel.2;
%           u(5)=ang.acceleration1;u(6)=ang.acceleration2
A1=J1+m2*l1^2;
A2=m2*l1*lG2;
A3=m2*l1*lG2;
A4=(m1*lG1+m2*l1)*g;
B1=m2*l1*lG2;
B2=J2+m2*lG2^2;
B3=m2*l1*lG2;
B4=m2*g*lG2;


%%%%%%%%%%%%%%%%%%%%%%
sim('Nonlineare10.slx')

fsa     = 12;           % fontsize axis 14
fsl     = 15;           % fontsize labels 18
fsc     = 11;           % fontsize commenti
font    = 'Times';
```

B2. Simulink diagrams for the updated model

In order to adapt the original Simulink diagrams two blocs had to be added in the functions of the non-linear system.

In this Annex the inside view of the modificated blocs can be found. The blocs that are not shown means that remain the same.

The general scheme remains the same as it can be seen below:

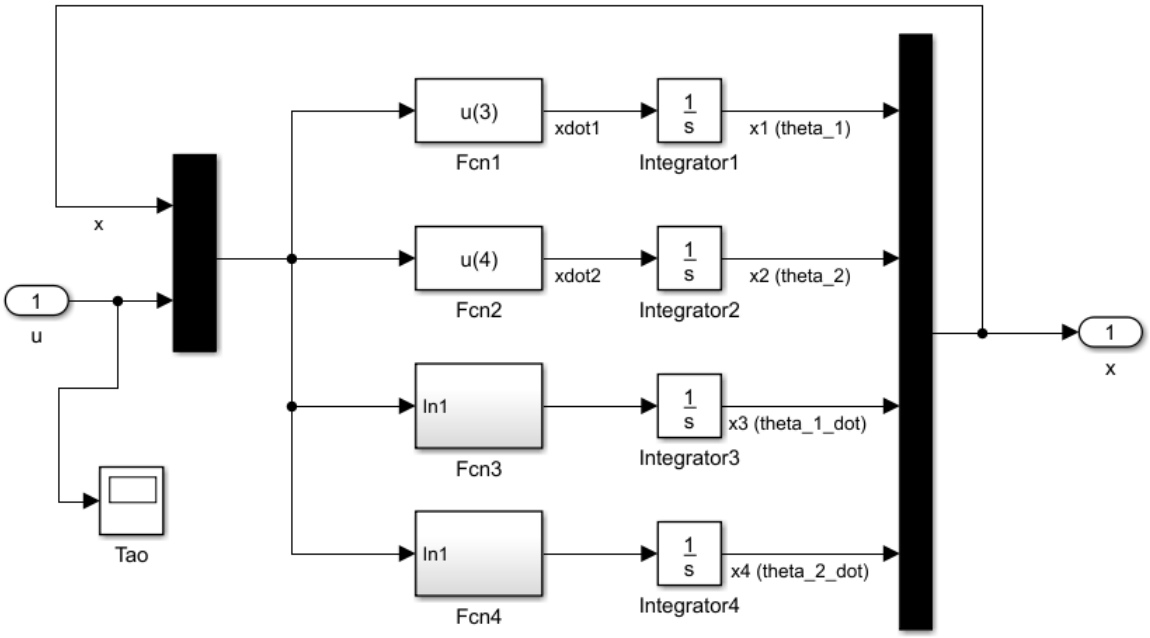

Inside view of the bloc "Numeratore 1" inside the bloc "Fcn3"

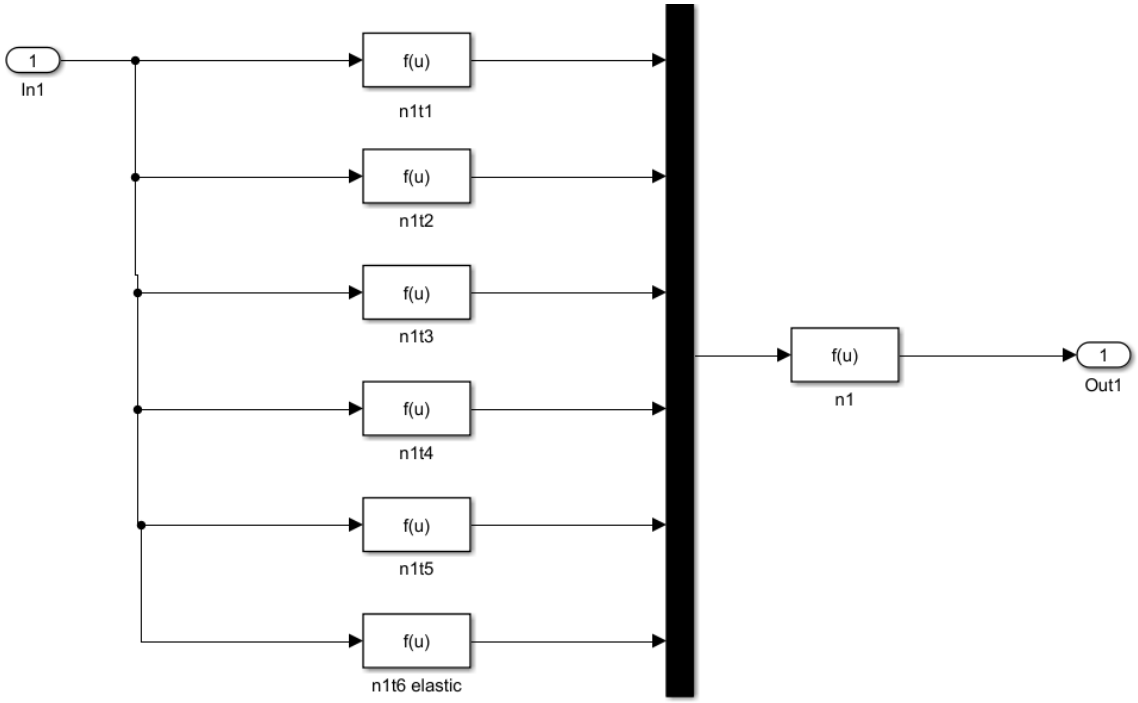

As it can be seen, a 6th bloc has been added corresponding to the elastic element.

n1t1: B2*A3*u(4)^2*sin(u(1)-u(2))

n1t2: B2*A4*sin(u(1))

n1t3: B3*A2*u(3)^2*sin(u(1)-u(2))*cos(u(1)-u(2))

n1t4: B4*A2*sin(u(2))*cos(u(1)-u(2))

n1t5: A2*cos(u(1)-u(2))*u(5)

n1n6 elastic B2*(-Kelas*(u(1)-u(2)))

n1: u(1)-u(2)+u(3)+u(4)+u(5)-u(6)

Inside view of the bloc "Numeratore 2" inside the bloc "Fcn4"

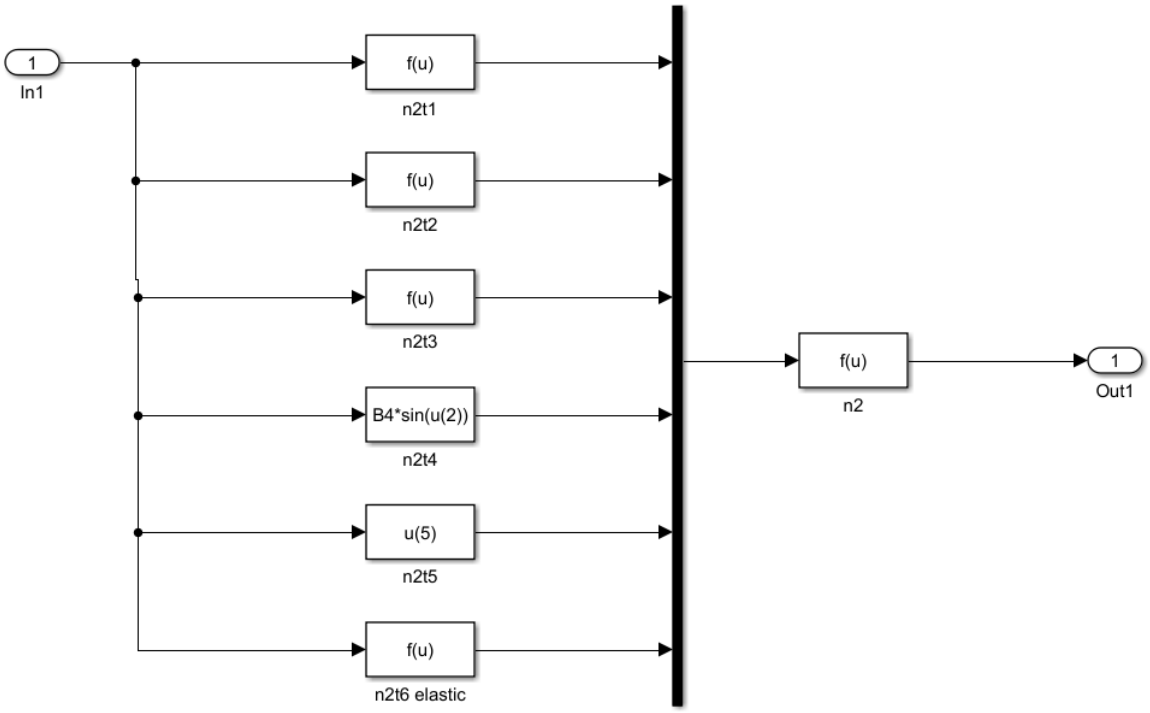

Again, a 6th bloc has been added corresponding to the elastic component.

n2t1: (B1*A3/A1)*u(4)^2*sin(u(1)-u(2))*cos(u(1)-u(2))

n2t2: (B1*A4/A1)*sin(u(1))*cos(u(1)-u(2))

n2t3: B3*u(3)^2*sin(u(1)-u(2))

n2t4:	B4*sin(u(2))
n2t5:	u(5)
n2t6 elastic	(B1/A1)*(-Kelas*(u(1)-u(2)))*cos(u(1)-u(2))
n2:	-u(1)+u(2)-u(3)-u(4)-u(5)+u(6)

Annex C

The implementation of the non-linear controller in Matlab can be found below.

C1. Matlab Script Non-linear control law

```
clear all
close all
%DATI
m1=32.34;
l1=0.9275;
lG1=l1/2;
m2=30.66+7; %taking into acount the arms (m2+m3)
l2=0.504;
lG2=(319/538)*l2;
g=9.81;

%Moments of inertia --> Body 1 and Body 23 as Slender rods
J1=9.4548;
J2=11.9831;

%Moments of inertia --> Body 1 as rectangular prism,
%and Body 23 as a composition of a rectangular prism and a slender rod
% J1=9.574656;
% J2=11.86929;


%P.Equilibrio
x0=[0.05 0 0 0];

%Costanti controllore
ke=1.5;
kp=1;
kd=1;


%NON LINEARE
%States var: u(1)=x1;u(2)=x2;u(3)=x3;u(4)=x4;u(5)=CM3
%Force var: u(1)=theta1;u(2)=theta2;u(3)=ang.vel.1;u(4)=ang.vel.2;
%           u(5)=ang.acceleration1;u(6)=ang.acceleration2
A1=J1+m2*l1^2;
A2=m2*l1*lG2;
A3=m2*l1*lG2;
A4=(m1*lG1+m2*l1)*g;
B1=m2*l1*lG2;
B2=J2+m2*lG2^2;
B3=m2*l1*lG2;
B4=m2*g*lG2;
```

```
43
44      %CONTROLLORE
45      %Costanti per il controllore
46 -    Q1=A1;
47 -    Q2=A2;
48 -    Q3=A4/g;
49 -    Q4=B2;
50 -    Q5=B4/g;
51
52
53
54      %%%%%%%%%%%%%%%%%%%%%%
55 -    sim('NonliniearNL1.slx')
56
57 -    fsa     = 12;           % fontsize axis 14
58 -    fsl     = 15;           % fontsize labels 18
59 -    fsc     = 11;           % fontsize commenti
60 -    font    = 'Times';
61
```

C2. Matlab Simulink Non-linear control law

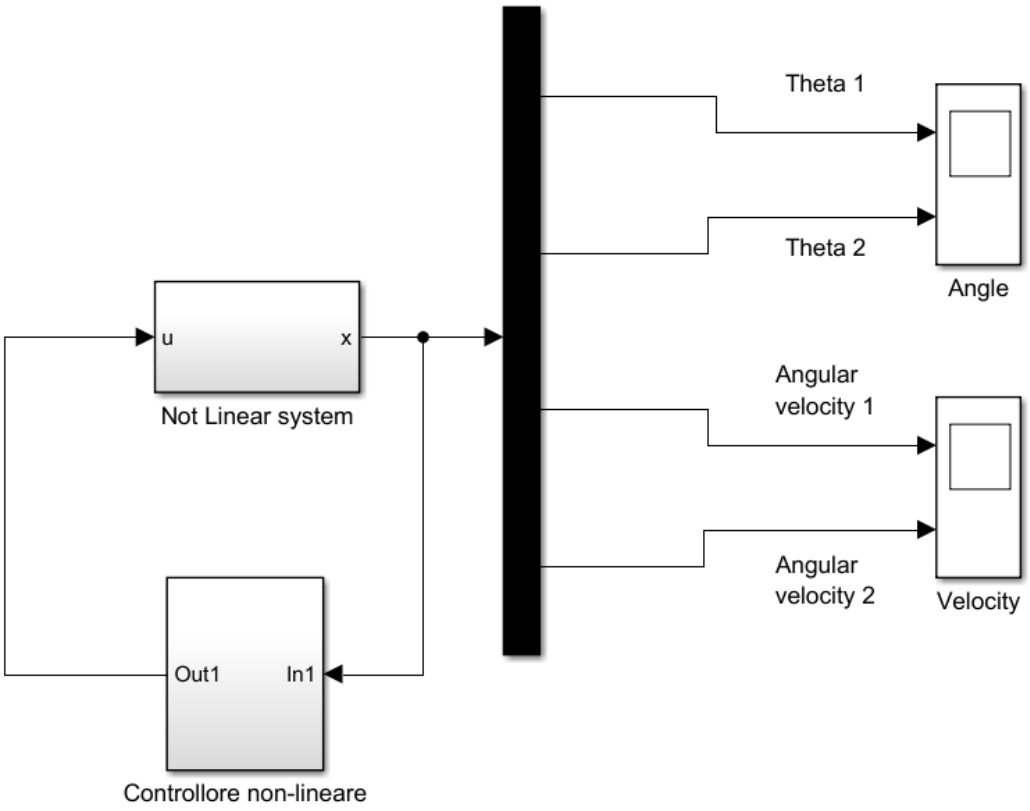

Inside view of the bloc "Controllore non-lineare"

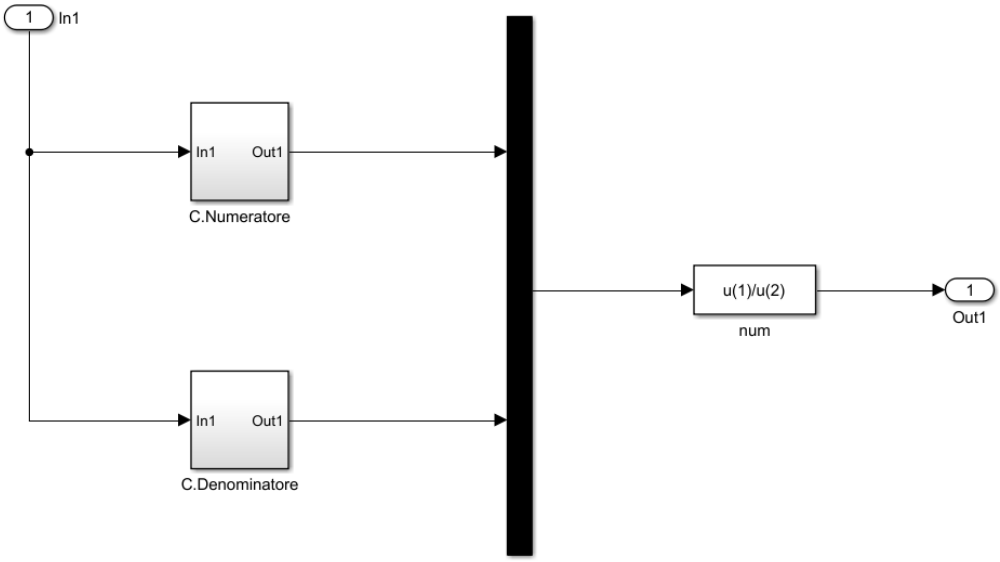

Inside view of the bloc "C.Numeratore" inside the bloc "Controllore non-lineare"

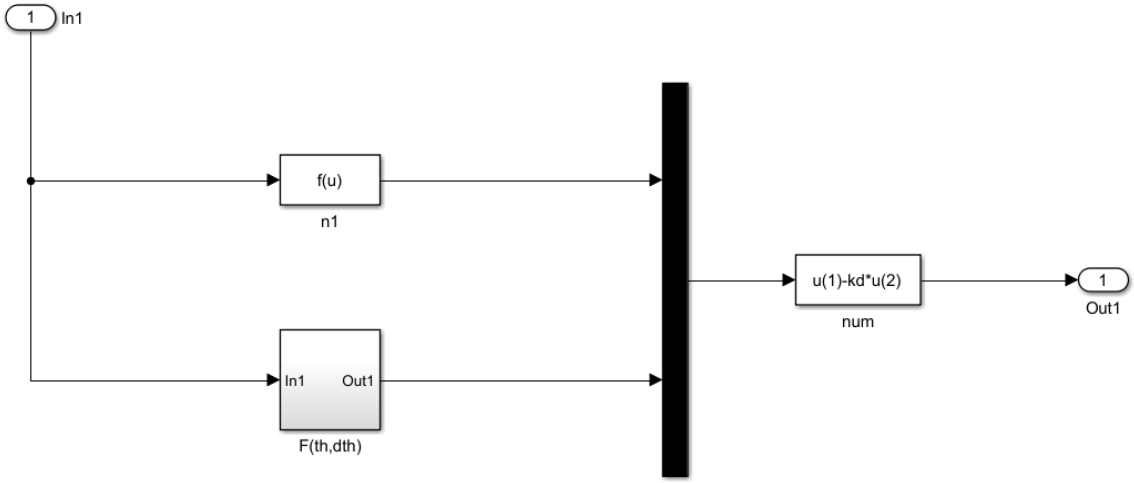

Being the block n1 equal to:

n1: -(Q1*Q4-Q2^2*(cos(u(1)-u(2)))^2)*(u(4)+kp*u(2))

And the block F(th,dth) following the next inner structure:

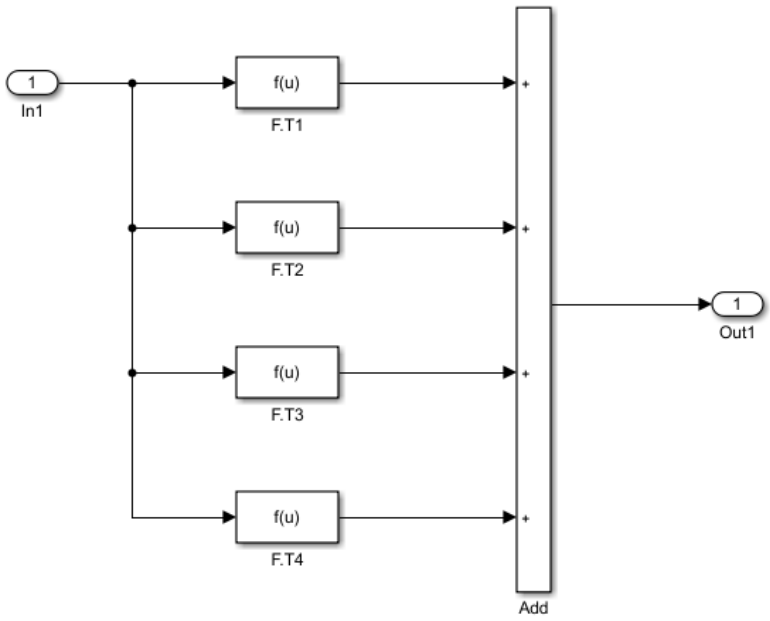

Where:

F.T1: Q2^2*cos(u(1)-u(2))*sin(u(1)-u(2))*(u(4))^2

F.T2: -Q2*Q3*g*cos(u(1)-u(2))-sin(u(1))

F.T3: Q1*Q2*sin(u(1)-u(2))*u(3)^2

F.T4: Q1*Q5*g*sin(u(2))

Inside view of the bloc "C.Denominatore" inside the bloc "Controllore non-lineare"

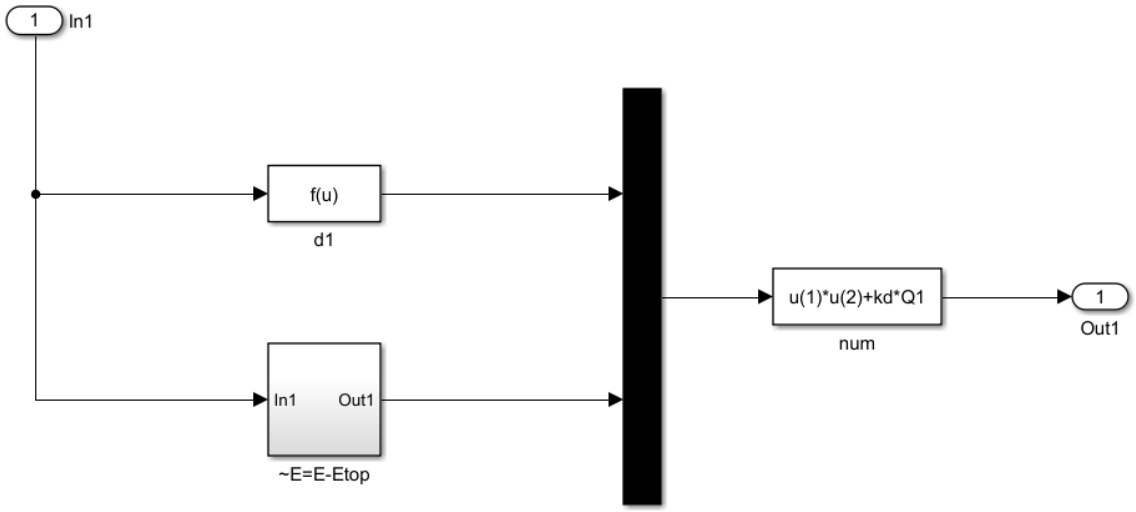

Being the block d1 equal to:

d1: ke*(Q1*Q4-Q2^2*(cos(u(1)-u(2)))^2)

And the block ~E=E-Etop following the next inner structure:

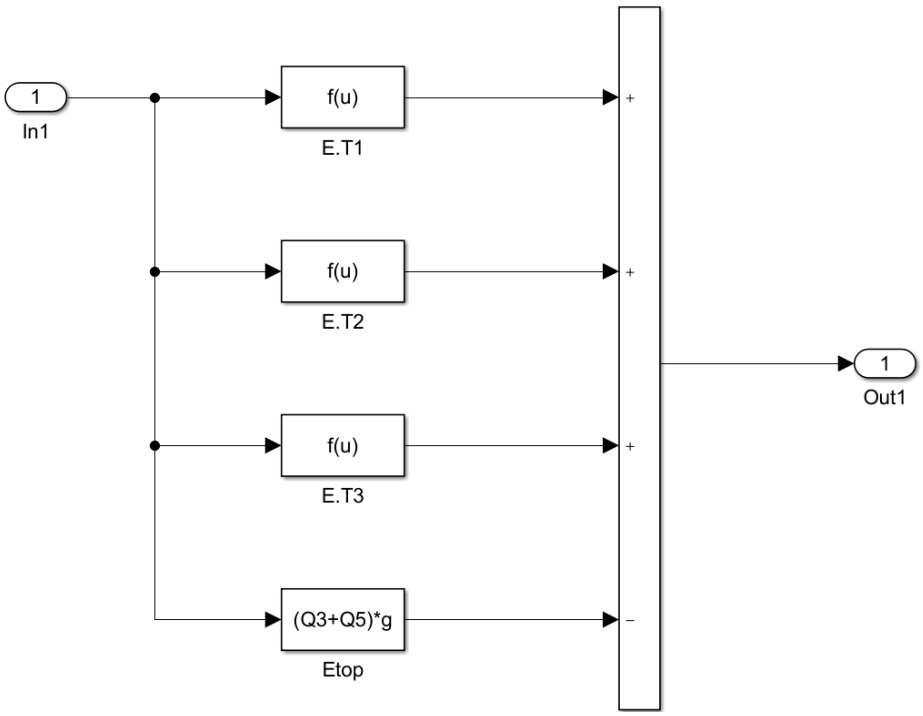

Where:

E.T1: 0.5*Q1*u(3)^2

E.T2: Q3*g*cos(u(1))

E.T3: Q5*g*cos(u(2))

Etop: (Q3+Q5)*g

Regarding the subtraction of "E_{top}", be aware of the negative sign in the "Add" block itself.

Annex D

Maple16 has been used to compute the partial derivatives from the Taylor's expansion and evaluate them in the equilibrium point in order to linearize the non-linear systems.

In this Annex all the detailed Matlab files and results can be found for both the original and updated model.

D1. Maple16 Initial model

```
> A1:=J1+m2*l1^2:
> A2:=m2*l1*lG2:
> A3:=m2*l1*lG2:
> A4:=(m1*lG1+m2*l1)*g:
> B1:=m2*l1*lG2:
> B2:=J2+m2*lG2^2:
> B3:=m2*l1*lG2:
> B4:=m2*g*lG2:
> f1:=(t1,t2,dt1,dt2,CM3)->(B2*A3*dt2*sin(t1-t2)-B2*A4*sin(t1)+B3*A2*
  (dt1)^2*sin(t1-t2)*cos(t1-t2)+B4*A2*sin(t2)*cos(t1-t2)+A2*cos(t1-t2)*
  CM3)/(B1*A2*(cos(t1-t2))^2-B2*A1);
```

$$f1 := (t1, t2, dt1, dt2, CM3) \rightarrow \frac{1}{B1\,A2\cos(t1-t2)^2 - B2\,A1}\left(B2\,A3\,dt2\sin(t1-t2)\right. \quad (1)$$
$$- B2\,A4\sin(t1) + B3\,A2\,dt1^2\sin(t1-t2)\cos(t1-t2) + B4\,A2\sin(t2)\cos(t1-t2)$$
$$\left. + A2\cos(t1-t2)\,CM3\right)$$

```
>
>
> f2:=(t1,t2,dt1,dt2,CM3)->((-B1*A3/A1)*(dt2)^2*sin(t1-t2)*cos(t1-t2)+
  (B1*A4/A1)*sin(t1)*cos(t1-t2)-B3*(dt1)^2*sin(t1-t2)-B4*sin(t2)-CM3)/(
  ((B1*A2)/A1)*(cos(t1-t2))^2-B2);
```

$$f2 := (t1, t2, dt1, dt2, CM3) \rightarrow \frac{1}{\frac{B1\,A2\cos(t1-t2)^2}{A1} - B2}\left(\quad (2)\right.$$
$$- \frac{B1\,A3\,dt2^2\sin(t1-t2)\cos(t1-t2)}{A1} + \frac{B1\,A4\sin(t1)\cos(t1-t2)}{A1} - B3\,dt1^2\sin(t1-t2)$$
$$\left. - B4\sin(t2) - CM3\right)$$

```
>
> f11:=diff(f1(t1,t2,dt1,dt2,CM3),t1);
```

$$f11 := \left(\left(J2 + m2\,lG2^2\right) m2\,l1\,lG2\,dt2\cos(t1-t2) - \left(J2 + m2\,lG2^2\right)(m1\,lG1 + m2\,l1)\,g\cos(t1) + m2^2\,l1^2\,lG2^2\,dt1^2\cos(t1-t2)^2 - m2^2\,l1^2\,lG2^2\,dt1^2\sin(t1-t2)^2 - m2^2\,g\,lG2^2\,l1\sin(t2)\sin(t1-t2) - m2\,l1\,lG2\sin(t1-t2)\,CM3\right) \Big/ \left(m2^2\,l1^2\,lG2^2\cos(t1-t2)^2 - \left(J2 + m2\,lG2^2\right)\left(J1 + m2\,l1^2\right)\right) + \left(2\left(\left(J2 + m2\,lG2^2\right) m2\,l1\,lG2\,dt2\sin(t1-t2) - \left(J2 + m2\,lG2^2\right)(m1\,lG1 + m2\,l1)\,g\sin(t1) + m2^2\,l1^2\,lG2^2\,dt1^2\sin(t1-t2)\cos(t1-t2) + m2^2\,g\,lG2^2\,l1\sin(t2)\cos(t1-t2) + m2\,l1\,lG2\cos(t1-t2)\,CM3\right) m2^2\,l1^2\,lG2^2\cos(t1-t2)\sin(t1-t2)\right) \Big/ \left(m2^2\,l1^2\,lG2^2\cos(t1-t2)^2 - \left(J2 + m2\,lG2^2\right)\left(J1 + m2\,l1^2\right)\right)^2 \quad (3)$$

```
>
> eval(f11,[t1=0,t2=0,dt1=0,dt2=0,CM3=0]);
```

$$-\frac{\left(J2 + m2\,lG2^2\right)(m1\,lG1 + m2\,l1)\,g}{m2^2\,l1^2\,lG2^2 - \left(J2 + m2\,lG2^2\right)\left(J1 + m2\,l1^2\right)} \quad (4)$$

```
> f12:=diff(f1(t1,t2,dt1,dt2,CM3),t2);
```

$$f12 := \left(-\left(J2 + m2\,lG2^2\right) m2\,l1\,lG2\,dt2\cos(t1-t2) - m2^2\,l1^2\,lG2^2\,dt1^2\cos(t1-t2)^2 + m2^2\,l1^2\,lG2^2\,dt1^2\sin(t1-t2)^2 + m2^2\,g\,lG2^2\,l1\cos(t2)\cos(t1-t2) + m2^2\,g\,lG2^2\,l1\sin(t2)\sin(t1-t2) + m2\,l1\,lG2\sin(t1-t2)\,CM3\right) \Big/ \left(m2^2\,l1^2\,lG2^2\cos(t1-t2)^2 - \left(J2 + m2\,lG2^2\right)\left(J1 + m2\,l1^2\right)\right) - \left(2\left(\left(J2 + m2\,lG2^2\right) m2\,l1\,lG2\,dt2\sin(t1-t2) - \left(J2 + m2\,lG2^2\right)(m1\,lG1 + m2\,l1)\,g\sin(t1) + m2^2\,l1^2\,lG2^2\,dt1^2\sin(t1-t2)\cos(t1-t2) + m2^2\,g\,lG2^2\,l1\sin(t2)\cos(t1-t2) + m2\,l1\,lG2\cos(t1-t2)\,CM3\right) m2^2\,l1^2\,lG2^2\cos(t1-t2)\sin(t1-t2)\right) \Big/ \left(m2^2\,l1^2\,lG2^2\cos(t1-t2)^2 - \left(J2 + m2\,lG2^2\right)\left(J1 + m2\,l1^2\right)\right)^2 \quad (5)$$

```
> eval(f12,[t1=0,t2=0,dt1=0,dt2=0,CM3=0]);
```

$$\frac{m2^2\,g\,lG2^2\,l1}{m2^2\,l1^2\,lG2^2 - \left(J2 + m2\,lG2^2\right)\left(J1 + m2\,l1^2\right)} \quad (6)$$

```
>
> f13:=diff(f1(t1,t2,dt1,dt2,CM3),dt1);
```

$$f13 := \frac{2\,m2^2\,l1^2\,lG2^2\,dt1\sin(t1-t2)\cos(t1-t2)}{m2^2\,l1^2\,lG2^2\cos(t1-t2)^2 - \left(J2 + m2\,lG2^2\right)\left(J1 + m2\,l1^2\right)} \quad (7)$$

```
> eval(f13,[t1=0,t2=0,dt1=0,dt2=0,CM3=0]);
```

$$0 \quad (8)$$

```
>
> f14:=diff(f1(t1,t2,dt1,dt2,CM3),dt2);
```

$$f14 := \frac{\left(J2 + m2\,lG2^2\right) m2\,l1\,lG2\sin(t1-t2)}{m2^2\,l1^2\,lG2^2\cos(t1-t2)^2 - \left(J2 + m2\,lG2^2\right)\left(J1 + m2\,l1^2\right)} \quad (9)$$

```
> eval(f14,[t1=0,t2=0,dt1=0,dt2=0,CM3=0]);
```

$$0 \quad (10)$$

```
>
```

```
> f21:=diff(f2(t1,t2,dt1,dt2,CM3),t1);
```

$$f21 := \frac{1}{\frac{m2^2\, l1^2\, lG2^2 \cos(t1-t2)^2}{J1 + m2\, l1^2} - J2 - m2\, lG2^2} \left(- \frac{m2^2\, l1^2\, lG2^2\, dt2^2 \cos(t1-t2)^2}{J1 + m2\, l1^2} + \frac{m2^2\, l1^2\, lG2^2\, dt2^2 \sin(t1-t2)^2}{J1 + m2\, l1^2} + \frac{m2\, l1\, lG2\, (m1\, lG1 + m2\, l1)\, g \cos(t1) \cos(t1-t2)}{J1 + m2\, l1^2} - \frac{m2\, l1\, lG2\, (m1\, lG1 + m2\, l1)\, g \sin(t1) \sin(t1-t2)}{J1 + m2\, l1^2} - m2\, l1\, lG2\, dt1^2 \cos(t1-t2) \right) + \left(2 \left(- \frac{m2^2\, l1^2\, lG2^2\, dt2^2 \sin(t1-t2) \cos(t1-t2)}{J1 + m2\, l1^2} + \frac{m2\, l1\, lG2\, (m1\, lG1 + m2\, l1)\, g \sin(t1)}{J1 + m2\, l1^2} \right. \right.$$

$$\left. \left. \cos(t1-t2) - m2\, l1\, lG2\, dt1^2 \sin(t1-t2) - m2\, g\, lG2 \sin(t2) - CM3 \right) m2^2\, l1^2\, lG2^2 \cos(t1-t2) \sin(t1-t2) \right) \Bigg/ \left(\left(\frac{m2^2\, l1^2\, lG2^2 \cos(t1-t2)^2}{J1 + m2\, l1^2} - J2 - m2\, lG2^2 \right)^2 (J1 + m2\, l1^2) \right)$$

```
> eval(f21,[t1=0,t2=0,dt1=0,dt2=0,CM3=0]);
```

$$\frac{m2\, l1\, lG2\, (m1\, lG1 + m2\, l1)\, g}{(J1 + m2\, l1^2) \left(\frac{m2^2\, l1^2\, lG2^2}{J1 + m2\, l1^2} - J2 - m2\, lG2^2 \right)} \tag{12}$$

```
> f22:=diff(f2(t1,t2,dt1,dt2,CM3),t2);
```

$$f22 := \frac{1}{\frac{m2^2\, l1^2\, lG2^2 \cos(t1-t2)^2}{J1 + m2\, l1^2} - J2 - m2\, lG2^2} \left(\frac{m2^2\, l1^2\, lG2^2\, dt2^2 \cos(t1-t2)^2}{J1 + m2\, l1^2} - \frac{m2^2\, l1^2\, lG2^2\, dt2^2 \sin(t1-t2)^2}{J1 + m2\, l1^2} + \frac{m2\, l1\, lG2\, (m1\, lG1 + m2\, l1)\, g \sin(t1) \sin(t1-t2)}{J1 + m2\, l1^2} + m2\, l1\, lG2\, dt1^2 \cos(t1-t2) - m2\, g\, lG2 \cos(t2) \right) - \left(2 \left(- \frac{m2^2\, l1^2\, lG2^2\, dt2^2 \sin(t1-t2) \cos(t1-t2)}{J1 + m2\, l1^2} + \frac{m2\, l1\, lG2\, (m1\, lG1 + m2\, l1)\, g \sin(t1) \cos(t1-t2)}{J1 + m2\, l1^2} - m2\, l1\, lG2\, dt1^2 \sin(t1-t2) - m2\, g\, lG2 \sin(t2) - CM3 \right) m2^2\, l1^2\, lG2^2 \cos(t1-t2) \sin(t1-t2) \right) \Bigg/ \left(\left(\frac{m2^2\, l1^2\, lG2^2 \cos(t1-t2)^2}{J1 + m2\, l1^2} - J2 - m2\, lG2^2 \right)^2 (J1 + m2\, l1^2) \right) \tag{13}$$

```
> eval(f22,[t1=0,t2=0,dt1=0,dt2=0,CM3=0]);
```

$$-\frac{m2\, g\, lG2}{\frac{m2^2\, l1^2\, lG2^2}{J1 + m2\, l1^2} - J2 - m2\, lG2^2} \tag{14}$$

```
>
> f23:=diff(f2(t1,t2,dt1,dt2,CM3),dt1);
```

$$f23 := -\frac{2\, m2\, l1\, lG2\, dt1 \sin(t1 - t2)}{\frac{m2^2\, l1^2\, lG2^2 \cos(t1 - t2)^2}{J1 + m2\, l1^2} - J2 - m2\, lG2^2} \tag{15}$$

```
> eval(f23,[t1=0,t2=0,dt1=0,dt2=0,CM3=0]);
```

$$0 \tag{16}$$

```
>
> f24:=diff(f2(t1,t2,dt1,dt2,CM3),dt2);
```

$$f24 := -\frac{2\, m2^2\, l1^2\, lG2^2\, dt2 \sin(t1 - t2) \cos(t1 - t2)}{(J1 + m2\, l1^2)\left(\frac{m2^2\, l1^2\, lG2^2 \cos(t1 - t2)^2}{J1 + m2\, l1^2} - J2 - m2\, lG2^2\right)} \tag{17}$$

```
> eval(f24,[t1=0,t2=0,dt1=0,dt2=0,CM3=0]);
```

$$0 \tag{18}$$

```
>
> g11:=diff(f1(t1,t2,dt1,dt2,CM3),CM3);
```

$$g11 := \frac{m2\, l1\, lG2 \cos(t1 - t2)}{m2^2\, l1^2\, lG2^2 \cos(t1 - t2)^2 - (J2 + m2\, lG2^2)(J1 + m2\, l1^2)} \tag{19}$$

```
> eval(g11,[t1=0,t2=0,dt1=0,dt2=0,CM3=0]);
```

$$\frac{m2\, l1\, lG2}{m2^2\, l1^2\, lG2^2 - (J2 + m2\, lG2^2)(J1 + m2\, l1^2)} \tag{20}$$

```
>
> g22:=diff(f2(t1,t2,dt1,dt2,CM3),CM3);
```

$$g22 := -\frac{1}{\frac{m2^2\, l1^2\, lG2^2 \cos(t1 - t2)^2}{J1 + m2\, l1^2} - J2 - m2\, lG2^2} \tag{21}$$

```
> eval(g22,[t1=0,t2=0,dt1=0,dt2=0,CM3=0]);
```

$$-\frac{1}{\frac{m2^2\, l1^2\, lG2^2}{J1 + m2\, l1^2} - J2 - m2\, lG2^2} \tag{22}$$

D2. Maple16 Updated model

Linearization of the model that includes the stiffness element for the hip joint.

```
> A1:=J1+m2*l1^2:
> A2:=m2*l1*lG2:
> A3:=m2*l1*lG2:
> A4:=(m1*lG1+m2*l1)*g:
> B1:=m2*l1*lG2:
> B2:=J2+m2*lG2^2:
> B3:=m2*l1*lG2:
> B4:=m2*g*lG2:
> Ca:=-Kelas*(t2-t1):
```

```
> f1:=(t1,t2,dt1,dt2,CM3)->(B2*A3*dt2*sin(t1-t2)-B2*A4*sin(t1)+B3*A2*
  (dt1)^2*sin(t1-t2)*cos(t1-t2)+B4*A2*sin(t2)*cos(t1-t2)+A2*cos(t1-t2)*
  CM3-B2*Ca)/(B1*A2*(cos(t1-t2))^2-B2*A1);
```

$$f1 := (t1, t2, dt1, dt2, CM3) \rightarrow \frac{1}{B1\,A2\cos(t1-t2)^2 - B2\,A1}\left(B2\,A3\,dt2\sin(t1-t2)\right. \tag{1}$$
$$- B2\,A4\sin(t1) + B3\,A2\,dt1^2\sin(t1-t2)\cos(t1-t2) + B4\,A2\sin(t2)\cos(t1-t2)$$
$$\left. + A2\cos(t1-t2)\,CM3 - B2\,Ca\right)$$

```
> f2:=(t1,t2,dt1,dt2,CM3)->((-B1*A3/A1)*(dt2)^2*sin(t1-t2)*cos(t1-t2)+
  (B1*A4/A1)*sin(t1)*cos(t1-t2)-B3*(dt1)^2*sin(t1-t2)-B4*sin(t2)-CM3+
  (B1/A1)*Ca*cos(dt1-dt2))/(((B1*A2)/A1)*(cos(t1-t2))^2-B2);
```

$$f2 := (t1, t2, dt1, dt2, CM3) \rightarrow \frac{1}{\frac{B1\,A2\cos(t1-t2)^2}{A1} - B2}\left(\right. \tag{2}$$
$$- \frac{B1\,A3\,dt2^2\sin(t1-t2)\cos(t1-t2)}{A1} + \frac{B1\,A4\sin(t1)\cos(t1-t2)}{A1} - B3\,dt1^2\sin(t1-t2)$$
$$\left. - B4\sin(t2) - CM3 + \frac{B1\,Ca\cos(dt1-dt2)}{A1}\right)$$

```
>
>
```

```
> f11:=diff(f1(t1,t2,dt1,dt2,CM3),t1);
```

$$f11 := \left(\left(J2 + m2\,lG2^2\right) m2\,l1\,lG2\,dt2\cos(t1-t2) - \left(J2 + m2\,lG2^2\right)(m1\,lG1 + m2\,l1)\,g\cos(t1)\right. \tag{3}$$
$$+ m2^2\,l1^2\,lG2^2\,dt1^2\cos(t1-t2)^2 - m2^2\,l1^2\,lG2^2\,dt1^2\sin(t1-t2)^2$$
$$- m2^2\,g\,lG2^2\,l1\sin(t2)\sin(t1-t2) - m2\,l1\,lG2\sin(t1-t2)\,CM3 - \left(J2 + m2\,lG2^2\right)Kelas\Big)$$
$$\Big/\left(m2^2\,l1^2\,lG2^2\cos(t1-t2)^2 - \left(J2 + m2\,lG2^2\right)\left(J1 + m2\,l1^2\right)\right) + \left(2\left(\left(J2\right.\right.\right.$$
$$+ m2\,lG2^2\Big)\,m2\,l1\,lG2\,dt2\sin(t1-t2) - \left(J2 + m2\,lG2^2\right)(m1\,lG1 + m2\,l1)\,g\sin(t1)$$
$$+ m2^2\,l1^2\,lG2^2\,dt1^2\sin(t1-t2)\cos(t1-t2) + m2^2\,g\,lG2^2\,l1\sin(t2)\cos(t1-t2)$$
$$+ m2\,l1\,lG2\cos(t1-t2)\,CM3 + \left(J2 + m2\,lG2^2\right)Kelas\,(-t1+t2)\Big)\,m2^2\,l1^2\,lG2^2\cos(t1$$
$$\left.\left.\left. - t2)\sin(t1-t2)\right)\Big/\left(m2^2\,l1^2\,lG2^2\cos(t1-t2)^2 - \left(J2 + m2\,lG2^2\right)\left(J1 + m2\,l1^2\right)\right)^2\right)$$

```
>
```

```
> eval(f11,[t1=0,t2=0,dt1=0,dt2=0,CM3=0]);
```

$$\frac{-\left(J2+m2\,lG2^2\right)\left(m1\,lG1+m2\,l1\right)g-\left(J2+m2\,lG2^2\right)Kelas}{m2^2\,l1^2\,lG2^2-\left(J2+m2\,lG2^2\right)\left(J1+m2\,l1^2\right)} \tag{4}$$

```
> f12:=diff(f1(t1,t2,dt1,dt2,CM3),t2);
```

$$\begin{aligned} f12 := {} & \left(-\left(J2+m2\,lG2^2\right)m2\,l1\,lG2\,dt2\cos(t1-t2)-m2^2\,l1^2\,lG2^2\,dt1^2\cos(t1-t2)^2\right. \\ & +m2^2\,l1^2\,lG2^2\,dt1^2\sin(t1-t2)^2+m2^2\,g\,lG2^2\,l1\cos(t2)\cos(t1-t2) \\ & +m2^2\,g\,lG2^2\,l1\sin(t2)\sin(t1-t2)+m2\,l1\,lG2\sin(t1-t2)\,CM3+\left(J2+m2\,lG2^2\right)Kelas\Big) \\ & \Big/\left(m2^2\,l1^2\,lG2^2\cos(t1-t2)^2-\left(J2+m2\,lG2^2\right)\left(J1+m2\,l1^2\right)\right)-\left(2\left(\left(J2\right.\right.\right. \\ & +m2\,lG2^2\Big)m2\,l1\,lG2\,dt2\sin(t1-t2)-\left(J2+m2\,lG2^2\right)\left(m1\,lG1+m2\,l1\right)g\sin(t1) \\ & +m2^2\,l1^2\,lG2^2\,dt1^2\sin(t1-t2)\cos(t1-t2)+m2^2\,g\,lG2^2\,l1\sin(t2)\cos(t1-t2) \\ & +m2\,l1\,lG2\cos(t1-t2)\,CM3+\left(J2+m2\,lG2^2\right)Kelas\,(-t1+t2)\Big)\,m2^2\,l1^2\,lG2^2\cos(t1 \\ & \left.\left.-t2)\sin(t1-t2)\right)\Big/\left(m2^2\,l1^2\,lG2^2\cos(t1-t2)^2-\left(J2+m2\,lG2^2\right)\left(J1+m2\,l1^2\right)\right)^2 \end{aligned} \tag{5}$$

```
> eval(f12,[t1=0,t2=0,dt1=0,dt2=0,CM3=0]);
```

$$\frac{m2^2\,g\,lG2^2\,l1+\left(J2+m2\,lG2^2\right)Kelas}{m2^2\,l1^2\,lG2^2-\left(J2+m2\,lG2^2\right)\left(J1+m2\,l1^2\right)} \tag{6}$$

```
>
> f13:=diff(f1(t1,t2,dt1,dt2,CM3),dt1);
```

$$f13 := \frac{2\,m2^2\,l1^2\,lG2^2\,dt1\sin(t1-t2)\cos(t1-t2)}{m2^2\,l1^2\,lG2^2\cos(t1-t2)^2-\left(J2+m2\,lG2^2\right)\left(J1+m2\,l1^2\right)} \tag{7}$$

```
> eval(f13,[t1=0,t2=0,dt1=0,dt2=0,CM3=0]);
```

$$0 \tag{8}$$

```
>
> f14:=diff(f1(t1,t2,dt1,dt2,CM3),dt2);
```

$$f14 := \frac{\left(J2+m2\,lG2^2\right)m2\,l1\,lG2\sin(t1-t2)}{m2^2\,l1^2\,lG2^2\cos(t1-t2)^2-\left(J2+m2\,lG2^2\right)\left(J1+m2\,l1^2\right)} \tag{9}$$

```
> eval(f14,[t1=0,t2=0,dt1=0,dt2=0,CM3=0]);
```

$$0 \tag{10}$$

```
>
```

```
> f21:=diff(f2(t1,t2,dt1,dt2,CM3),t1);
```

$$f21 := \frac{1}{\frac{m2^2\, l1^2\, lG2^2 \cos(t1-t2)^2}{J1+m2\, l1^2} - J2 - m2\, lG2^2}\left(-\frac{m2^2\, l1^2\, lG2^2\, dt2^2 \cos(t1-t2)^2}{J1+m2\, l1^2} + \frac{m2^2\, l1^2\, lG2^2\, dt2^2 \sin(t1-t2)^2}{J1+m2\, l1^2} + \frac{m2\, l1\, lG2\,(m1\, lG1+m2\, l1)\, g \cos(t1)\cos(t1-t2)}{J1+m2\, l1^2} - \frac{m2\, l1\, lG2\,(m1\, lG1+m2\, l1)\, g \sin(t1)\sin(t1-t2)}{J1+m2\, l1^2} - m2\, l1\, lG2\, dt1^2 \cos(t1-t2) + \frac{m2\, l1\, lG2\, Kelas \cos(dt1-dt2)}{J1+m2\, l1^2}\right) + \left(2\left(-\frac{m2^2\, l1^2\, lG2^2\, dt2^2 \sin(t1-t2)\cos(t1-t2)}{J1+m2\, l1^2} + \frac{m2\, l1\, lG2\,(m1\, lG1+m2\, l1)\, g \sin(t1)\cos(t1-t2)}{J1+m2\, l1^2} - m2\, l1\, lG2\, dt1^2 \sin(t1-t2) - m2\, g\, lG2 \sin(t2) - CM3 - \frac{m2\, l1\, lG2\, Kelas\,(-t1+t2)\cos(dt1-dt2)}{J1+m2\, l1^2}\right) m2^2\, l1^2\, lG2^2 \cos(t1-t2)\sin(t1-t2)\right) \Big/ \left(\left(\frac{m2^2\, l1^2\, lG2^2 \cos(t1-t2)^2}{J1+m2\, l1^2} - J2 - m2\, lG2^2\right)^2 (J1+m2\, l1^2)\right) \tag{11}$$

```
> f22:=diff(f2(t1,t2,dt1,dt2,CM3),t2);
```

$$f22 := \frac{1}{\frac{m2^2\, l1^2\, lG2^2 \cos(t1-t2)^2}{J1+m2\, l1^2} - J2 - m2\, lG2^2}\left(\frac{m2^2\, l1^2\, lG2^2\, dt2^2 \cos(t1-t2)^2}{J1+m2\, l1^2} - \frac{m2^2\, l1^2\, lG2^2\, dt2^2 \sin(t1-t2)^2}{J1+m2\, l1^2} + \frac{m2\, l1\, lG2\,(m1\, lG1+m2\, l1)\, g \sin(t1)\sin(t1-t2)}{J1+m2\, l1^2} + m2\, l1\, lG2\, dt1^2 \cos(t1-t2) - m2\, g\, lG2 \cos(t2) - \frac{m2\, l1\, lG2\, Kelas \cos(dt1-dt2)}{J1+m2\, l1^2}\right) - \left(2\left(-\frac{m2^2\, l1^2\, lG2^2\, dt2^2 \sin(t1-t2)\cos(t1-t2)}{J1+m2\, l1^2} + \frac{m2\, l1\, lG2\,(m1\, lG1+m2\, l1)\, g \sin(t1)}{J1+m2\, l1^2}\right.\right.$$

$$\left.\left.\frac{\cos(t1-t2)}{} - m2\, l1\, lG2\, dt1^2 \sin(t1-t2) - m2\, g\, lG2 \sin(t2) - CM3 - \frac{m2\, l1\, lG2\, Kelas\,(-t1+t2)}{J1+m2\, l1^2}\right.\right.$$

$$m2^2\, l1^2\, lG2^2 \cos(t1 - t2) \sin(t1 - t2) \Big) \Big/ \left(\left(\frac{m2^2\, l1^2\, lG2^2 \cos(t1 - t2)^2}{J1 + m2\, l1^2} - J2 - m2\, lG2^2 \right)^2 (J1 + m2\, l1^2) \right)$$

```
> eval(f22,[t1=0,t2=0,dt1=0,dt2=0,CM3=0]);
```

$$\frac{-m2\, g\, lG2 - \dfrac{m2\, l1\, lG2\, Kelas}{J1 + m2\, l1^2}}{\dfrac{m2^2\, l1^2\, lG2^2}{J1 + m2\, l1^2} - J2 - m2\, lG2^2} \tag{14}$$

```
>
> f23:=diff(f2(t1,t2,dt1,dt2,CM3),dt1);
```

$$f23 := \frac{-2\, m2\, l1\, lG2\, dt1 \sin(t1 - t2) + \dfrac{m2\, l1\, lG2\, Kelas\, (-t1 + t2) \sin(dt1 - dt2)}{J1 + m2\, l1^2}}{\dfrac{m2^2\, l1^2\, lG2^2 \cos(t1 - t2)^2}{J1 + m2\, l1^2} - J2 - m2\, lG2^2} \tag{15}$$

```
> eval(f23,[t1=0,t2=0,dt1=0,dt2=0,CM3=0]);
```

$$0 \tag{16}$$

```
>
> f24:=diff(f2(t1,t2,dt1,dt2,CM3),dt2);
```

$$f24 := \tag{17}$$

$$\frac{1}{\dfrac{m2^2\, l1^2\, lG2^2 \cos(t1 - t2)^2}{J1 + m2\, l1^2} - J2 - m2\, lG2^2} \left(- \frac{2\, m2^2\, l1^2\, lG2^2\, dt2 \sin(t1 - t2) \cos(t1 - t2)}{J1 + m2\, l1^2} - \frac{m2\, l1\, lG2\, Kelas\, (-t1 + t2) \sin(dt1 - dt2)}{J1 + m2\, l1^2} \right)$$

```
> eval(f24,[t1=0,t2=0,dt1=0,dt2=0,CM3=0]);
```

$$0 \tag{18}$$

```
>
> g11:=diff(f1(t1,t2,dt1,dt2,CM3),CM3);
```

$$g11 := \frac{m2\, l1\, lG2 \cos(t1 - t2)}{m2^2\, l1^2\, lG2^2 \cos(t1 - t2)^2 - (J2 + m2\, lG2^2)\, (J1 + m2\, l1^2)} \tag{19}$$

```
> eval(g11,[t1=0,t2=0,dt1=0,dt2=0,CM3=0]);
```

$$\frac{m2\, l1\, lG2}{m2^2\, l1^2\, lG2^2 - (J2 + m2\, lG2^2)\, (J1 + m2\, l1^2)} \tag{20}$$

```
> g22:=diff(f2(t1,t2,dt1,dt2,CM3),CM3);
```

$$g22 := -\frac{1}{\frac{m2^2\, l1^2\, lG2^2 \cos(t1-t2)^2}{J1 + m2\, l1^2} - J2 - m2\, lG2^2} \tag{21}$$

```
> eval(g22,[t1=0,t2=0,dt1=0,dt2=0,CM3=0]);
```

$$-\frac{1}{\frac{m2^2\, l1^2\, lG2^2}{J1 + m2\, l1^2} - J2 - m2\, lG2^2} \tag{22}$$

D3. Maple16 Non-linear Controller

```
> with(LinearAlgebra):
> mD:=Matrix([[Q1,Q2*cos(th1-th2)],[Q2*cos(th1-th2),Q4]]);
```

$$mD := \begin{bmatrix} Q1 & Q2\cos(th1-th2) \\ Q2\cos(th1-th2) & Q4 \end{bmatrix} \tag{1}$$

```
> mC:=Matrix([[0,Q2*sin(th1-th2)*dth2],[-Q2*sin(th1-th2)*
  dth1,0]]);
```

$$mC := \begin{bmatrix} 0 & Q2\sin(th1-th2)\, dth2 \\ -Q2\sin(th1-th2)\, dth1 & 0 \end{bmatrix} \tag{2}$$

```
> mG:=Matrix([[-Q3*g*sin(th1)],[-Q5*g*sin(th2)]]);
```

$$mG := \begin{bmatrix} -Q3\, g\sin(th1) \\ -Q5\, g\sin(th2) \end{bmatrix} \tag{3}$$

```
> mddth:=Matrix([[ddth1],[ddth2]]);
```

$$mddth := \begin{bmatrix} ddth1 \\ ddth2 \end{bmatrix} \tag{4}$$

```
> mdth:=Matrix([[dth1],[dth2]]);
```

$$mdth := \begin{bmatrix} dth1 \\ dth2 \end{bmatrix} \tag{5}$$

```
> mtao:=Matrix([[0],[tao]]);
```

$$mtao := \begin{bmatrix} 0 \\ tao \end{bmatrix} \tag{6}$$

```
> mDi:=MatrixInverse(mD);
```

$$mDi := \begin{bmatrix} -\dfrac{Q4}{-Q1\,Q4 + Q2^2\cos(th1-th2)^2} & \dfrac{Q2\cos(th1-th2)}{-Q1\,Q4 + Q2^2\cos(th1-th2)^2} \\ \dfrac{Q2\cos(th1-th2)}{-Q1\,Q4 + Q2^2\cos(th1-th2)^2} & -\dfrac{Q1}{-Q1\,Q4 + Q2^2\cos(th1-th2)^2} \end{bmatrix} \quad (7)$$

```
>
> mCmdth:=Multiply(mC,mdth);
```

$$mCmdth := \begin{bmatrix} Q2\sin(th1-th2)\,dth2^2 \\ -Q2\sin(th1-th2)\,dth1^2 \end{bmatrix} \quad (8)$$

```
> mtaomCmdthmG:=mtao-mCmdth-mG;
```

$$mtaomCmdthmG := \begin{bmatrix} -Q2\sin(th1-th2)\,dth2^2 + Q3\,g\sin(th1) \\ tao + Q2\sin(th1-th2)\,dth1^2 + Q5\,g\sin(th2) \end{bmatrix} \quad (9)$$

```
> ddthfinal:=Multiply(mDi,mtaomCmdthmG);
```

$$ddthfinal := \left[\left[-\frac{Q4\left(-Q2\sin(th1-th2)\,dth2^2 + Q3\,g\sin(th1)\right)}{-Q1\,Q4 + Q2^2\cos(th1-th2)^2} + \frac{Q2\cos(th1-th2)\left(tao + Q2\sin(th1-th2)\,dth1^2 + Q5\,g\sin(th2)\right)}{-Q1\,Q4 + Q2^2\cos(th1-th2)^2} \right], \left[\frac{Q2\cos(th1-th2)\left(-Q2\sin(th1-th2)\,dth2^2 + Q3\,g\sin(th1)\right)}{-Q1\,Q4 + Q2^2\cos(th1-th2)^2} - \frac{Q1\left(tao + Q2\sin(th1-th2)\,dth1^2 + Q5\,g\sin(th2)\right)}{-Q1\,Q4 + Q2^2\cos(th1-th2)^2} \right]\right] \quad (10)$$

```
> ddth2:= Q2*cos(th1-th2)*(-Q2*sin(th1-th2)*dth2^2+Q3*g*sin
  (th1))/(-Q1*Q4+Q2^2*cos(th1-th2)^2)-Q1*(tao+Q2*sin(th1-
  th2)*dth1^2+Q5*g*sin(th2))/(-Q1*Q4+Q2^2*cos(th1-th2)^2);
```

$$ddth2 := \frac{Q2\cos(th1-th2)\left(-Q2\sin(th1-th2)\,dth2^2 + Q3\,g\sin(th1)\right)}{-Q1\,Q4 + Q2^2\cos(th1-th2)^2} - \frac{Q1\left(tao + Q2\sin(th1-th2)\,dth1^2 + Q5\,g\sin(th2)\right)}{-Q1\,Q4 + Q2^2\cos(th1-th2)^2} \quad (11)$$

```
> fcomddth2:=-Q2*cos(th1-th2)*(-Q2*sin(th1-th2)*dth2^2+Q3*g*
  sin(th1))+Q1*(tao+Q2*sin(th1-th2)*dth1^2+Q5*g*sin(th2));
```

$$fcomddth2 := -Q2\cos(th1 - th2)\left(-Q2\sin(th1 - th2)\,dth2^2 + Q3\,g\sin(th1)\right) + Q1\left(tao + Q2\sin(th1 - th2)\,dth1^2 + Q5\,g\sin(th2)\right) \quad (12)$$

```
> mF:=Q2^2*cos(th1-th2)*sin(th1-th2)*dth2^2-Q2*Q3*g*cos(th1-
  th2)*sin(th1)+Q1*Q2*sin(th1-th2)*dth1^2+Q1*Q5*g*sin(th2);
```

$$mF := Q2^2\cos(th1 - th2)\sin(th1 - th2)\,dth2^2 - Q2\,Q3\,g\cos(th1 - th2)\sin(th1) + Q1\,Q2\sin(th1 - th2)\,dth1^2 + Q1\,Q5\,g\sin(th2) \quad (13)$$

```
> mQ1tao:= Q1*tao;
```

$$mQ1tao := Q1\,tao \quad (14)$$